1983

Electronic Structure of Iron.

Diola Bagayoko
Louisiana State University and Agricultural & Mechanical College

Bagayoko, Diola

ELECTRONIC STRUCTURE OF IRON

The Louisiana State University and Agricultural and Mechanical Col. PH.D. 1983

PLEASE NOTE:

In all cases this material has been filmed in the best possible way from the available copy. Problems encountered with this document have been identified here with a check mark __✓__.

1. Glossy photographs or pages _____
2. Colored illustrations, paper or print _____
3. Photographs with dark background _____
4. Illustrations are poor copy _____
5. Pages with black marks, not original copy _____
6. Print shows through as there is text on both sides of page _____
7. Indistinct, broken or small print on several pages ✓
8. Print exceeds margin requirements _____
9. Tightly bound copy with print lost in spine _____
10. Computer printout pages with indistinct print ✓
11. Page(s) _____ lacking when material received, and not available from school or author.
12. Page(s) _____ seem to be missing in numbering only as text follows.
13. Two pages numbered _____. Text follows.
14. Curling and wrinkled pages _____
15. Other _____

University
Microfilms
International

ELECTRONIC STRUCTURE OF IRON

A Dissertation
Submitted to the Graduate Faculty of the
Louisiana State University and
Agricultural and Mechanical College
in Partial Fulfillment of the
Requirements for the Degree of
Doctor of Philosophy

in

The Department of Physics and Astronomy

by

Diola Bagayoko
B.S., Ecole Normale Superieure de Bamako, Mali, 1973
M.S., Lehigh University, Bethlehem, Pennsylvania, USA, 1978
August 1983

DEDICATION

As an expression of my gratitude for their love and support, I dedicate this dissertation to my mother, Nagnouma (kind mother) Keita; my father, Djigui (the reliant) Bagayoko; my grandfather, Namory (the great leader) Keita; my grandmother, Mariam Traore; my wife, Ella Kelley; and my son, Namory Djigui Bagayoko.

I extend this dedication to the memories of my ancestor, Professor "Cheik" Mohamed Bagayoko of the University of Timbuctu, whose hard work, intellectual accomplishments, and great human qualities are a continual source of inspiration for me. In doing so I am hereby presenting this dissertation to my sons and daughters, present and future, as an invitation to uphold the family tradition.

ACKNOWLEDGEMENTS

I am deeply grateful to Professor Joseph Callaway for supporting and guiding me throughout this research. I have immensely benefited from his broad and profound understanding of physics. His personal habit of working hard, material and moral assistances constituted a quintessence of the successful completion of this endeavor and serve as inspirational examples for me in my career as a scientist.

I thank the African-American Institute, Lehigh and Brandeis Universities for the gracious AFGRAD fellowship which enabled me to undertake this Ph.D. program. The financial support of Louisiana State University and the U.S. National Science Foundation for large computations as well as participation to several conferences i to be commended. Dr. Charles E. Coates Memorial Fund of The L.S.U. Foundation assisted for the publication of this dissertation.

Faculty members, post-doctoral researchers and students of the Department of Physics and Astronomy provided me with a stimulating academic atmosphere I highly appreciated. I particularly thank Professors A. K. Rajagopal, Jerry Draayer, Claude Grenier, A. R. P. Rau, Roy Goodrich, Ronald J. Henry, R. G. Hussey, and Drs. Xianwu Zou, Alfred Ziegler, S. P. Singhal, Uday Gupta, M. V. Ramana, Alfred Msezane, Samir Bhattacharya, Lou Adams, J. Perez-Mercader, Eugene Ho, and Graduate Students Khachig Jerjian, S. Dhar, Gonzalo Fuster, Dipak Oza, and Yosua Namba for their help and support. I am indebted to Professor Norman M. Mach for invaluable suggestions. I thank Professor Alan Marshak for sparing some of his time for me. I am

grateful to Dr. D. G. Laurent who taught me the essentials of the original band package and to Dr. Nathalie Zongo N'Guessan for her support. The L.S.U. System Network Computer Center and the System Analyst Ms. Hortensia Delgado played a key role in the success of my interface with the IBM 3033. To help, and always with pleasure is a distinction Ms. Delgado has earned. Artist N. P. Harris kindly reinked and photographed the figures in this document. The typing services of Linda Gauthier and Daisy Mehrotra have been very helpful in the production of this publication.

I finally wish to express my profound gratitude to Dj'gui Bagayoko, Namory Keita, Ella Kelley, C. M. Cherif Keita, and families for their love and encouragement.

TABLE OF CONTENTS

LIST OF TABLES

LIST OF FIGURES

ABSTRACT

A survey of previous theoretical and experimental works on iron in some Bravais lattices and at various temperature and pressures shows this 3d transition metal to exhibit a wealth of allotropic transformations and to possess, along with some of its alloys, peculiar magnetic properties in the face centered cubic (FCC) phase. We present an ab-initio self-consistent spin polarized band structure study of this metal in the body (BCC) and face centered cubic lattices at absolute zero and at various atomic volumes. Our calculations employed gaussian basis functions in a LCAO scheme and used the RSK local density potential. In contrast to previous attempts, the structural and atomic volume dependences of the electronic and magnetic states of iron are analysed using the fundamental parameters, band widths and exchange splittings, of the energy bands.

While the smooth variation of the magnetic moment in BCC iron with lattice spacings greater or equal to 4.8 a.u. is attributed to the atomic origin of magnetism in that structural phase, its drastic change in FCC iron between a = 6.5516 a.u. and 7.0 a.u. is ascribed to a transition from an itinerant picture to a localized one. This analysis sheds some light on the nature of magnetism in other metals like cobalt. The relevance of the above transition to the properties of FCC iron based alloys is illustrated. Applications of the numerically established local quadratic dependence of the charge and spin form factors on the lattice spacing are discussed.

CHAPTER 1

INTRODUCTION

The BCC phase of iron is known to be the most stable one in ordinary conditions of temperature and pressure. The Curie or critical temperature of this ferromagnet is 1043 K. The equilibrium lattice spacing at 0 K is around 5.4057 a.u. A quasi-exhaustive list of theoretical band structure calculations of iron (Fe) at the equilibrium lattice constant (slightly different for different calculations) is provided by Tawil and Callaway[1], Callaway and Wang[2], and recent reviews[3,4,5,6]. Unlike the case of nickel, there is a general agreement between theory[2,3,6] and experiment[5,7,8,9] for BCC iron as far as band widths and exchange splittings are concerned. The experimental spin splitting obtained at P_4 by Eastman et al.[5], 1.5 electron volts (eV) compares to the 1.34 eV theoretical result of Callaway and Wang[2]. This is a significant agreement as the theoretical splittings for FCC nickel are generally double that of the experimental ones. The majority (or up) spin sub-band width at P is reported to be 3 and 2.6 eV by photo-emission experiment[5] and theory[2], respectively. Danan and coworkers[7] measured the magnetic moment to be 2.12 Bohr magneton (μ_B) while theory predicted 2.16 μ_B. Eastman et al.[5] discussed the Fermi surface of iron and found theory[2] and experiment to support one another.

The industrial importance of iron partly explains the continual growth of the number of experimental works on this 3d metal at finite temperature and under hydrostatic pressure[10,11,12,13]. Under the

above conditions iron undergoes several allotropic transformations[11,14] and exhibit a variety of magnetic properties. Liu and Bassett[14] presented an experimental temperature versus pressure (T-P) phase diagram[15,16] of iron. This diagram, whose general features are reproduced in Figure 1, illustrates the regions of stability for the alpha (α), epsilon (ϵ), gamma (γ), and delta (δ) iron. The respective crystal structures are the body centered cubic (BCC), the hexagonal close packed (HCP), the face centered cubic (FCC), and a BCC with magnetic disorder.

A major obstacle in the study of FCC iron, as intimated by Figure 1, is the difficulty there is to stabilize it a low temperature[11,17]. Several conclusions relevant to FCC iron are drawn from knowledge of various iron based alloys[11]. While there seems to be agreement on the paramagnetism of a high pressure HCP phase of iron, the question of magnetism in the FCC phase is yet to be totally settled. A high temperature FCC phase (i.e., T = 1320 K) is known to display spatial ferromagnetic correlations[17]. Conflicting views exist on the magnetic state of the FCC phase assuming that it could be prepared at low temperature, and/or under high pressures. Kaufman et al.[11] discussed the Mossbauer effect, neutron diffraction experiments as well as susceptibility measurements for various FCC alloys containing iron. It was concluded that at low temperatures, FCC iron would be antiferromagnetic (AF) with a moment less than one Bohr magneton (μ_B). Two extrapolated lattice constants are obtained[11] for FCC iron at 25 degree celsius using the atomic separation versus solute concentration curves[18] of iron based alloys. The curves for Fe-Pt, Fe-Pd, Fe-Ni alloys in which iron

atoms possess a high moment (2.8 μ_B) lead to 6.878 a.u. while those for Fe-C, Fe-Mn, Fe-N give 6.727 a.u. This was considered as supporting Tauer and Weiss[19] hypothesis of low moment low volume (γ_1) and high moment and high volume (γ_2) states of FCC iron. The issue of magnetic order in FCC Fe has been closely related to that of its alloys in general and of the invar alloys in particular[20]. These invar alloys are characterized, among other things[21], by an almost zero, if not negative, expansion coefficient in certain temperature and solute concentration ranges.

In contrast to some of the above works where the properties of FCC iron are infered from those of alloys, Wright[22], Gradmann et al.[23], and Keune et al.[24] considered pure gamma iron films. Wright studied by electron spin resonance 30 angstroms thick gamma Fe films grown by electrodeposition on the (110) copper (Cu) single crystal face. He found these films to display ferromagnetism at room temperature. A moment of 1.1 μ_B and a lattice spacing of 6.8027 were estimated. Gradmann et al. performed magnetization measurements on gamma Fe thin films grown on the (111) copper surface. They utilized an oscillation type magnetometer. For temperatures in the range 70-300 K a ferromagnetic ordering was observed in these films. Keune and coworkers carried out Mossbauer spectroscopy measurements on gamma Fe films. The films were grown on the (001) copper face and were reported to exhibit antiferromagnetism for temperatures between 2 and 295 K. These authors[24], considering the two previous results[22,23], suggested a dependence of the magnetic ordering on the film orientation.

Figure 1. Major features of the temperature versus pressure (T-P) experimental phase diagram of iron according to Liu and Basset.[14] The full, dotted, and dashed curves are respectively from references 14, 15, and 16.

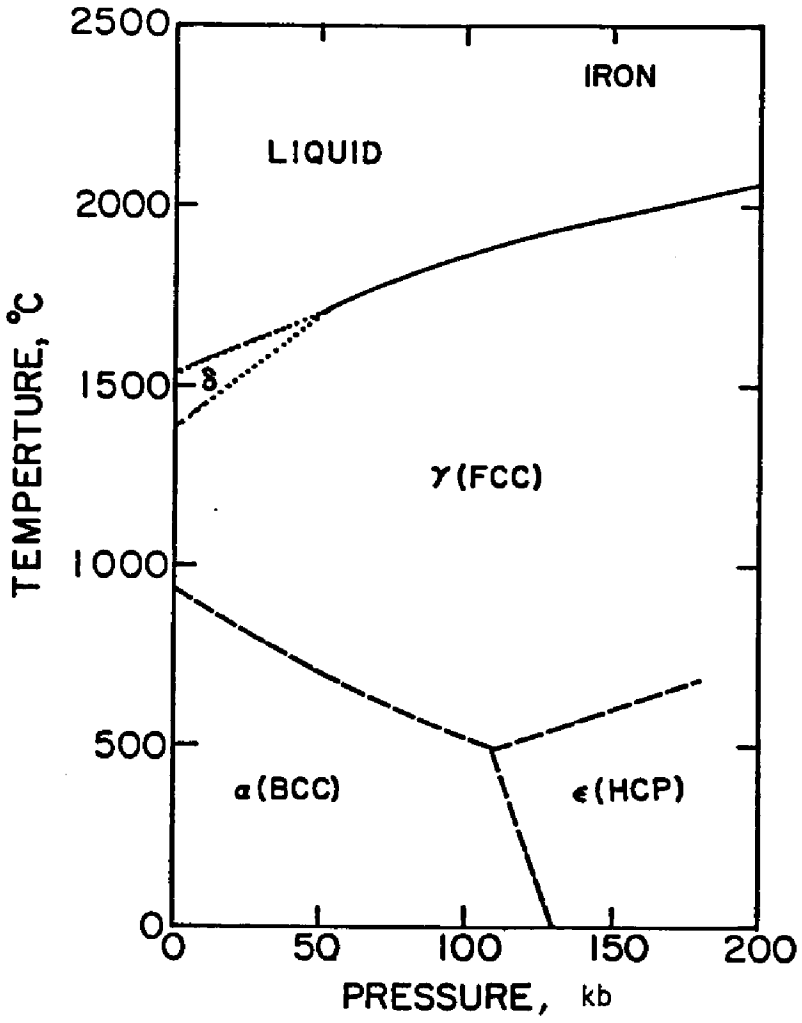

Gonser et al.[25] presented Mossbaur spectra of coherent FCC iron precipitates in a $Cu_{69}Au_{30}$ matrix. Contrary to the antiferromagnetic results of previous works on gamma Fe precipitates, as reviewed by Kaufman et al.[11], these authors found ferromagnetic ones. They made measurements at 4.2, 77, and 295 K. They estimated an iron atom separation of at least 5.0227 a.u. using Vegards Law. Antiferromagnetism and ferromagnetism were intimated to occur for atomic separations respectively below and above this value. A significant result is the observation of ferromagnetism in gamma Fe by the microscopic Mossbauer technique as opposed to the macroscopic ones used in references 22 and 23. Very recently Brown et al.[17], on the basis of their ferromagnetic results from neutron diffraction experiments on FCC iron at high temperatures, concluded that the low temperature FCC iron, if it could be stabilized, would be ferromagnetic.

Several other theoretical works on FCC iron exist in the literature[26-32]. The APW band structure calculations of Wood[26] were followed by those of Deegan[27] who used the narrow band approximation to the Korringa-Kohn-Rostoker (KKR) or the Green function method. Dalton[28] presented density of state curves for BCC and FCC iron along with other metals.

More recently Madsen et al.[29], and Poulsen and coworkers[30] addressed, among other issues, the question of magnetic order in BCC and FCC iron for various lattice parameters. They employed a local density potential and the atomic sphere approximation (ASA) to the KKR method. Their results and procedure of calculation are reviewed by Andersen et al.[31]. For Wigner-Seitz radii (R_s) between 2.66 and

2.85 Madsen et al. found the magnetic moment of an assumed FCC phase to be between 3 and 3.5 μ_B. The moment drops rapidly below 1.5 μ_B around R_s = 2.60 and goes to zero at R_s = 2.47. Poulsen et al., unlike Madsen and coworkers, included the sp-d hybridization in all their calculatins and found no moment for FCC iron for R_s values less than 2.60.

Kubler[32] considered antiferromagnetism which was not addressed by the authors just mentioned. He also utilized a local density potential to carry out self-consistent band structure calculations in an augmented spherical wave approximation[33]. He studied non-magnetic ferro and antiferromagnetic orderings in BCC and FCC iron. From the total energy curves he found the stable magnetic order to be ferro and antiferromagnetic for BCC and FCC iron phases, respectively. A difficulty connected with the FCC phase consists in having its total energy lower than that of ferromagnetic BCC iron for the R_s values considered. We shall discuss this subsequently. The moment of the ferromagnetic FCC phase was found to exhibit the sharp drop described above around R_s = 2.63 and goes to zero in the vicinity of R_s = 2.55 a.u.

Roy and Pettifor[34] reported to have obtained the γ_1 and γ_2 states from Stoner theory[35]. The ASA and local density calculations of these authors predicted both states to be ferromagnetic. The experimental T-P diagram of iron in Figure 1 has very recently been qualitatively reproduced by Hasegawa and Pettifor[36]. Their calculations were based on the spin fluctuation theory of band magnetism[37,38]. They found the magnetic contribution to the free energy to be the driving force in the phase transitions

and questioned previous explanations[11] which employed the two gamma states.

From this survey it appears that the magnetic state of FCC (γ) iron at low temperature is yet to be determined as there are experimental and theoretical results to support opposite views.

Our goal is to study the problem of the stability of the magnetic structures by means of ab-initio self consistent electronic band structures of ferromagnetic iron in BCC and FCC Bravais lattices for some R_s values between 2 and 5. Paramagnetism is indirectly allowed for. A close analysis of first principle energy bands and related fundamental parameters, band widths and splittings, is intended to explain essential electronic and magnetic properties of iron in the above phases as the lattice constant changes. The structural dependence of magnetism in iron is not only of importance in its own right but also is expected to be relevant to a complete understanding of invar anomalies.

The second chapter of this dissertation is devoted to an outline of our method of band structure calculation, the choice of a potential and the formalism for the calculation of the total energy of a metal recently developed by this group. The contraction procedure and other computational details are described in chapter two. The analysis of the results follows in chapter three and four. The electronic structure of BCC and FCC Fe are presented in the former while the latter addresses the magnetic properties. The discussions in the last chapter include some suggestions for future investigations believed to be of relevance to the properties of transition ferromagnets and a summary.

CHAPTER 2

GENERAL THEORY

A modern treatment of energy band theory for a metal generally amounts to solving the Kohn-Sham equations[39] of density functional theory[39,40,41]. Indeed, assuming a potential describing the many particle system is known[39,42] there exist several methods of obtaining the energy levels. These band calculation procedures have been reviewed by Callaway[43].

In the first section of this chapter we shall outline the linear combination of atomic orbital (LCAO) version of the tight-binding[44] method. Our choice of an effective one particle density functional potential is discussed in the second section. A new formalism for the calculation of the total energy of a metal is then covered in the last one.

A. The LCAO Method

Our aim is to solve the single particle Schrodinger equation:

$$(-\nabla^2 + V_\sigma(\vec{r}))\ \Psi_n\ (\vec{k},\vec{r}) = E_n(\vec{k})\ \Psi_n\ (\vec{k},\vec{r}) \qquad (1)$$

where

$$V_\sigma(\vec{r}) = -\sum_\mu \frac{2z}{|\vec{r} - \vec{R}_\mu|} + 2\int \frac{\rho(\vec{r}')}{|\vec{r} - \vec{r}'|}\, d^3r' + V_{xc\sigma}(\vec{r}) \qquad (2)$$

and

$$\psi_n(\vec{k},\vec{r}) = e^{-i\vec{k}\cdot\vec{R}_\mu} \psi_n(\vec{k},\vec{r}+\vec{R}_\mu), \tag{3}$$

satisfies Bloch theorem. The band index n, the coordinate vector $\vec{r}$, and the position vector $\vec{R}_\mu$ for lattice site μ are defined as usual. The potential $V_\sigma(\vec{r})$ comprises coulomb terms and an exchange correlation contribution $V_{xc\sigma}(\vec{r})$ where σ indicates the spin. The nuclear charge is Z and the units of energy are Rydbergs (Ry) with $\hbar = c = 1$, $e^2 = 2$, $m = 1/2$.

The tight-binding method consists in searching for solutions to equation 1 by expanding the wave function $\psi_n(\vec{k},\vec{r})$ in a finite set of atomic like (i.e., localized) functions. When the radial parts of these functions are taken to be those obtained for atoms the method is referred to as the LCAO method. The term LCGO, for linear combination of gaussian orbitals, is used if the above radial parts are gaussians. The basis functions $\phi_i(\vec{k},\vec{r})$ satisfy

$$\phi_i(\vec{k},\vec{r}) = N^{-1/2} \sum_\mu e^{i\vec{k}\cdot\vec{R}_\mu} U_i(\vec{r}-R_\mu) \tag{4}$$

with

$$U_i(\vec{r}) = R_{\ell_i}(r)\, K_{\ell_i,m}(\Theta,\psi) \tag{5}$$

in which $K_{\ell_i,m}(\Theta,\psi)$ and $R_{\ell_i}(r)$, respectively, contain the angular and radial dependences. The orbital quantum number is ℓ_i and m is the magnetic quantum number when the $K_{\ell_i,m}(\Theta,\psi)$ are taken to be

spherical harmonics. In general the choices of $R_{\ell_i}(r)$ are

$$R_{\ell_i} = N_i r^{\ell_i} e^{-\alpha_i r} \quad \text{or} \quad R_{\ell_i} = N_i r^{\ell_i} e^{-\alpha_i r^2} \tag{6}$$

where N_i is a normalization constant. For treatment of cubic crystals the angular functions are often chosen to be cubic harmonics[45]. The substitution of

$$\Psi_n(\vec{k},\vec{r}) = \sum_i C_{ni}(\vec{k})\, \phi_i(\vec{k},\vec{r}) \tag{7}$$

into equation 1 leads to

$$\sum_j H_{ij}(\vec{k})\, C_{nj}(\vec{k}) = E_n(\vec{k}) \sum_i S_{ij}(\vec{k})\, C_{nj}(\vec{k}) \tag{8}$$

where

$$H_{ij}(\vec{k}) = \sum_\mu e^{-i\vec{k}\cdot\vec{R}_\mu} \langle U_i(\vec{r} - \vec{R}_\mu) \mid -\nabla^2 + V_\sigma(\vec{r}) \mid U_j(\vec{r}) \rangle \tag{9}$$

and the overlap matrix elements are

$$S_{ij}(\vec{k}) = \sum_\mu e^{-i\vec{k}\cdot\vec{R}_\mu} \langle U_i(\vec{r} - \vec{R}_\mu) \mid U_j(\vec{r}) \rangle \tag{10}$$

The matrix equation 8 is solved for the eigenvalues $E_n(\vec{k})$ and the expansion coefficients $C_{ni}(\vec{k})$.

It appears from equation 8 that the mathematical foundation of the LCAO method is the Rayleigh-Ritz variational formalism. In the absence of orthogonality between the basis functions, as is the case

here, the overlap matrix elements, $S_{ij}(\vec{k})$, appear explicitly.

To construct the potential $V_\sigma(\vec{r})$ one needs the charge density $\rho(\vec{r})$ which is generally obtained only when the correct wave functions of the occupied states of the system are known. For this reason, the most recent applications of the LCAO method involved an iterative procedure. The reader is referred to Wang and Callaway[45] for details on the iterations. A second major problem in energy band theory, besides finding a method of solution to equation 1, is the choice of an effective potential as we shall discuss in the following section.

B. The RSK Local Density Functional Potential

The Slater exchange potential, proportional to the 1/3 power of the charge density, is a well known example of an effective, local and single particle exchange potential. Hohenberg and Kohn[41] proved that the ground state energy of a many electron system is a unique functional of its ground state charge density. Based on this theorem, Kohn and Sham[39] and Sham and Kohn[40] derived the equations describing real systems like metals. This led to the constructions of various exchange-correlation potentials, referred to as density functional potentials, which differ in their estimations of the unknown exact exchange-correlation contribution to the unique functional. One of the most used form is due to Von-Barth and Hedin (VBH)[42], a more soundly based version of which has been presented by Rajagopal, Singhal and Kimball (RSK)[46]. This RSK potential has been fitted to the VBH functional forms, but possesses slightly different parameters.

The exchange or exchange-correlation potentials to be discussed depend on the spin, σ. This leads to a splitting of equation 1 into two, one for each spin. For ferromagnetic systems this leads to differences between eigenvalues $E_{n+}(\vec{k})$ and $E_{n-}(\vec{k})$, i.e., the exchange splittings.

Following Von Barth and Hedin, the exchange-correlation potential is written:

$$V_{xc\sigma}(\vec{r}) = \frac{\partial}{\partial \rho_\sigma(\vec{r})} \left[\rho(\vec{r})\, e_{xc}(\rho_+(\vec{r}),\, \rho_-(\vec{r}))\right] \tag{11}$$

where

$$\rho(\vec{r}) = \rho_+(\vec{r}) + \rho_-(\vec{r}),\; e_{xc}(\rho_+(\vec{r}),\rho_-(\vec{r})) = e_x + e_c \tag{12}$$

with

$$e_x = -3\,\left(\frac{3}{4\pi}\right)^{1/3}\,\left(\frac{\rho_+(\vec{r})^{4/3} + \rho_-(\vec{r})^{3/4}}{\rho(\vec{r})}\right)\,,$$

$$e_c == \varepsilon_c^p + (\varepsilon_c^f - \varepsilon_c^f)\, f(x). \tag{13}$$

For

$$x_+ = \frac{\rho_+(\vec{r})}{\rho(\vec{r})}\,, \quad x_- = \frac{\rho_-(\vec{r})}{\rho(\vec{r})} \tag{14}$$

and $a_0 = 2^{-1/3}$ one has

$$f(x) = \frac{1}{1-a_0}\,(x_+^{4/3} + x_-^{4/3} - a_0) \tag{15}$$

The quantities ε_c^f and ε_c^f are expressed in terms of four constant parameters:

$$c^p = 0.0504,\ r^p = 30,\ c^f = 0.0254,\ r^f = 75 \text{ for VBH} \qquad (16)$$

potential while

$$c^p = 0.04612,\ r^p = 39.7,\ c^f = 0.02628,\ r^f = 70.6 \qquad (17)$$

for RSK potential.

The merits of local density potentials are discussed in several review articles[46,47,48]. In particular, as discussed by Callaway, the VBH type potentials give quite reasonable values of the band widths for metals while a typical Hartree-Fock treatment yields widths which are double that of the experimental ones. The recent work on lithium[49,50] demonstrated that the RSK potential correctly describe the limit behavior of this metal for lattice constant larger than normal. In contrast to some Hartree-Fock results, the energy levels of metallic lithium unambiguously go to the atomic ones for lattice constants larger than about 14 a.u.

As for possible limitation of a local density potential as compared to non-local ones, the very recent study by Wang[51] is a case in point. Wang performed self-consistent band structure calculations for FCC nickel utilizing a non-local density functional potential. This potential comprises a non-local exchange part constructed according to Gunnarson et al.[52] weighted density approximation scheme and a local correlation contribution.[53] The resulting exchange correlation energy per particle, contrary to the case of local approximations, goes to 1/r at large distance. It therefore formally reproduces the correct behavior away from a point charge. However

the results of Wang calculations, as compared to those obtained[54] with the local VBH potential have mixed behaviors. Indeed, while the observed decrease of the exchange splitting from 0.6 eV to 0.4 eV was desired, the somewhat increase obtained for the band width was not.

A generally shared contention at present is that non-local forms of density functional potentials[51,48] have yet to prove themselves to be superior to the local ones in practical applications. Perdew and coworkers[55] obtained some results in that direction for atoms and other systems but the case of metals is not yet resolved.

In a LCAO scheme and using any VBH type potential we shall derive in the next section a formalism for the calculation of the total energy of a metal.

C. Evaluation of the Total Energy of a Metal

Callaway et al.[49,50] recently presented a formalism for the evaluation of the total energy of a metal in the framework of an LCGO band structure calculation. After expressing the kinetic energy in terms of eigenvalues $E_{n\sigma}(\vec{k})$ one can write the total energy of a solid as:

$$N E_T = \sum_{n\sigma} E_{n\sigma}(\vec{k}) - \int \frac{\rho(\vec{r})\,\rho(\vec{r}')}{|\vec{r}-\vec{r}'|}\, d^3r d^3r' + \sum_{\substack{\mu\nu \\ \mu\neq\nu}} \frac{Z_\mu Z_\nu}{|\vec{R}_\mu - \vec{R}_\nu|}$$

$$+ E_{xc} - \sum_{\sigma} \int \rho_\sigma(\vec{r})\, V_{xc\sigma}(\vec{r})\, d^3r; \qquad (18)$$

where the sum over n and σ is limited to occupied states. For a single specy system as metallic lithium $Z_\mu = Z_\nu = Z$, the nuclear charge. The explicit exchange-correlation terms in equation 18 are

combined into Δ_{xc} .

$$\Delta_{xc} = - E_{xc} + \sum_{\sigma} \int \rho_{\sigma}(\vec{r})\, V_{xc\sigma}(\vec{r})\, d^3r = \sum_{\sigma} \int \rho_{\sigma}(\vec{r})\, W_{\sigma}(\vec{r})\, d^3r \qquad (19)$$

where

$$W_{\sigma}(\vec{r}) = \rho(\vec{r}) \frac{\partial e_{xc}(\rho_{+}(\vec{r}),\rho_{-}(\vec{r}))}{\partial \rho_{\sigma}(\vec{r})} \qquad (20)$$

It is to be noted that E_{xc} is the exchange correlation contribution to the total energy not Δ_{xc}. A major difficulty overcome by this group is that of evaluating the infinite Coulomb terms. These terms have been rearranged so as to obtain finite quantities U and D by setting

$$U + D = - \int \frac{\rho(\vec{r})\, \rho(\vec{r}')}{|\vec{r} - \vec{r}'|} \, d^3r \, d^3r' + \sum_{\substack{\mu\nu \\ \mu\neq\nu}} \frac{Z_{\mu} Z_{\nu}}{|\vec{R}_{\mu} - \vec{R}_{\nu}|}$$

with

$$U = \sum_{\nu} Z_{\nu} \int \frac{\rho(\vec{r})}{|\vec{r} - \vec{R}_{\nu}|} \, d^3r - \int \frac{\rho(\vec{r})\, \rho(\vec{r}')}{|\vec{r} - \vec{r}'|} \, d^3r \, d^3r' \qquad (21)$$

and

$$D = \sum_{\substack{\mu\nu \\ \mu\neq\nu}} \frac{Z_{\mu} Z_{\nu}}{|\vec{R}_{\mu} - \vec{R}_{\nu}|} - \sum_{\nu} Z_{\nu} \int \frac{\rho(\vec{r})}{|\vec{r} - \vec{R}_{\nu}|} \, d^3r \qquad (22)$$

For reasons to become clear in the following chapter, U and D are evaluated in reciprocal space.

$$U = - \frac{1}{2} \, N \, \Omega \sum_{S} V_T \, (\vec{K}_S)\, \rho_{\rho}(\vec{K}_S) \qquad (23)$$

and

$$D = \frac{1}{2} \; N \; Z \left[\left(-\frac{Z}{\pi} \right) C - V_T(0) - \sum_{s \neq 0} V_e(\vec{K}_s) \right]. \tag{24}$$

In these expressions, restricted to a monotomic system, Ω is the cell volume and the index e denotes the electronic contribution. $V_T(K_s)$ is the Fourier transform of the total Coulomb potential, including the nuclear-nuclear repulsion, and K_s is a reciprocal lattice vector. $V_T(0)$ is described by Callaway[43] and the constant C:

$$C = \left(\frac{8\pi^3}{\Omega} \right) \sum_{s \neq 0} \frac{1}{K_s^2} - \int \frac{1}{q^2} \, d^3q, \tag{25}$$

has been evaluated by Pack et al.[56] for various lattice structures. Following these authors' approach, this constant has been reevaluated to more significant figures in the course of the work on lithium[49]. Boettcher[57] went farther and found, in units of $\frac{2\pi}{a}$:

$$\begin{aligned} C &= -8.913632917586 \quad \text{for simple cubic lattice} \\ C &= -11.432989069675 \quad \text{for body centered cubic} \\ C &= -14.403769009759 \quad \text{for face centered cubic.} \end{aligned} \tag{26}$$

The calculation of Δ_{xc} is basically that of $W_\sigma(\vec{r})$ which, after some algebra, can be written

$$W_\sigma(\vec{r}) = \left(\frac{1}{4} \; \mu_x^p + \nu_c + G \right) (2 \, x_\sigma)^{1/3} + Q - G \tag{27}$$

with

$$Q = \mu_c^p - \varepsilon_c^p - \nu_c,\ G = \frac{a_o}{1-a_o}\left[\mu_c^F - \mu_c^p - \frac{7}{3}\left(\varepsilon_c^F - \varepsilon_c^p\right)\right]$$

The parameters in the expressions of W are as defined in reference 42 and $a_o = 2^{-1/3}$.

The total energy is thus obtained as:

$$N E_T = \sum_{n\sigma} E_{n\sigma}(\vec{k}) + U + D - \Delta_{xc}. \qquad (28)$$

Wang and Callaway[45] implemented the LGCO method of band structure calculation using Slater type or VBH potentials. The resulting program package, BNDPKG, has been extended to evaluate the total energy [49,50]. This program package has been used in the present study of iron, and the following chapter is devoted to the salient features of the computations.

CHAPTER 3

COMPUTATIONAL PROCEDURE

By computational procedure, what is meant here is the set of numerical techniques and details pertaining to the implementation of the formalisms in the preceding chapter. The major steps of the calculation are described, followed in the second section by the discussion of the contractions of basis sets.

A. BNDPKG

In a single particle approximation the band package, BNDPKG, produces the energy bands of a cubic material with one atom per unit cell. The calculations are non-relativistic and at absolute zero temperature. Para- or ferromagnetic orderings are allowed for and the LCGO method is chosen. The angular functions are cubic harmonics. The eigenvalues and wave functions are obtained at as many number of $\vec{k}$ points in $1/48^{th}$ of the first Brillouin zone as desired or economically feasible. Emphasis, in what follows, will be put on general features and new ones pertaining to the evaluation of the total energy. For further details we refer to Wang and Callaway[45] and appendix A where some extended programs are provided.

FCOF is the first program of the package. It employs gaussians orbitals provided by atomic calculations to construct an initial charge density and then generates the fourier coefficients of the various terms in the potential, i.e., the electronic and total Coulomb and exchange-correlation potentials. The innocent looking

matrix elements, $H_{ij}(\vec{k})$, contain three dimensional multi-center integrals. As shown by Lafon and Lin[58], the use of Fourier expansion, i.e.

$$V_\sigma(\vec{r}) = \sum_{\vec{K}_s} V_\sigma(\vec{K}_s) \cos \vec{K}_s \cdot \vec{r}, \tag{29}$$

reduces the difficulties in the evaluation to at most two-center integrals. In the above expressions, the use of the cosine function is justified by the inversion symmetry of the potentials. The resulting two center integrals can be evaluated analytically if gaussian functions are used[59,60,61].

An Ewald split technique is used to remedy a possible slow convergence of Fourier sums due to the screening potential of tightly bound electrons and the contribution of the nuclear terms. The choice of an effective exchange-correlation potential is determined by the input to subroutine VXCRS. Slater or VBH type potentials are currently allowed for. The new version of FCOF produces the Fourier coefficients of $W_\sigma(\vec{r})$ needed for the total energy calculation and contains a new approach to the computation of $V_I(0)$. This quantity has little bearing on the relative position of the energy levels but strongly affects the total energy as can be seen from equations 24 and 28.

Program ESINT evaluates integrals needed in the Hamiltonian and overlaps matrices and BND forms, using properties of the cubic group, the appropriate combinations to generate the matrix elements. In the event where self-consistency is not needed, the diagonalization option in BND is chosen to obtain the energies and wave functions.

We recall that only $\vec{k}$ points in the irreducible wedge ($1/48^{th}$ of the first Brillouin zone) need be considered for cubic crystals. For self-consistency procedure the necessary Fourier transforms of the overlap integrals are generated and properly arranged in the fourth (SIJ) and fifth (INVSIJ) programs respectively.

The iterations toward self consistency are performed in SCF1 and SCF2 for paramagnetic and ferromagnetic calculations respectively. Changes to the Fourier coefficients of the charge density, Coulomb and exchange-correlations potentials, are obtained and added to the appropriate quantities. Self-consistency is assumed to be reached when the Fourier coefficients of the Coulomb potentials from two consecutive iterations differ by no more than 10^{-4} for any $\vec{K}_s$ vector. A judicious choice of the damping parameter FACT (i.e., 0.2 - 0.4) reduces the number of necessary iterations. SCF1 AND SCF2 has been extended to obtain the self-consistent Fourier transforms of W or W_σ respectively. The new version of SCF2 play a key role in the forthcoming discussion of the magnetic properties of iron. Indeed, in the course of the study of metallic lithium[49,50] the total energy of this material was computed using both para- and ferromagnetic inputs. For lattice constants less than 10.5 a.u. the paramagnetic calculations yielded energy bands identical to the up and down spin sub-bands of the ferromagnetic results and the two total energies agreed to over 5 decimal places. On the contrary, for lattice parameters above 10.7 a.u., lithium was found to be ferromagnetic. In this range the total energies for the ferromagnetic calculations were clearly lower than those resulting from the paramagnetic ones[50]. These results did not depend on the

input magnetic moment which was chosen between 0 and 1. Similar results have been obtained for copper. The important point here is that ferromagnetic calculations for iron, at various atomic volumes, are expected to yield a paramagnetic result if indeed iron is paramagnetic at the lattice constants considered.

The self-consistent results are fed into ESINT which outputs are used by BND to calculate the final self-consistent band structure. The last program of the package, DENST, generates the electronic density of states. This program has been extensively modified to evaluate the total energy expression in equation 28.

Bagayoko et al.[62] used BNDPKG to obtain the electronic energies and other quantities for FCC copper at a lattice constant a = 6.80915 a.u. A basis set of 75 gaussian functions[63] has been used and it took 417 CPU minutes (on an IBM 3033) to obtain self-consistent eigenvalues at 505 $\vec{k}$ points of the irreducible wedge. The computations employed a paramagnetic input. Similar calculations with ferromagnetic inputs take about twice as much time. This makes it financially intractable to study BCC and FCC iron, with ferromagnetic inputs, at several lattice constants unless a method is found to significantly reduce the time needed. The contraction of the basis set is one such procedure as is discussed in the next section.

B. Contractions

Despite its advantages, i.e. analytical evaluation of integrals, the use of gaussian ($r^{\ell_i} e^{-\alpha_i r^2}$) basis sets has a drawback. Namely, the size of the Hamiltonian matrix is about twice as much as it would

be with exponential basis functions ($r^{\ell_i} e^{-\alpha_i r}$). Contraction schemes has been developed [63-69] in order to reduce the dimension Nd of the Hamiltonian matrices for atomic and molecular calculations. Two methods generally utilized are the least square fit[66,68] and the formation of linear combinations with fixed coefficients, of single Gaussian type orbital (GTO)[63,65,69]. The basis functions resulting from the latter will be referred to as contracted Gaussian type orbitals (CGTO), not to be confused with Gaussian type orbitals obtained through a scaling of the exponents[70]. Bagayoko[71] presented guidelines for the construction of CGTO suitable for solid state computations. Those are only surveyed here as further details are available in reference 71.

The sets of GTO or CGTO provided for atoms are generally not sufficient for molecular or solid state calculations. A major reason for this is the difference between the electronic distributions in atoms, molecules and solids. While the bond formation characterizes molecules[69], the quasi-free electron behavior distinguish metals from the latters and from atoms. One solution to the above inadequacy of atomic GTO basis is the inclusion of supplementary orbitals[72,73]. In particular the atomic GTO must be supplemented by a 4p orbital in order to correctly reproduce the electronic energy bands of 3d metals around the fermi energy. A specific example is the disappearance of copper fermi surface neck at L, as shown by Bagayoko[73], if a 4p like orbital is not used. Another, relatively minor, modification of the atomic GTO sets is the dropping of the atomic s orbital with the smallest exponent for calculations on 3d metals.

The similarity of the core electronic cloud in atoms, molecules,

and solid supplemented by the fact that the largest number of orbitals, for a given symmetry (s, p, d, or f), contribute to the innermost atomic functions lead to an obvious first rule to follow in forming CGTO. It consists in grouping orbitals with consecutive exponents so that the number of single GTO involved in a CGTO decreases with decreasing exponents as shown in Table 1, relaxing the contraction of the outer orbitals in going from atoms to molecules and solids in that order. To facilitate the forthcoming discussion, this prescription will be referred to as bond or free electron rule for molecules or metals respectively.

The constant factors multiplying each orbital present in a CGTO remain to be specified. The atomic calculations provide 1, 2, and 4 sets of expansion coefficients for the d, p, and s orbitals of copper respectively. In the absence of further exponent optimization in forming the CGTO one employs the atomic coefficients. The question is then the choice of the sets of coefficients to use. Given the exponents pertaining to the s symmetry, one has to choose among the expansion coefficients for the 1s, 2s, 3s, or 4s atomic states to form the CGTO describing the s symmetry functions. Basch et al.[67] found the 1s atomic coefficients to describe all s orbitals far better than do the 3s coefficients. They mentioned a similar result reported by Huzinaga. Their finding has been verified for copper and nickel. This result could be expected, considering that the largest contribution to the total energy for a given symmetry is that belonging to the lowest principal quantum number, i.e., 1s for s, 2p for p, and 3d for d symmetries. This conclusion will be referred to as the lowest n rule. In the following all the CGTO have been

constructed using the 1s, 2p, 3d atomic coefficients for the s, p, and d orbitals.

If one utilizes the atomic coefficients as described above then elementary mathematics shows that grouping together two orbitals with expansion coefficients of different signs and exponents not far apart, is almost equivalent to eliminating them both as far as the charge density is concerned. The sign rule simply consists in avoiding such combinations.

In the Rayleigh-Ritz variational formalism the m^{th} variational eigenvalue, λ_m^{Nd} where Nd is the number of basis functions, tends to the true m^{th} eigenvalue when Nd increases. Therefore, energy levels obtained with CGTO (reduced basis set) will generally not be lower than those generated using single GTO. A consequence of this is the upward shift of the energy levels to be expected when employing CGTO. This may appear as a drawback of the use of CGTO but should be of no effects on relative quantities such as exchange splittings and band widths resulting from solid state calculations.

The program package BNDPKG has been run to produce the non self-consistent energy levels of copper at high symmetry points of the Brillouin zone. The input for subroutine GTO determine the choice of contraction. The criterion for best contraction is the lowering of the energy levels. The above discussion of the limit behavior of variational eigenvalues as Nd increases makes it difficult to compare two contractions employing different numbers of CGTO. The 18 contractions in Table I, all of which involved 32 CGTO, has been used in these test calculations for copper. They are ranked in Table II from the best to the worst. One difficulty in choosing the overall

TABLE I. Contractions,eighteen different contractions (Nd = 32) used in the non self-consistent band calculations. The GTO utilized are those provided by Wachters. For a given symmetry the orbitals are numbered in the order of decreasing exponents.

Contrac-tions	S orbitals	P orbitals	D orbitals
1	(1,2,3,4,5,6) (7,8) (9) (10) (11) (12) (13)	(1,2,3,4,5,6) (7) (8) (9) (10)	(1,2,3,4) (5)
2	(1,2,3,4,5,6,7) (8) (9) (10) (11) (12) (13)	(1,2,3,4,5,6) (7) (8) (9) (10)	(1,2,3,4) (5)
3	" " " "	" " "	(1,2,3) (4,5)
4	(1,2,3,4,5,6) (7) (8,9) (10) (11) (12) (13)	" " "	" "
5	(1,2,3,4,5,6) (7) (8) (9,10) (11) (12) (13)	" " "	" "
6	(1,2,3,4,5,6) (7,8) (9) (10) (11) (12) (13)	(1,2,3,4,5) (6,7) (8) (9) (10)	(1,2) (3,4,5)
7	" " " "	(1,2,3) (4,5) (6,7) (8,9) (10)	(1,2,3,4) (5)
8	" " " "	(1,2,3) (4,5) (6,7) (8) (9,10)	(1,2,3) (4,5)
9	" " " "	(1,2,3,4,5) (6,7) (8) (8) (10)	" "
10	" " " "	(1,2,3,4,5) (6) (7) (8,9) (10)	(1,2,3,4) (5)
11	" " " "	(1,2,3,4,5) (6) (7,8) (9) (10)	(1,2,3) (4,5)
12	" " " "	(1,2,3,4) (5,6) (7) (8,9) (10)	(1,2,3) (4,5)
13	" " " "	(1,2,3,4,5) (6) (7) (8,9) (10)	(1,2) (3,4,5)
14	" " " "	" " "	(1,2,3) (4,5)
15	" " " "	" " "	(1) (2,3,4,5)
16	" " " "	(1,2,3) (4,5) (6,7) (8,9) (10)	(1,2,3) (4,5)
17	" " " "	" " "	(1,2) (3,4,5)
18	" " " "	" " "	(1) (2,3,4,5)

TABLE II. Comparison of different contractions. The contractions are those in table I and are ranked from best to worst. The best is the one giving the lowest eigenvalues. The rankings change with symmetry points.

States		Contraction Numbers	Δ max = max $(\lambda_m^w - \lambda_m^b)$
Core	S	1,4,5,2,3,8,9,6,11,10,14,12,13,15,7,16,17,18	+3.053 Ryd
	P	1,7,10,8,9,11,12,14,16,6,13,15,17,18,2,3,4,5	+1.035
Valence Bands	Γ	1,2,7,10,6,13,17,8,9,11,12,14,16,15,18,4,5,3	+0.011
	L	1,2,3,4,6,8,9,5,11,7,10,13,17,16,14,15,18,12	+0.166
	K	1,2,3,4,5,6,8,9,11,10,7,12,14,13,15,16,17,18	+0.120
	X	1,2,3,4,5,8,9,6,11,10,7,12,14,16,13,17,15,18	+0.111
	W	1,2,3,4,5,6,8,11,9,10,12,13,14,15,7,16,17,18	+0.122
Higher Bands		2,3,1,4,5,9,11,10,14,12,6,13,8,7,16,17,15,18	

best contraction is the change of the ranking from one state to another. One refers to the system specificities in order to make a choice. The electrical, thermal and optical properties of a metal being primarily determined by the valence and higher bands these levels will be considered the most important for copper. Let λ_m^b and λ_m^w designate the m^{th} eigenvalues obtained with the best and worst contractions, respectively. At the Γ point there exists 6 eigenvalues corresponding
to the valence states (degeneracy included) of copper. The quantity

$$\Delta_{max} = \max\ (\lambda_m^w - \lambda_m^b), \tag{30}$$

where m takes 6 different values, has been used to compare the contractions. The values of Δ_{max} in column 3 of Table II refer to the comparison of the best and worst contractions which are respectively the 1st and last ones as they appear in a row of Table II.

The detailed discussion of the contents of Table I and II is available in reference 71. With the knowledge that the twelfth 1s and the eight 2p orbitals have negative expansion coefficients the verification of the guidelines set above become apparent from these tables. Contractions 1-2 and to some extent 3-4, are the best for valence and higher bands while 15-18 are the worst for the same states. The best ones follow the guidelines best while the worst ones violate one or more of the rules. Interestingly, except for the deletion of the s tail and the inclusion of a tenth p orbital, contraction 14 corresponds to the best obtained by Wachters[63] for

atomic copper. Contractions 1, 2, 3, and 4 are in this order, except at Γ, for the valence states. This means, Δ_{max} being relatively small at Γ, that either one is expected to give good results.

The best contraction in Table II (contraction 1) has been chosen to perform self-consistent band structure calculations for FCC copper. At the exception of the contraction of the basis set every other parameter entering these computations has been kept as it was in the work of Bagayoko et al.[62] where 75 GTO have constituted the basis set. Let λ^{32}_m and λ^{75}_m be the m^{th} eigenvalues, beginning with the 1s state, resulting from the former and latter calculations. A detailed comparison of the valence bands for the high symmetry points, show:

$$\lambda^{75}_m < \lambda^{32}_m \ , \ E^{75}_F < E^{32}_F$$

and

$$\lambda^{75}_m - E^{75}_F = \lambda^{32}_m - E^{32}_F \pm 0.0025 \text{ Ry}, \qquad (31)$$

In the above expressions the Fermi energies E^{75}_F and E^{32}_F as well as λ^{75}_m and λ^{32}_m are negative quantities. This relation therefore shows that while the λ^{32}_m has been shifted upward as compared to the corresponding λ^{75}_m, relative quantities like the occupied band widths have practically not been changed. This is the rigid upward shift (0.0142 Ry), due to the use of small basis set expected on variational grounds. The shift is illustrated by figure

Figure 2. Density of states N(E) for paramagnetic FCC copper , in states/atom per Rydberg ,obtained using bases of 75 and 32 GTO and CGTO respectively. The rigid upward shift of the bands for Nd = 32 is seen in the shift to the right of the Fermi level and the peaks in the density of states curve . a = 6.80915 a.u.

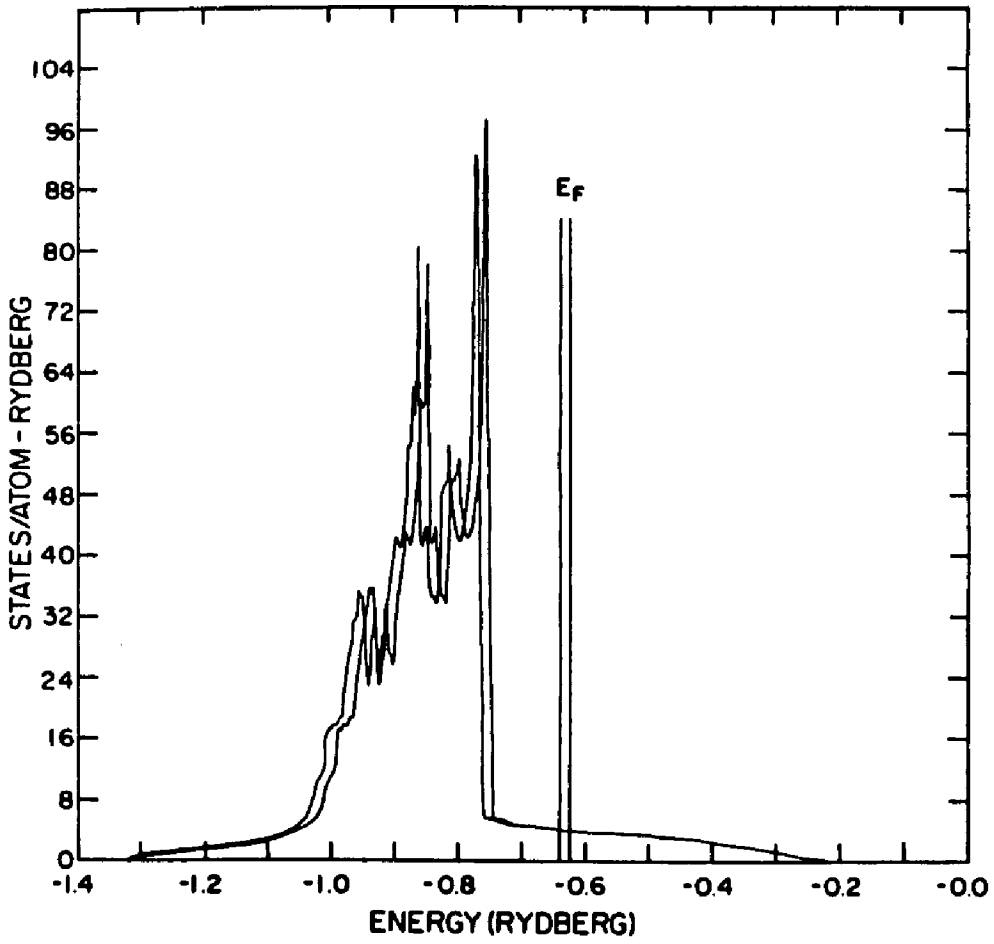

2 where the density of states resulting from both calculations are shown.

Another test of the guidelines for contraction is provided by the total energy calculation results[71]. Not only a minimum is obtained in the total energy curve, but also it occurs around a lattice constant of 6.80915 a.u. which is almost identical to the experimental value[6] for the equilibrium spacing at absolute zero. The above results on a 3d metal like copper leave no doubt about the adequacy of the above contraction procedure for the study of other 3d materials or lighter ones. The self-consistent calculations with 32 CGTO and 75 single GTO have been performed on an IBM 3033. The total CPU time required for the former was 6.8 times smaller than that (417 minutes) needed for the latter. This is the significant reduction of CPU time we were aiming for. Other miscellaneous benefits of this procedure are described in reference 71. In particular we have explicitly shown the inadequacy of some contractions for atoms and molecules in solid state calculations. BNDPKG has been used with a contraction option, following the above guidelines, to extensively study iron at 0°K. The results of those calculations are presented in the next chapter.

CHAPTER 4

ELECTRONIC STRUCTURES OF BCC AND FCC IRON

The new version of the band package, BNDPKG, has been used in this work. We employed the RSK local density potential. Choosing the contraction option of BNKPKG we constructed 8s,5p, and 4d CGTO according to the guidelines set forth in the preceding chapter. The atomic GTO entering the CGTO were those provided by Wachters[63]. Only ferromagnetic inputs were considered and the ab-initio self-consistent band energies have been produced at 505 and 506 $\vec{k}$ points of the respective irreducible wedges of the FCC and BCC structures. The input configurations, for both structures, were $3d^7 4s^1$. These calculations have been carried out for several values of the atomic volume. The electronic structure of BCC iron at a = 5.4057 a.u. will be discussed in section A, followed by the studies of the variations of the bands with atomic volume for BCC and FCC lattices in sections B and C. The last section is devoted to the charge and spin form factors.

A. BCC Iron, a = 5.4057 a.u.

As previously stated most of the previous calculations for BCC iron at normal lattice constant (i.e., a = 5.4057 a.u., R_S = 2.6616 a.u.) are listed in the aforementioned references [1-6]. A comparison of our results to those of Callaway and Wang[2] is particularly meaningful as the differences between the two works reside in our use of 43 CGTO and the RSK potential instead of 75 GTO and the VBH

potential. The present calculations basically reproduced the results of Callaway and Wang. The present eigenenergies are rigidly shifted upwards as expected on variational grounds. However, in this case, contrary to the work on copper described in Chapter 3, the shift is primarily due to the use of a different method of evaluating $V_T(0)$. This Fourier coeffficient of the Coulomb potential, as previously stated, does not affect the relative position of the bands. The algebraic values of the differences between the present and previous $V_T(0)$ and Fermi energies (E_F) are respectively 0.4376 and 0.4402 Ry. On the scales of the graphs in reference 2, the band structures these authors obtained are indistinguishable from ours if the Fermi levels are superposed. Tables III and IV contain major quantities describing these bands.

The magnetic moment, 2.15 μ_B, is 0.01 μ_B less than the value they found. The up spin d band width at p is 2.5 eV, 0.1 eV less than their result. The exchange spliting at P_4, 1.31 eV, is 0.03 smaller than the previous value[2]. We found charge and spin form factors almost identical to those obtained by Callaway and Wang. The analysis by Van Laar et al.[74] therefore shows than the spherical parts of both spin form factors are in accord with experiment. The above agreements between our results and previous theoretical as well as experimental ones justify the application of a contracted basis set to the study of iron at several atomic volumes. The slight reductions in the magnetic moment and the exchange splitting seem to indicate a somewhat stronger correlation effect in the RSK potential as compared to the VBH. Further discussion of the electronic structure of iron at normal lattice constant is presented in

conjunction with that of the variations of the bands with the lattice parameter.

Table III. Representative band widths (W) and exchange splittings (δE_{ex}) for BCC iron-in Rydbergs (Ry) - for various atomic radii (R_s), lattice constants (a) in a.u. Up or down spin is indicated by ↑ or ↓, respectively.

R_s a.u.	a a.u.	$W_{sp\downarrow}$ $(H_{15\downarrow}-\Gamma_{1\downarrow})$ (Ry)	$w_d^{p\uparrow}$ $(P_{3\uparrow}-P_{4\uparrow})$ (Ry)	$w_d^{p\downarrow}$ $(P_{3\downarrow}-P_{4\downarrow})$ (Ry)	$w_{d(\uparrow\downarrow)}^{p}$ $(P_{3\downarrow}-P_{4\uparrow})$ (Ry)	$\delta E_{ex}(\Gamma_1)$ (Ry)	$\delta E_{ex}(N_1)$ (Ry)	$\delta E_{ex}(P_4)$ (Ry)	$\delta E_{ex}(P_3)$ (Ry)
2.4619	5.0	1.5533	0.2579	0.3262	0.4017	0.0176	0.0691	0.0755	0.1438
2.5603	5.2	1.4326	0.2165	0.2913	0.3798	0.0159	0.0794	0.0885	0.1632
2.6616	5.4057	1.3211	0.1822	0.2579	0.3540	0.0150	0.0855	0.0961	0.1718
2.7573	5.6	1.2269	0.1557	0.2310	0.3349	0.0147	0.0916	0.1039	0.1793
2.9542	6.0	1.0626	0.1114	0.1857	0.3094	0.0157	0.1079	0.1237	0.1980
3.4466	7.0	0.7742	0.0425	0.1141	0.2758	0.0212	0.1417	0.1617	0.2332
4.4313	9.0	0.3808	0.0062	0.0617	0.2792	0.0533	0.1881	0.2176	0.2534

Table IV. Representative band widths (W) and exchange splittings (δE_{ex}) for BCC-iron - in Rydbergs (Ry) - for various atomic radii (R_s) or lattice constants (a). W_d^{occ} is the occupied d band width. Up or down spin is indicated by ↑ or ↓, respectively.

R_s (a.u.)	a (a.u.)	W_d^{occ} (Ry)	$W_d^{H\uparrow}$ $(H_{12\uparrow}-H_{25'\uparrow})$ (Ry)	$W_d^{H\downarrow}$ $(H_{12\downarrow}-H_{25'\downarrow})$ (Ry)	$\delta E_{ex}(H_{12})$ (Ry)	$\delta E_{ex}(H_{25'})$ (Ry)
2.4619	5.0	0.4602	0.5003	0.5287	0.0900	0.1183
2.5603	5.2	0.4031	0.4159	0.4498	0.1054	0.1393
2.6616	5.4057	0.3507	0.3435	0.3764	0.1169	0.1499
2.7573	5.6	0.3091	0.2844	0.3151	0.1292	0.1599
2.9542	6.0	0.2732	0.1838	0.2061	0.1612	0.1835
3.4466	7.0	0.2421	0.0546	0.0419	0.2243	0.2116
4.4313	9.0	0.2266	0.0002	0.0496	0.2729	0.2235

B. Volume Dependence of BCC Iron Band Structure

The up and down spin sub-bands of BCC iron at a = 5.2 a.u. in Figures 3 and 4 are shown to facilitate the forthcoming discussion. Figure 5 shows the total density of states. Fundamental parameters describing the bands, widths and exchange splittings, are provided in Tables III and IV.

Appendix B contains the valence state energy levels, at high symmetry points, for a = 5.2, 5.4057, and 5.6 a.u. The band widths decrease with increasing lattice constant and more up or down spin bands are respectively filled or emptied. These patterns can be described in terms of a competition between the kinetic and the exchange energies which get respectively smaller and larger in magnitude as the lattice constant increases.

One drastic change in the band structure of ferromagnetic BCC iron occurs at the N point. For a = 5.2 a.u., Fig. 3, the upper G_4 and lower D_3 branches are connected to N_1' which lies below N_3 where G_2 and the upper D_3 meet for the up spin sub-bands. In the down spin case, Fig. 4, G_2 and the upper D_3 meet at N_3 which lies above N_4 where the upper G_4 and D_2 are branching off. For the minority sub-bands this picture remains the same up to a = 7.0 a.u. where the upper N_1, N_4, and N_3 are in that order of increasing energy but are almost degenerate ($E(N_4) - E(N_1) = 6.9$ mRy; $E(N_3) - E(N_4) = 5.6$ mRy). For the majority spin sub-bands N_1' and N_3 become degenerate around a = 5.4057 (see Fig. 1 of Callaway and Wang[2], RS = 2.6616). This degeneracy no longer exists at a = 5.6 a.u. and above and the G_2 branch is connected to D_3 at N_3 which has moved below N_1' where the upper G_4 and D_3 meet.

Figure 3. Energy bands in ferromagnetic BCC iron along some lines of high symmetry for the majority or up spin. Energies are in Rydberg(Ry). The lattice constant is a = 5.2 a.u.

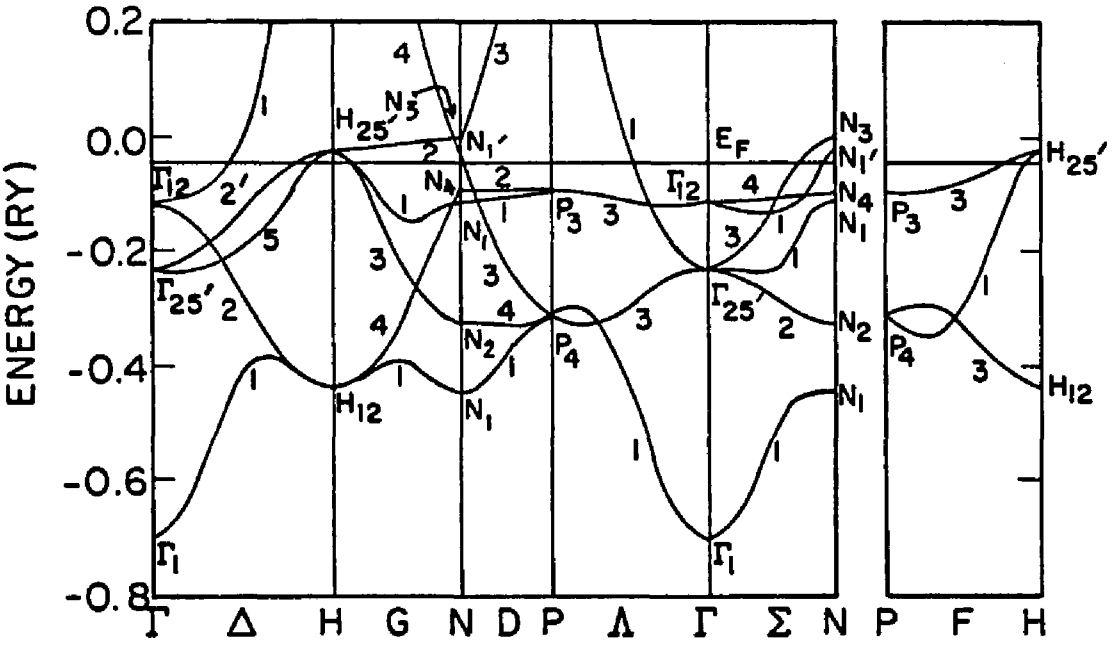

Figure 4. Energy bands in ferromagnetic BCC iron along some lines of high symmetry for the minority or down spin. Energies are in Rydberg(Ry). The lattice constant is a = 5.2 a.u.

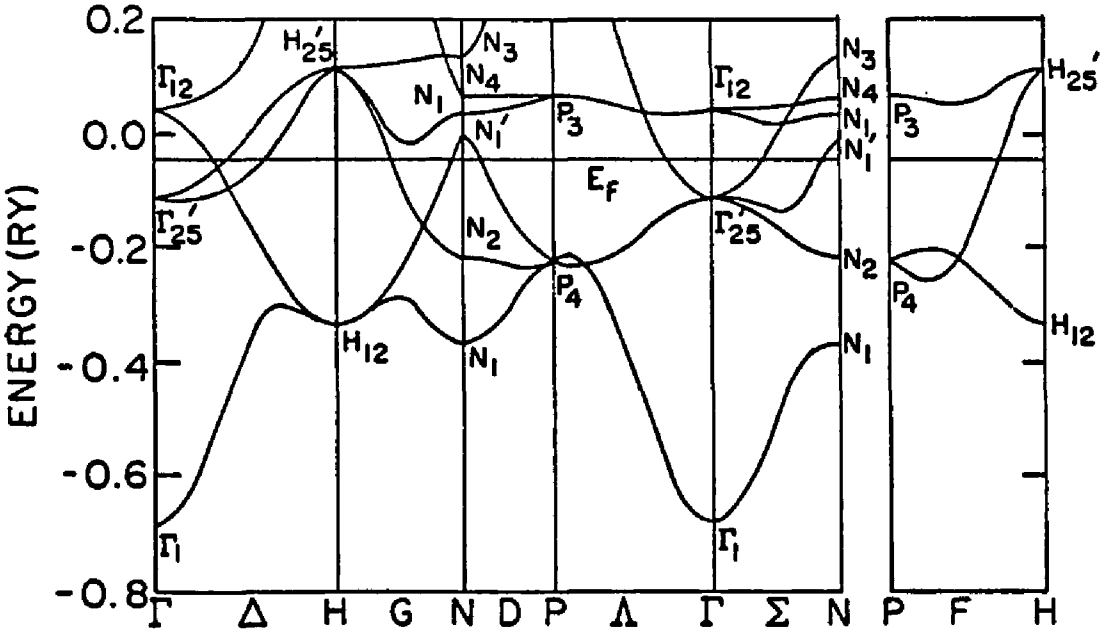

Figure 5. Total density of states N(E),in states/atom per Rydberg, and the valence electron number for ferromagnetic BCC iron. The lattice constant is a = 5.2 a.u.

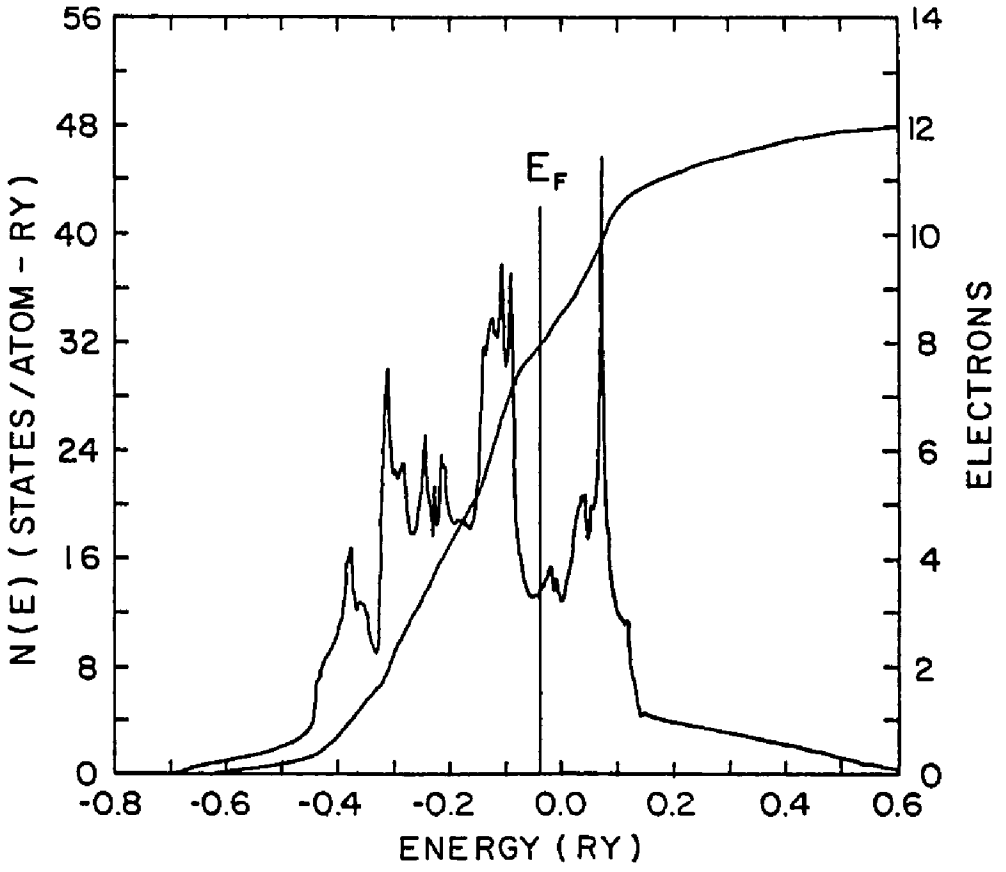

The passage of the N_3 representation below N_1' in the majority spin sub-band is a direct consequence of the above mentioned competitions between kinetic and exchange energies. The d states (N_3) are far more sensitive to the exchange effect than are the P ones (N_1'). When the lattice constant increases so does the exchange effect and N_3, for the up spin sub-bands, passes below (N_1'). There follows a change of connections to avoid the crossing of bands of the same symmetry, i.e., the upper and lower D_3.

A second major change in the structure of the d bands is observed at a value of the lattice constant around 9 a.u. Figure 6 shows the up and down spin sub-bands for this lattice parameter at which the crystal field splitting is larger than the overlap effects; t_{2g} and e_g sub-bands are consequently split. It is apparent from figure 6 that the exchange splitting of the d bands is then much larger than sub-band widths. In other words, the crystal field splitting is larger than the overlap effect and t_{2g} and e_g sub-bands are consequently split.

The values of the exchange splittings and band widths in Table III and IV, deserve comments. Callaway and Wang[2] reported a rather large difference between the splittings at P_4 and P_3. This result has been reproduced here for a = 5.4057 as discussed in Section A of this chapter. One further observes, from Table III, that the increase of lattice constant is accompanied by a decrease of the ratio of the splitting at P_3 to that at P_4. For a = 5.2 a.u. this ratio is about 2; it tends to 1 as the lattice spacing increases because both splitting approach the same value which is that for the atoms. While the total d band width at P, $W^P_{d(\uparrow\uparrow)}$ approaches that same atomic splitting, the widths for up and down spin sub-band go to zero. A known measure of the

Figure 6. Up (full) and down (dashed) spin energy bands of BCC iron at a lattice constant of 9.0 a.u. The following representations are in the order of increasing energy for both sub-bands: $\Gamma_{25'}$, Γ_{12}; $H_{25'}$, H_{12}; P_4, P_3.

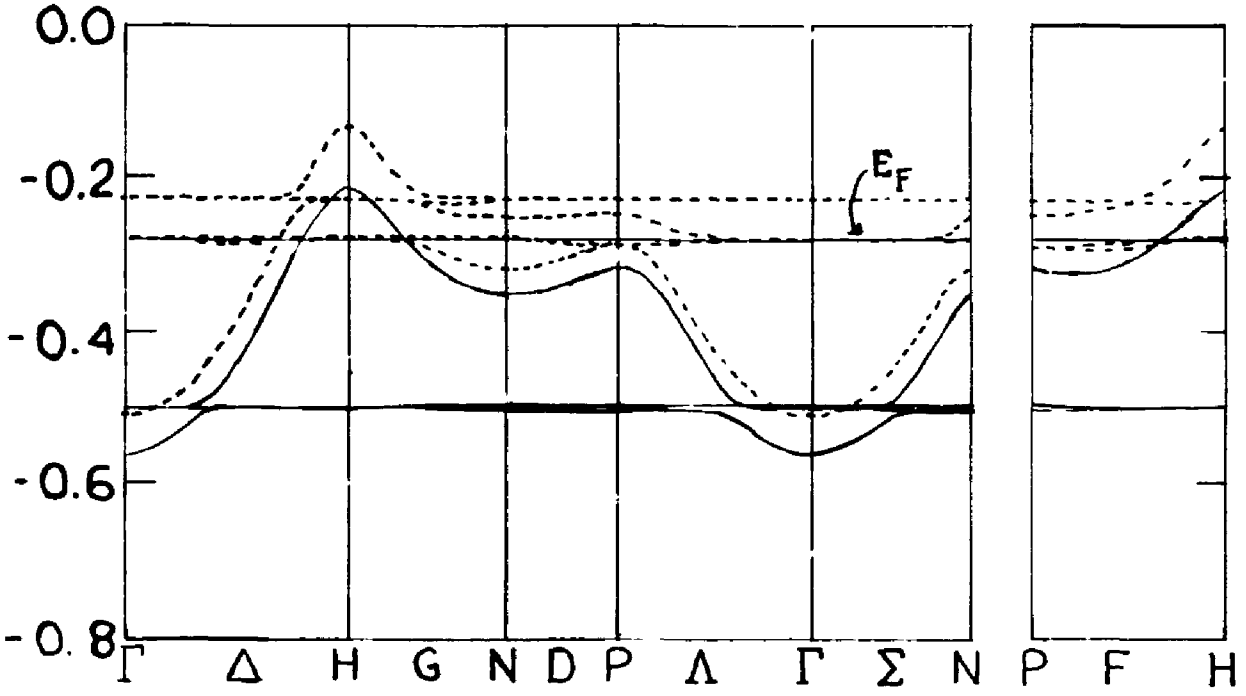

hopping time for an electron occupying a given band is h/w where h is the Plank constant and W is the band width. The smaller W, the more time the electron will spend on a given site. The relatively small d band widths as compared to the sp band widths is a result of the relative localization of the d electrons as compared to sp electrons.

A major characteristic of the BCC band structure of iron is the quasi-flatness of the D_1, D_2, upper Λ_3 and Σ_4 branches at lattice parameters equal or greater than 4.8 a.u. To this flat portion in the band corresponds a sharp peak in the density of state curve as shown in Fig. 5. These branches do not participate to the fermi surface. They therefore seem to possess a highly localized character as we shall discuss in connection with the study of the magnetic properties.

C. Electronic Structure of FCC Iron

The band structures of FCC iron at a = 6.5516 and 7.0 a.u. are shown in Figs. 7 through 10. Tables V and VI contain representative band widths and exchange splittings which describe variations of the bands with atomic volume. The valence band energies, at high symmetry points, can be found in Appendix B for the above lattice constants and a = 6.8107 a.u.

Drastic changes in the FCC band structure occur at the L point. In the majority spin sub-band L_3 and L_2' are quasi degenerate [75] for a = 6.8107 a.u. (R_s = 2.6616); for smaller R_s values, L_2' lies below L_3 and the branchings are as in Fig. 7 (a = 6.5516 a.u.) while for larger ones L_2' lies above L_3 and the branchings are as in Fig. 9 (a = 7.0 a.u.). A somewhat similar branch switching is described above for BCC iron.

Figure 7. Energy bands in ferromagnetic FCC iron along some lines of high symmetry for the majority or up spin. Energies are in Rydberg(Ry). The lattice constant is 6.5516 a.u.

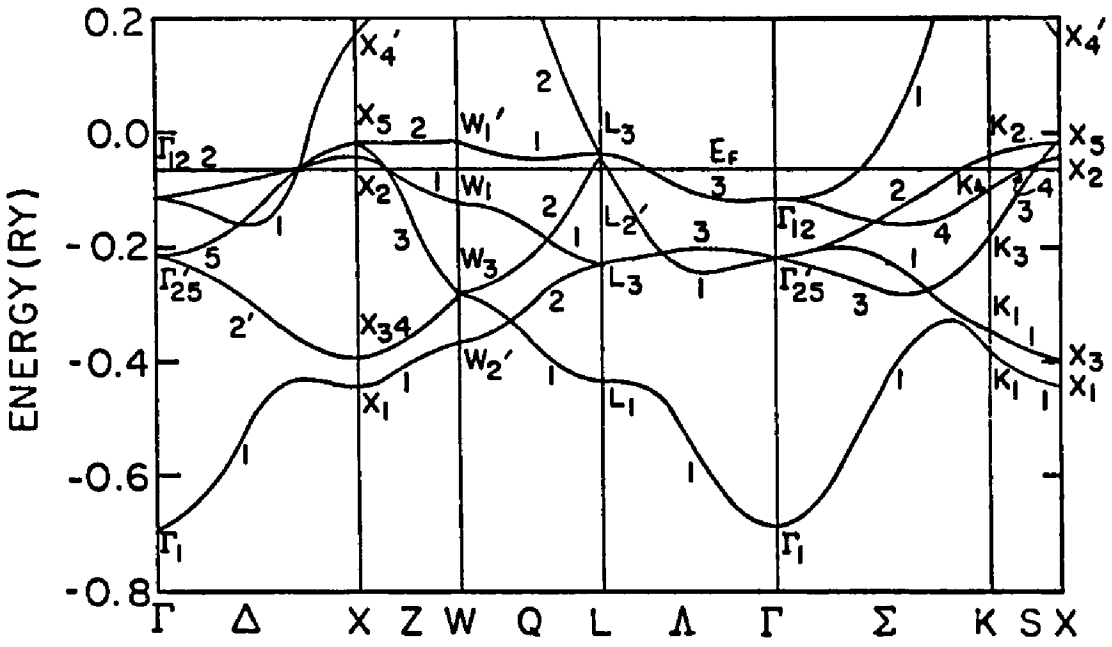

Figure 8. Energy bands in ferromagnetic FCC iron along some lines of high symmetry for the minority spin. Energies are in Rydberg(Ry). The lattice constant is 6.5516 a.u

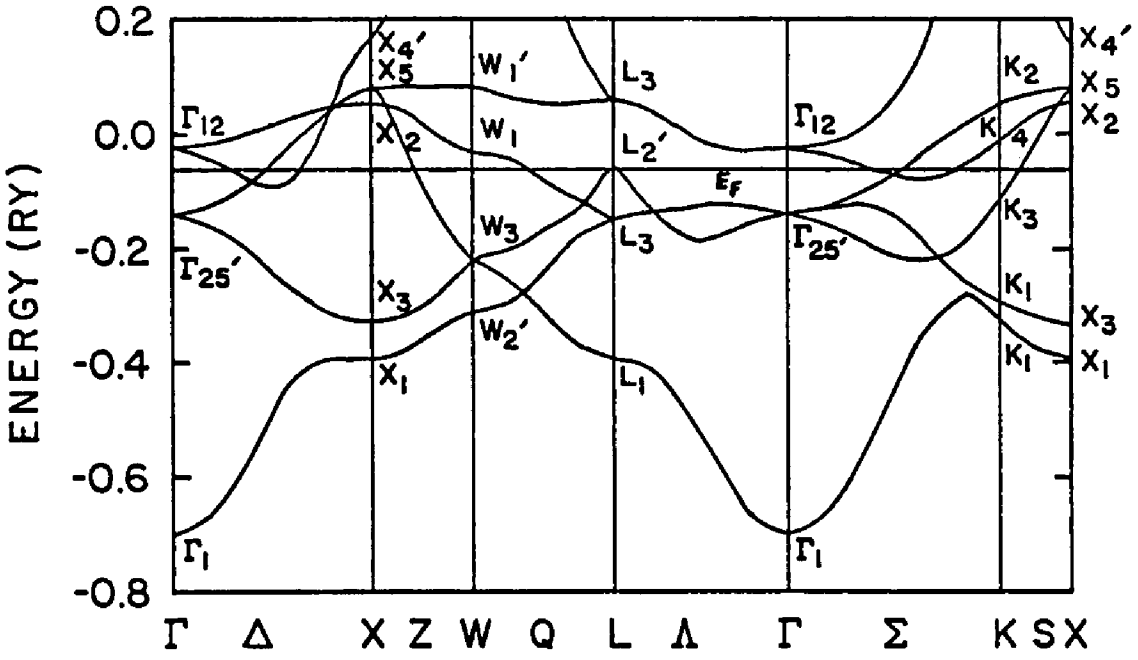

Figure 9. Energy bands in ferromagnetic FCC iron along some lines of high symmetry for the majority or up spin. Energies are in Rydberg(Ry). The lattice constant is 7.0 a.u.

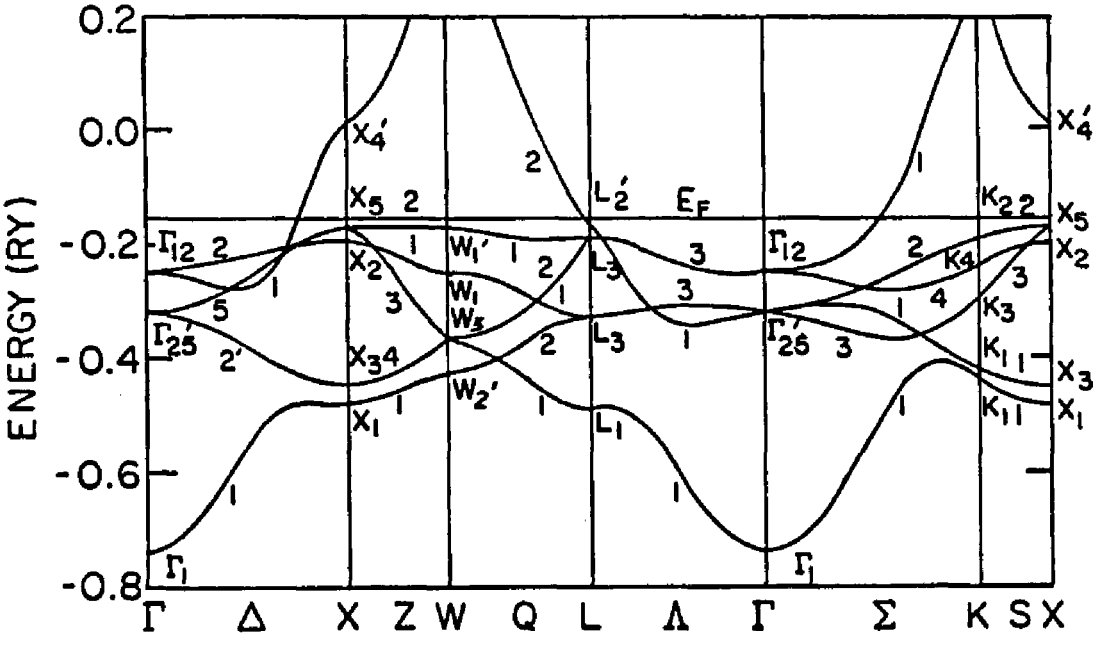

Figure 10. Energy bands in ferromagnetic FCC iron along some lines of high symmetry for the minority spin. Energies are in Rydberg(Ry). The lattice constant is 7.0 a.u

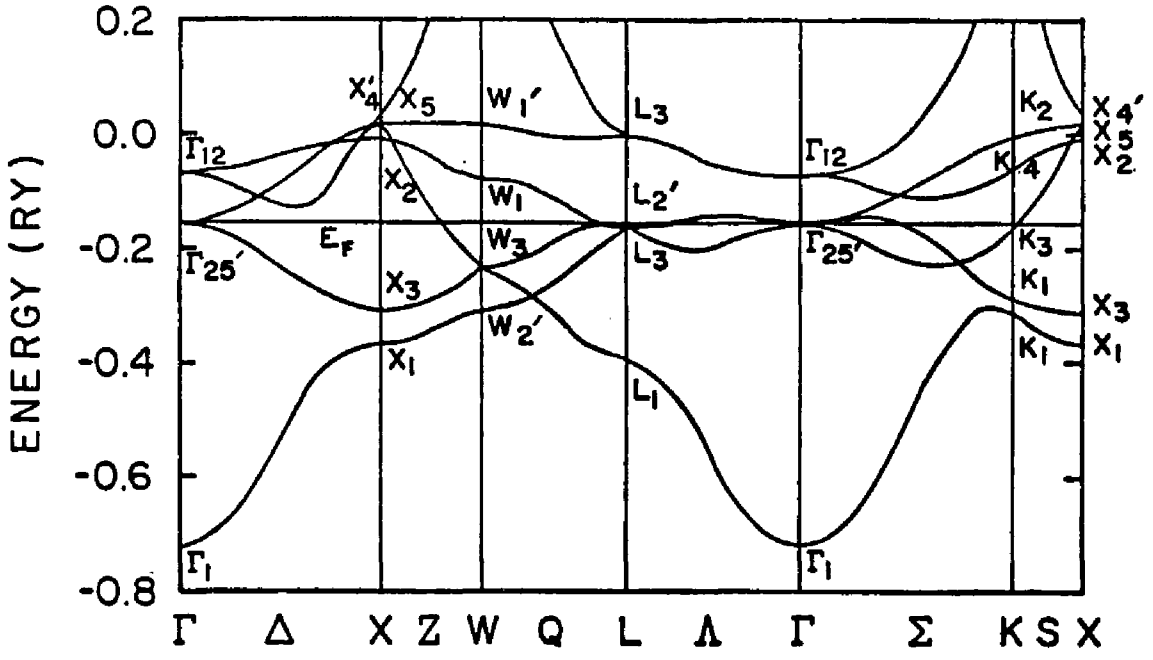

Table V. Representative band widths (W) and exchange splittings (δE_{ex}) for FCC iron - in Rydbergs (Ry) - for various atomic radii (R_s) or lattice constants (a) in a.u. Up or down spin is indicated by ↑ or ↓, respectively.

R_s (a.u.)	a (a.u.)	$W_{sp\downarrow}$ $(X_{4',\downarrow}-\Gamma_{1\downarrow})$ (Ry)	$W_d^{x\uparrow}$ $(X_{2\uparrow}-X_{3\uparrow})$ (Ry)	$W_d^{x\downarrow}$ $(X_{2\downarrow}-X_{3\downarrow})$ (Ry)	$W_{d(\uparrow\downarrow)}$ $(X_{2\downarrow}-X_{3\uparrow})$ (Ry)	$\delta E_{ex}(X_3)$ (Ry)	$\delta E_{ex}(X_2)$ (Ry)	$\delta E_{ex}(\Gamma_{25'})$ (Ry)	$\delta E_{ex}(\Gamma_{12})$ (Ry)
2.1125	5.4057	1.3111	0.8316	0.8537	0.8631	0.0094	0.0314	0.0224	0.0266
2.1885	5.6	1.2158	0.7164	0.7410	0.7552	0.0141	0.0388	0.0286	0.0338
2.3448	6.0	1.0479	0.5302	0.5603	0.5886	0.0283	0.0584	0.0449	0.0530
2.5603	6.5516	0.8695	0.3532	0.3928	0.4508	0.0580	0.0976	0.0771	0.0918
2.6616	6.8107	0.8026	0.2927	0.3365	0.4184	0.0818	0.1257	0.1020	0.1195
2.7356	7.0	0.7602	0.2544	0.3080	0.4443	0.1362	0.1899	0.1639	0.1814
3.5172	9.0	0.4698	0.0365	0.0503	0.2680	0.2177	0.2315	0.2221	0.2278

Table VI. Representative band width (W_d) and exchange splittings (δE_{ex}) for FCC iron - in Rydbergs (Ry) - for various atomic radii (R_s) or lattice constants (a) in a.u.. W_d^{occ} is the occupied d band width. Up or down spin is indicated by ↑ or ↓, respectively.

R_s (a.u.)	a (a.u.)	W_d^{occ} (Ry)	$W_d^{x\uparrow}$ $(X_{5\uparrow}-X_{1\downarrow})$ (Ry)	$W_d^{x\downarrow}$ $(X_{5\downarrow}-X_{1\downarrow})$ (Ry)	$\delta E_{ex}^{(L_3)}$ Lowest	$\delta E_{ex}^{(L_3)}$ Highest
2.1125	5.4057	0.7745	0.9629	1.0053	0.0181	0.0345
2.1885	5.6	0.6734	0.3353	0.8799	0.0246	0.0415
2.3448	6.0	0.5205	0.6283	0.6749	0.0426	0.0596
2.5603	6.5516	0.3828	0.4305	0.4776	0.0782	0.0952
2.6616	6.8107	0.3361	0.3623	0.4109	0.1047	0.1218
2.7356	7.0	0.3376	0.3146	0.3887	0.1639	0.1887
3.5172	9.0	0.2620	0.0636	0.1001	0.2237	0.2310

In both cases the representation reordering occurs around R_s = 2.6616 a.u. and is limited to the majority sub-bands.

For lattice parameters less than 6.5516 a.u. the exchange splittings of the two uppermost d bands (Λ_3 branches included), almost constant in the zone, double for 0.5 a.u. increase while for values above 7.0 a.u. the splittings change by less than 10% for such increase. At a = 6.5515 a.u. the ratio of the splitting to the width for these bands are around 1/3 while their values are slightly less or greater than one for the lower and upper (as at W) ones at a = 7.0 a.u. If one limits consideration to the W-L- Γ branches of thes bands one still finds the ratio less than one for both bands at a = 6.5516 a.u. while it is greater than one for both at a = 7.0 a.u. The above points are particularly meaningful for the up spin sub-bands. The two uppermost d bands for the minority spin are either empty or clearly participate to the Fermi surface. However, for lattice spacings equal to or greater than 7.0 a.u. these bands are fully occupied for the majority spin. The above discussion, the first of its kind on the details of the band structures of iron will be of importance in the understanding of the magnetic properties of this metal. Some by products of these band structure calculations, using BNKPKG, are the charge and spin form factors. We shall discuss these in the next section.

D. BCC and FCC Iron Form Factors

The x-rays and neutron scattering form factors are gauge of the quality of the wave functions resulting from calculations as the present. This is so because these quantities, also respectively

referred to as charge (f_c) and spin (f_s) form factors, are directly related to the Fourier transform of the charge density:

$$f_c(k, \ell,m) = \rho(k,\ell,m) \cdot \Omega$$

and

$$f_s(k, \ell,m) = \frac{\rho_+(k,\ell,m) - \rho_-(k,\ell,m)}{\rho_+(0,0,0) - \rho_-(0,0,0)} \qquad (32)$$

In these expressions Ω is the cell volume and $\rho(k,\ell,m)$ stands for the Fourier transforms of the charge density with k, ℓ, m designating the x, y, and z components of the reciprocal lattice vectors in units of $2\pi/a$. Charge and spin form factors of BCC iron are in Tables VII through IX for a = 5.0, 5.4057, and 6.0 while those of FCC iron are in Tables X through XII for a = 6.5516, 6.8107. 7.0 a.u. It is to be recalled that Van Laar and coworkers[74] have established that the spin form factors for BCC iron for a = 5.4057, which are the same as those provided by Callaway and Wang[2], agree with experiment. The content of Table X-XII constitutes the first, at the author's knowledge, published form factors for FCC iron.

These data are provided for three different lattice parameters in order to allow much better comparison with experiment. Indeed, several tests have revealed that over a range of 1 a.u., the form factors can be fitted to a polynomial in a (lattice constant) of degree two for a given $\vec{K}_s$ vector:

$$f_c(k, \ell,m) = a^c_{0,k\ell m} + a^c_{1,k\ell m} \cdot a + a^c_{2,k\ell m} \cdot a^2$$

Table VII. The charge (f_c) and spin (f_s) form factors for BCC iron. The coordinates k, ℓ, m of the reciprocal lattice vectors are in units of $\frac{2\pi}{a}$. a = 5.0 a.u.

k	ℓ	m	f_c	f_s
1	1	0	17.6058	0.5945
2	0	0	14.3124	0.3749
2	1	1	12.2635	0.2099
2	2	0	10.8240	0.1323
3	1	0	9.7607	0.1168
2	2	2	9.0183	0.0286
3	2	1	8.4298	0.0253
4	0	0	7.9512	0.0673
3	3	0	7.6130	-0.0014
4	1	1	7.5985	0.0323
4	4	2	5.9619	-0.0325
6	0	0	5.9453	0.0188
5	3	2	5.8448	-0.0240
6	1	1	5.8341	0.0093
6	2	0	5.7271	0.0024
5	4	1	5.6299	-0.0227
6	2	2	5.5236	-0.0080
6	3	1	5.4255	-0.0102

Table VIII. The charge (f_c) and spin (f_s) form factors for BCC iron. The coordinates k, ℓ, m of the reciprocal lattice vectors are in units of $\frac{2\pi}{a}$. a = 5.4057 a.u.

k	ℓ	m	f_c	f_s
1	1	0	18.2942	0.6423
2	0	0	15.1038	0.4182
2	1	1	13.0747	0.2590
2	2	0	11.5991	0.1740
3	1	0	10.4721	0.1410
2	2	2	9.6713	0.0657
3	2	1	9.0192	0.0512
4	0	0	8.4778	0.0712
3	3	0	8.1023	0.0170
4	1	1	8.0823	0.0405
4	4	2	6.2954	-0.0272
6	0	0	6.2681	0.0109
5	3	2	6.1759	-0.0216
6	1	1	6.1582	0.0033
6	2	0	6.0536	-0.0023
5	4	1	5.9642	-0.0215
6	2	2	5.8582	-0.0107
6	3	1	5.7650	-0.0125

Table IX. The charge (f_c) and spin (f_s) form factors for BCC iron. The coordinates k, ℓ, m of the reciprocal lattice vectors are in units of $\frac{2\pi}{a}$. a = 6.00 a.u.

k	ℓ	m	f_c	f_s
1	1	0	19.1808	0.6919
2	0	0	16.1511	0.4717
2	1	1	14.1687	0.3213
2	2	0	12.6756	0.2302
3	1	0	11.4969	0.1800
2	2	2	10.6255	0.1159
3	2	1	9.9013	0.0897
4	0	0	9.2905	0.0868
3	3	0	8.8507	0.0461
4	1	1	8.8306	0.0592
4	4	2	6.7604	-0.0170
6	0	0	6.7285	0.0060
5	3	2	6.6311	-0.0150
6	1	1	6.6103	0.0001
6	2	0	6.5000	-0.0044
5	4	1	6.4091	-0.0171
6	2	2	6.2996	-0.0112
6	3	1	6.2064	-0.0129

Table X. The charge (f_c) and spin (f_s) form factors for FCC iron. The coordinates k, ℓ, m of the reciprocal lattice vectors are in units of $\frac{2\pi}{a}$. a = 6.5516 a.u.

k	ℓ	m	f_c	f_s
1	1	1	18.1917	0.6716
2	0	0	16.9126	0.5960
2	2	0	13.5527	0.3124
3	1	1	11.9193	0.2256
2	2	2	11.4913	0.1612
4	0	0	10.0970	0.1656
3	3	1	9.3336	0.0610
4	2	0	9.1251	0.0804
4	2	2	8.4287	0.0273
3	3	3	8.0233	-0.0096
5	1	1	8.0327	0.0585
4	4	0	7.5032	-0.0053
5	3	1	7.2574	-0.0027
4	4	2	7.1794	-0.0255
6	0	0	7.1937	0.0474
6	2	0	6.9230	0.0181
5	3	3	6.7417	-0.0317
6	2	2	6.6944	-0.0025

Table XI. The charge (f_c) and spin (f_s) form factors for FCC iron. The coordinates k, ℓ, m of the reciprocal lattice vectors are in units of $\frac{2\pi}{a}$. a = 6.8107 a.u.

k	ℓ	m	f_c	f_s
1	1	1	18.5324	0.6684
2	0	0	17.2753	0.5920
2	2	0	13.9609	0.3243
3	1	1	12.3174	0.2347
2	2	2	11.8915	0.1795
4	0	0	10.4475	0.1646
3	3	1	9.6683	0.0752
4	2	0	9.4442	0.0876
4	2	2	8.7158	0.0386
3	3	3	8.2907	0.0056
5	1	1	8.2867	0.0586
4	4	0	7.7344	0.0038
5	3	1	7.4712	0.0037
4	4	2	7.3928	-0.0150
6	0	0	7.3925	0.0425
6	2	0	7.1112	0.0174
5	3	3	6.9302	-0.0232
6	2	2	6.8745	-0.0004

Table XII. The charge (f_c) and spin (f_s) form factors for FCC iron. The coordinates k, ℓ, m of the reciprocal lattice vectors are in units of $\frac{2\pi}{a}$. a = 7.0 a.u.

k	ℓ	m	f_c	f_s
1	1	1	18.7783	0.6665
2	0	0	17.5382	0.5834
2	2	0	14.2619	0.3330
3	1	1	12.6055	0.2373
2	2	2	12.1850	0.2007
4	0	0	10.6927	0.1482
3	3	1	9.9190	0.0910
4	2	0	9.6779	0.0891
4	2	2	8.9314	0.0509
3	3	3	8.4967	0.0281
5	1	1	8.4676	0.0473
4	4	0	7.9093	0.0146
5	3	1	7.6306	0.0092
4	4	2	7.5567	0.0010
6	0	0	7.5278	0.0217
6	2	0	7.2437	0.0076
5	3	3	7.0740	-0.0099
6	2	2	7.0042	-0.0024

and

$$f_s(k, \ell, m) = a^s_{0,k\ell m} + a^s_{1,k\ell m} \quad a + a^s_{2,k\ell m} \quad a^2 \qquad (33)$$

The relevant coefficients, a^c_i or a^s_i are provided in Appendix B for the BCC iron form factors in Tables VII through IX. It is easily verified that the contents of these tables are exactly reproduced by these fits. Intermediate values, i.e., the form factors at a = 5.2, are obtained well beyond the second decimal place. Clearly, this signifies that experimental form factors can be judiciously compared to the theoretical ones for a lattice parameter equal to that existing in the conditions of measurements (i.e., non-zero temperature). The above locally quadratic dependence of the form factors of BCC or FCC iron is not unique to this metal. It applies equally well to lithium and copper.

CHAPTER 5

MAGNETISM IN IRON

The present calculations, with ferromagnetic inputs, resulted in magnetic moments, for BCC and FCC iron which are plotted in Fig. 11 versus R_s. Table XIII displays the moments, the density of state at the Fermi level as well as the characteristic exchange splittings. The latters are the energy differences between the absolute maxima in the majority and minority spin density of state curves. Density of states curves for FCC iron at a = 6.5516, 6.8107, and 7.0 a.u. are respectively shown in Figures 12, 13, and 14.

BNDPKG yields from a ferromagnetic input a paramagnetic ordering provided the latter is the most stable one. In light of this, Fig. 11 indicates that BCC and FCC iron are not paramagnetic for the R_s values in the range considered. These calculations predict ferromagnetism for BCC and FCC iron but they do not exclude antiferromagnetism[32] (in FCC iron) which is not addressed here.

The first section of this chapter is devoted to the discussion of the results in Table XIII and Fig. 11. The following sections, B and C address the relevance of our findings to properties of some iron based alloys after a comparison with experiment.

A. Ferromagnetism in BCC and FCC Iron

Figure 11 indicates a rather smooth variation of the magnetic moment per atom in BCC iron for R_s values greater or equal to

Figure 11. The magnetic moment ,in Bohr magneton, versus Wigner-Seitz radius(R_S),in atomic units (a.u), for BCC(dashed curve) and FCC(full curve) iron.

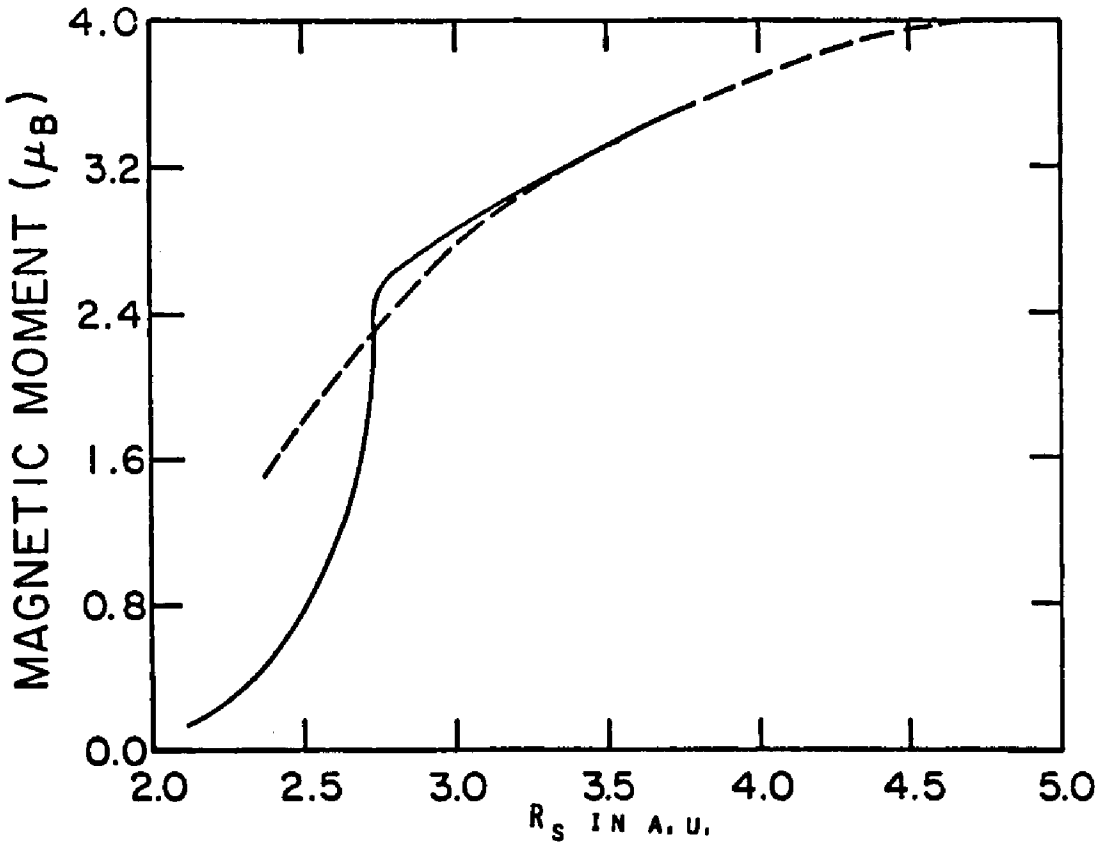

Table XIII. Density of states (states/atom-Rydberg) for majority (↑) and minority (↓) spin electron at the Fermi energy ((Rydberg-atom)$^{-1}$),magnetic moment per atom (in Bohr magneton) m, and the characteristic exchange splitting delta in Rydberg (Ry) for BCC and FCC iron.

BCC					FCC				
R_s	$N_\uparrow(E_F)$	$N_\downarrow(E_F)$	m	Δ_c	R_s	$N_\uparrow(E_F)$	$N_\downarrow(E_F)$	m	Δ_c
2.462	8.321	6.736	1.735	0.142	2.112	5.219	5.206	0.126	0.017
2.560	9.263	3.892	1.987	0.162	2.188	5.985	5.832	0.186	0.042
2.661	11.036	3.341	2.153	0.172	2.345	7.639	9.140	0.397	0.057
2.757	13.906	4.802	2.317	0.177	2.560	12.068	10.097	0.966	0.090
2.954	2.582	19.649	2.717	0.197	2.661	23.826	10.330	1.517	0.120
3.447	2.923	60.269	3.269	0.232	2.736	2.470	13.346	2.549	0.187
4.431	1.106	484.124	3.943	0.277	3.517	2.739	36.140	3.359	0.215

Figure 12. Total density of states N(E),in states/atom per Rydberg, and the valence electron number for ferromagnetic FCC iron. The lattice constant is a = 6.5516 a.u.

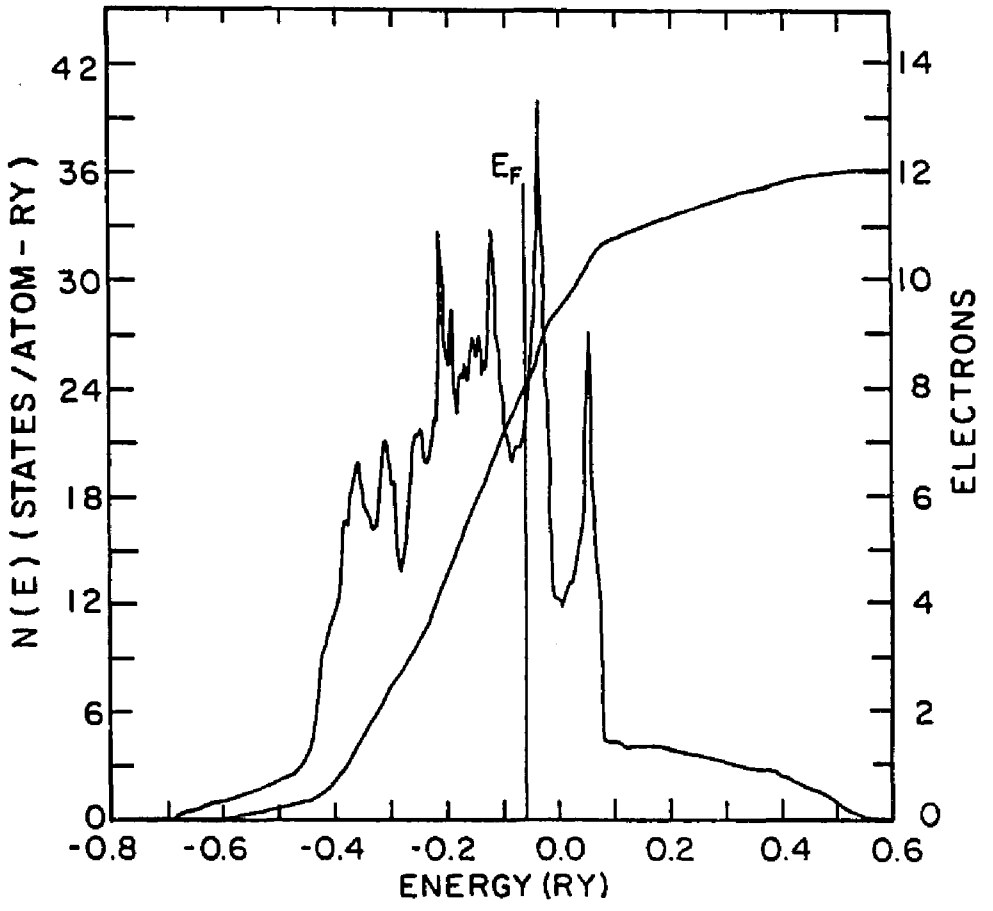

Figure 13. Total density of states N(E), in states/atom per Rydberg, and the valence electron number for ferromagnetic FCC iron .The lattice constant is a = 6.8107 a.u.

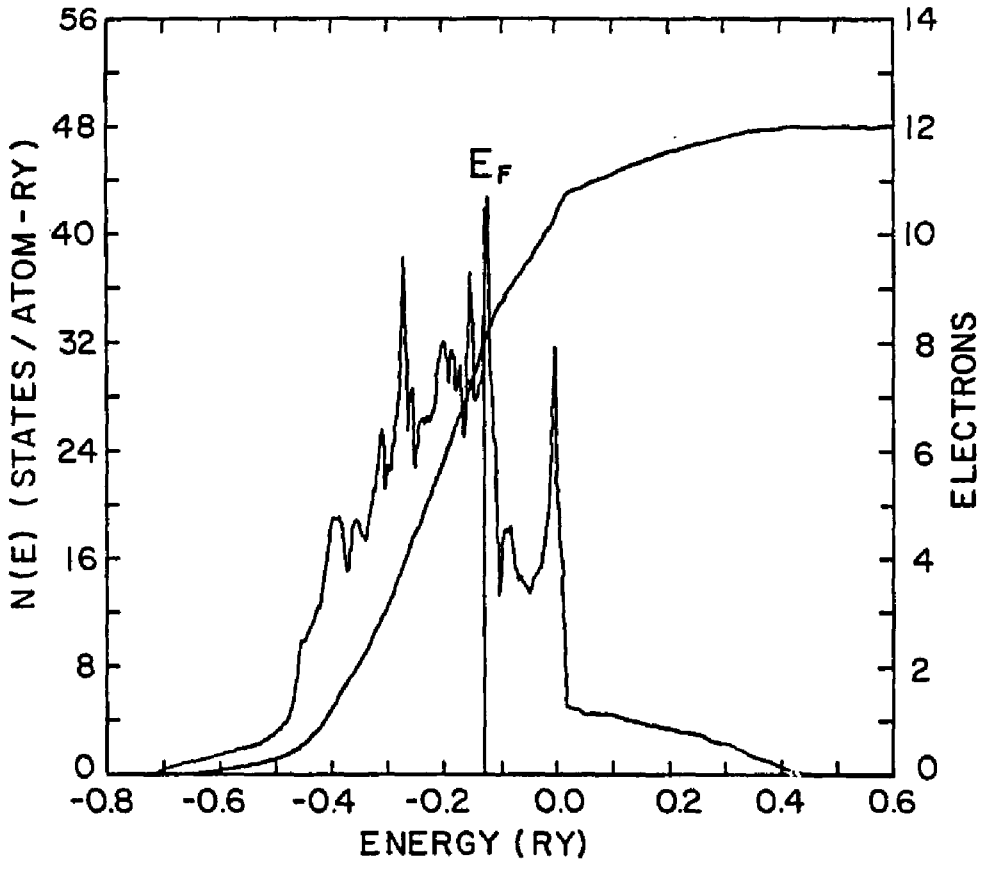

Figure 14. Total density of states N(E),in states/atom per Rydberg, and the valence electron number for ferromagnetic FCC iron. The lattice constant is a = 7.0 a.u

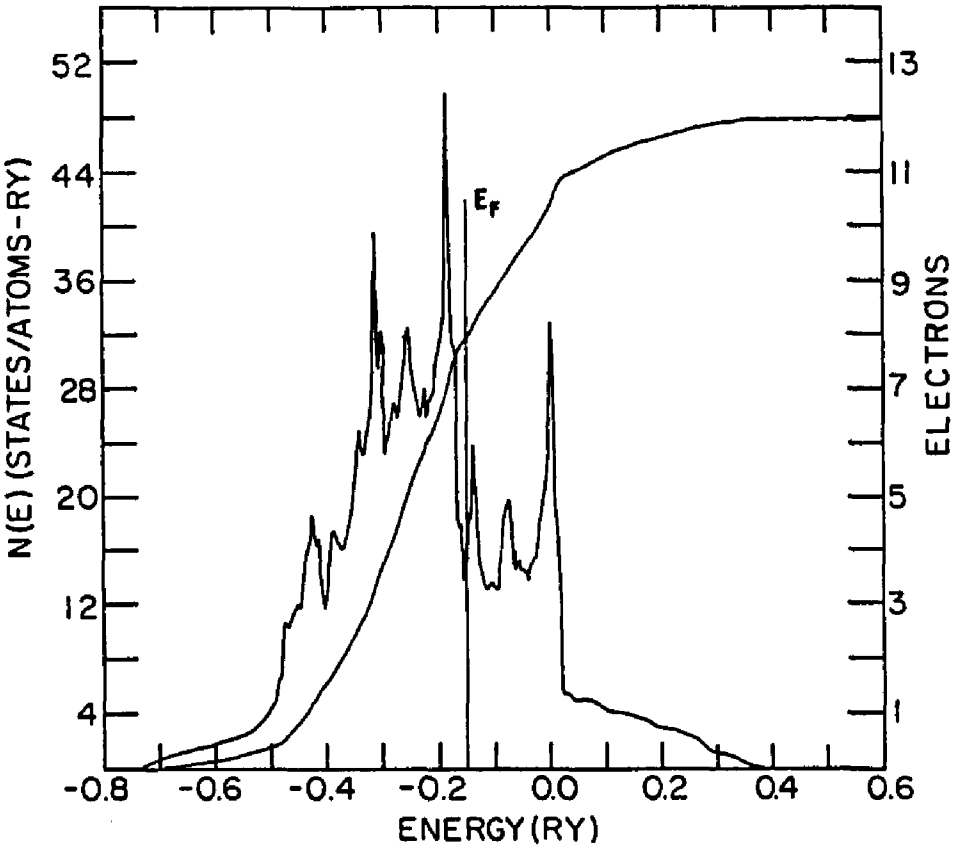

2.462 a.u. This behavior of the moment is explained, in general terms, by the gradual and continuously filling of the majority spin bands as compared to the minority ones. Due in part to the increase of the exchange effect, the majority spin bands are lowered with respect to the Fermi level while the minority energy levels are pushed upwards. BCC iron becomes a strong ferromagnet between the lattice constants of 5.6 and 6.0 a.u. This corresponds to the sinking below E_F of the G_2 branch in the up spin band. The smooth increase of the moment is basically the result of the progressive (see Fig. 4) transfer of electrons from the minority spin bands. A drastic change is not observed simply because no flat band crosses the Fermi level. We recall that the relatively flat bands in the structure, at ordinary lattice parameters, are the two uppermost d bands (D_1, D_2, Λ_3, and Σ_4 branches) which, as previously stated are respectively full or empty for the majority or minority sub-bands. This behavior of the bands, which fully explain the moment versus R_s curve of BCC iron is not unique to this metal.

Walmsley and coworker[76] recently have grown a BCC cobalt film, for the first time, on a chromium substrate. The moment was believed to be around that of the ordinarily stable HCP phase of this metal. Bagayoko, et al.[77] performed ab-initio band structure calculations on this novel phase of cobalt at lattice constants of 5.0, 5.2346 (experimental value), 5.3099 and 5.4456 a.u. The magnetic moments these authors reported, as shown in Table XIV, behave like those of BCC iron when the atomic volume changes. The flat bands which are believed to play a stabilizing role as to the variation of the moment are equally below and above the Fermi level, for up and down spin respectively, for the lattice constants considered. Like the case of BCC iron, no drastic

TABLE XIV. The magnetic moment(m),in Bohr magneton, for BCC cobalt at various atomic radii(R_S) or lattice constants(a) in atomic units(a.u).

R_S (a.u.)	a (a.u.)	m (μ_B)
2.4619	5.0	1.545
2.5774	5.2346	1.646
2.6144	5.3099	1.678
2.6813	5.4456	1.736

change with lattice parameter is expected for values of the latters above 5.0 a.u.

This behavior of the magnetic moment of BCC iron is quite similar to that of FCC iron at lattice parameters above 7.0 a.u. Figure 11 shows the two curves become indistinguishable between the R_s values of 3.25 and 3.75 a.u. However, the magnetic moment of FCC iron for R_s values below 2.73 (a less than 7.0 a.u.) behave quite differently than does the BCC moment. There is a rather steep rise of the moment around R_s = 2.71 a.u. This has been first observed theoretically by Madsen and Andersen[29]; these authors found a different R_s value for the transition ($R_s \simeq 2.61$ a.u.). This transition has been very recently explained in terms of the band structures by Bagayoko and Callaway[75]. The following explanation parallels the one given by these authors.

A relatively flat portion of the uppermost up spin d band, see Fig. 7, crosses the Fermi level for a = 6.5516 a.u. Specifically we are referring to the z_2, uppermost Q_1 and Λ_3 branches. These branches, as shown in Fig. 8, are above the Fermi level in the minority spin bands for the same lattice constant. The combination of the increase of the exchange effect and the decrease of kinetic energy lower these branches, in the majority sub-bands, while it pushes them upwards in the down spin bands, relative to the Fermi level as the lattice parameter increases. For the majority spin these branches are below E_F at a = 7.0 a.u. The abrupt increase in the magnetic moment of FCC iron when the lattice constant change from 6.5516 to 7.0 is due to this transition, i.e., the passage of the uppermost up spin d bands below the Fermi energy and the subsequent disappearance of portions of the Fermi surface. This transition is continuous in the sense that these bands progressively

sink below the Fermi level.

There is a second aspect of this transition equally as important as the filling of these up spin bands, i.e., the increased flatness of the bands which is the manisfestation of a relative localization. We have observed, see Figs. 7 through 10, that the ratio of the exchange splitting to the width of the uppermost d bands in FCC iron is less that unity for lattice constants less than or equal to 6.5516 a.u. This ratio is a quantitative measure of the degree of flatness of these bands. For R_s values above 2.73 a.u., the ratio is greater than one, indicating relatively flat bands or an increase in atomic character of the electrons occupying them. As explained in the discussion of the magnetic properties of BCC iron, once these flattened d bands lie below E_F, in the majority spin, no drastic variation of the moment with lattice parameter is expected, because the corresponding ones in the minority spin bands are above the Fermi energy. Bagayoko and Callaway estimated the transition atomic radius to be R_s = 2.71 a.u. At the transition atomic volume z_2 branch is expected to lie at the fermi level in the up spin sub-band.

The data in Table XIII show the onset of the transition to strong ferromagnetism for BCC and FCC iron. In both cases it is indicated by a relatively large density of down spin states as compared to that for the up spin ones at the Fermi level. Figures 12, 13 and 14 illustrate the same transition for FCC iron. It should be noted that while these figures are indicative of the establishment of strong ferromagnetism, one needs the detail band structure to ascertain the otherwise conjectural observation.

If the moment of BCC cobalt behaves like that of BCC iron for

varying atomic volume, the situation in nickel seems to resemble that of FCC iron. Indeed, Wang and Callaway[54] presented the band structure of this 3d metal for a lattice constant of 6.644 a.u. Weling and Callaway[78] produced semi-empirical bands of FCC nickel which fitted the experimentally observed[79] structure. Bagayoko[73], in the course of testing the new version of BNKPKG obtained results qualitatively similar to those of Wang and Callaway[54]. The magnetic moment obtained by the various calculations is around 0.55 μ_B. The important feature of the structures of FCC nickel of particular interest here is the itinerant character they possess as compared to BCC iron. The ratio of the exchange splitting to the total individual widths for the uppermost d bands of nickel (a = 6.644 a.u.) is less than one; a result similar to that found for FCC iron at a = 6.5516 a.u. However, if one considers only the Γ-L-W branches of these bands, in calculating the widths, the above ratio remains less than 1 for the down spin cases and becomes greater than one for the uppermost up spin ($\Gamma_{12\uparrow}$-$L_{3\uparrow}$-$W_{1\uparrow}$') in the case of nickel.

B. Comparison with Experiment

Our prediction of ferromagnetism for FCC iron is in agreement with the most recent experimental conclusions[17,25] as we shall discuss. At first a comparison with the theoretical works seems appropriate.

Andersen and coworkers[31] reported two different results on the magnetic ordering in FCC iron. Madsen and Andersen[29] found FCC iron to be ferromagnetic for R_s values above 2.47 while Poulsen et al.[30] found a non-zero moment only for R_s larger than 2.6 a.u. Poulsen et al., unlike Madsen and Andersen, included the sp-d hybridization in all their

calculations. The zero moment result of Poulsen et al. could be attributed to an overestimate of the correction to the unhybridized results. The drastic changes in the d band branchings as described here are indeed difficult to account for by the positioning and scaling of the projected density of states as was done by Madsen and Andersen or Poulsen et al. when the sp-d hybridization is included. The rather good results these authors obtained for normal volume (i.e., a magnetic moment of 2.17 μ_B) do not contradict the above contention as a full band structure calculation was used in that case instead of scaling procedures.

Bagayoko and Callaway[75] recently discussed the results of Kubler[32]. There is a qualitative agreement between this author's results and ours on the ferromagnetism of FCC iron below R_s = 2.60. There exist quantitative differences. In particular we find the moment not to vanish at R_s = 2.50 a.u. and we place the abrupt increase of the moment of FCC iron around R_s = 2.71 instead of about 2.645 a.u. The total energy curves obtained by Kubler indicate the stable phase of this metal to be an anti-ferromagnetic FCC, contrary to experiment, for R_s values between 2.5 and 2.7 a.u. The spherical averaging of the charge density inherent to the augmented spherical wave method is suspected[32] to cause this problem.

Roy and Pettifor[34] found the Tauer and Weiss γ_1 and γ_2 states to be both ferromagnetic. Their unhybridized ASA calculations are therefore in qualitative agreement with our results. However we should emphasize the continuity in the steep rise of the moment between R_s = 2.56 and R_s = 2.736 a.u. which is apparent from Fig. 1 as opposed to the discontinuity implied by the original γ_1 (antiferromagnetic) and γ_2

(ferromagnetic) hypothesis. Even though it is difficult to draw a conclusion from Kubler's results, several experimental ones found antiferromagnetic FCC iron at some R_s value less than 2.76.

As discussed in the first chapter, the magnetic ordering in FCC iron is suspected to depend on both film orientation[24] and atomic separation[25]. The difficulty connected with the experimental determination of the lattice constant compounds the problem. Still the results of Wright seem to be in good agreement with ours. This author found a ferromagnetic γ Fe film to possess a moment of 1.1 μ_B, for a lattice spacing estimated to be 6.8 a.u. At a lattice constant of 6.8107 a.u. the present result shows a moment of 1.517 μ_B. Considering that 6.8 a.u. was an upper limit for the experimental value and the rapid variation of the moment around this lattice parameter, this appears as a good agreement between experiment and theory. Gonser et al.[25] estimated a transition from anti-ferromagnetism to ferromagnetism to occur between R_s = 2.67 and R_s = 2.78 a.u. These authors, as mentioned in the introduction, found FCC iron precipitate in Cu_{69} Au_{30} to be ferromagnetic. We found the atomic radius for the transition to strong ferromagnetism to be about 2.71 a.u. for FCC iron. Their estimate of the smallest R_s value (2.67) compatible with ferromagnetism in FCC iron seems to be in disagreement with Wright's result where ferromagnetism is found at an R_s value below 2.66 a.u. The difficulties in the evaluation of the lattice parameter, due in part to possible pseudomorphic phase for the film, could account for the difference and vindicate either finding.

C. Relevance to Iron Based Alloys

The present study of ferromagnetic γ iron is quite relevant to the properties of FCC iron based alloys in general and the invar alloys in particular. That is so in part because at most two shells of neighboring iron atoms are believed to be needed for the central atom to exhibit bulk properties[32].

The most recent explanations of the invar anomalies do not assume γ iron to be antiferromagnetic[21,80,81,82]. While the explanation of Kaspar and Salahub[21] assume ferromagnetic order, Gavoille[82] reaches the conclusion that antiferromagnetically coupled iron atoms cannot be responsible for invar phenomena. The band structure of FCC iron in Fig. 7 through 10 could be used to support arguments of the type presented by Kaspar and Salahub. These authors obtained the ferromagnetic energy levels of Fe_{13}, $Fe_{12}Ni$ and Ni_{13} clusters; the respective non-bonding and anti-bonding characters of the minority and majority spin sub-levels just above the Fermi level (E_F) are used to discuss invar effects in Fe_{64} Ni_{36} (for Ni concentrations around 35%) through filling and emptying of levels. Two factors entering the analysis are the smaller atomic volume and excess electrons (2) nickel possesses as compared to iron. Hattox and coworkers[83] studies some properties of BCC vanadium as a function of the lattice constant. They described the possible usefulness as well as the limitations of the properties of pure metals in understanding alloys. The relevance of the present results to a complete theory of invar phenomena is illustrated by the work of Shiga[84] who studied the magneto-volume invar effects for Fe-Ni alloys among others. This author fits rather well the lattice constant (a(X)) versus nickel concentration (X) curves of Fe-Ni alloys with a modified Vegard's Law:

$$a(X) = a_1 \quad (1 - X) + a_2 \quad X + c \quad \mu(X)$$

where a_1, a_2 and c are adjustable parameters and $\mu(X)$ an average atomic moment. At absolute zero the curve shows the maximum lattice constant for the alloy to be about 6.77 a.u. at approximately 38% nickel; this spacing is in the region of steep rise of the moment of FCC iron. The deviations from the Vegard's Law are attributed to a magnetic contribution to the expansion as recently discussed by Morruzi et al.[6] for pure metals.

CHAPTER 6

DISCUSSION AND SUMMARY

It is apparent from the survey of previous works as well as the preceding description of magnetism in BCC and FCC iron that the present results and their analysis could be of importance for future investigations. We shall elaborate on such investigations as they appear through further discussion in section A. We present a summary of our findings in section B.

A. Discussion for Future Work

While experiments agree on the absence of paramagnetism in FCC iron, as found here, they disagree somewhat on the magnetic ordering in this metal. Antiferromagnetism[11,24] and ferromagnetism[17,22,23,25] are found in both gamma iron precipitates and films. Film orientation[24] or atomic separation[25] are suggested to be factors determining the magnetic order in FCC iron. However, we mentioned the observation of ferromagnetism in iron film[22] at a lattice constant smaller than the minimum required, according to Gonser et al.,[25] for the establishment of this magnetic ordering. The present results could allow meaningful comparison with experimental ones provided progress is made in the determination of the atomic separation in films or precipitates.

A first possible continuation of this work would be to extend the band package, BNDPKG, in order to produce the band structure of materials with two atoms per cell. The treatment of antiferromagnetism requires such a modification. These changes could be made in a manner

to allow for the calculation of the total energy. Although it might still be difficult to accommodate such factors as pseudomorphism in films or defects, this will permit the determination, from the total energy curve, of the most stable ordering at a given atomic volume for the pure metal. This is needed because any inference of the stability of the antiferromagnetic ordering from Kubler's[32] results requires iron to be in the FCC structure, contrary to reality, in ordinary conditions of temperature and pressure.

These total energy calculations could be supplemented by the concomitant evaluation of the pressure. Indeed the infinite terms which appear in the expression of the pressure as given by Janak[85] are easily avoided by expressing the Coulomb contributions to the potential energy in terms of U and D as defined in Chapter 2. This of importance as previous evaluation of the pressure necessitated approximations, like the Muffin-Tin one,[85] in order to avoid divergences. All the required entities are obtained in the process of band structure calculations using the new version of BNDPKG as shown in appendix c.

The above total energy and pressure calculations might require an large amount of CPU time for iron due to a slow convergence of the sums in U and D as defined in Chapter 2. This is so because of the very large gaussian exponents used to describe the core and also the nuclear repulsion term in the potential. In the work on copper the sums had to be carried out to a value of the square of K_s over 12,000 to obtain convergence. Such a summation appears impractical at over 20 lattice parameters as would be the case here for iron. Based on the rather slow variations of the Fourier coefficients at large K_s values one could replace the sums by integrals. This non-trivial honing of the total

energy calculation procedure is not only of potential use in the above suggested work on iron but also will enable one to study, from band calculations, the central pair potentials as described by Matthai et al.[86] and March[87]. Besides their obvious usefulness in metallurgy, these pair potentials can by applied to the study of defects.[87]

An important result obtained here has been the observation of the atomic behavior of some valence states in BCC iron. In FCC iron we have similar results for lattice constants above 7.0 a.u. These characteristics show up in the values and variations of the band widths and exchange splittings. Experimental[88] and theoretical[89] works intimated these results. In particular, Stearns[88] obtained evidence for quasi-localized states in BCC iron as well as other 3d metals which are hybridized with itinerant or continuum ones. The shake up structures observed in nickel[79] could be seen as further confirmation of Stearn's[88] observations. The increased directionality[86] from FCC to HCP and BCC, in that order, implied a somewhat atomic character in BCC iron. A more direct observation of this fact was the failure of the cluster approach calculation to yield an acceptable value of the critical temperature (T_c) of iron for any size of the cluster. On the contrary, Ziegler[89] reproduced the experimental value of this quantity for nickel.

Despite the above wealth of information on the localization of valence electrons in BCC iron, a detailed conceptual understanding of it is not yet available. It is not clear what interpretation one can give to parabola like portions of the bands they occupy. Various forms of hybridization (sp-d, d-d) can be invoked but lack a firm footing.

The data obtained here can be used to compute the probability that an electron occupying a band $n\sigma$ at a given site at time t be found at

time t' at another site. The basic formalism to do this has been provided by Callaway and Hughes[90] in their study of localized defects in semi-conductors using Wannier functions. Such transition time or probability will allow a quantitative description of the degree of localization at any lattice constant.

The above suggested experimental as well as theoretical works can benefit from our findings. In particular most computations we mentioned can use the present data as input. Other studies as those of the Compton profile, the Fermi surface, or the optical conductivity can, in a straight forward manner, utilize the results we wish to summarize in the following section.

B. Summary

We have reviewed previous theoretical and experimental works on BCC and FCC iron. A new formalism for the calculation of the total energy and pressure of a metal has been described. We extended Wang and Callaway's program package in order to implement this formalism. We described the general and new features of this package, BNDPKG, which utilizes Gaussian basis in a LCAO scheme. Local density potentials (i.e., VBH, RSK) are allowed for in BNDPKG. The large size of the Hamiltonian matrix resulting from the use of GTO or CGTO led to a careful study of contraction of basis sets. The most important successful test of the guidelines set forth for contraction has been the obtention of a minimum, at about the experimental lattice constant, in the total energy curve of FCC copper, a 3d metal. The large reduction of CPU time resulting from the use of CGTO opened the way for the present detailed study of the electronic structure of BCC and FCC iron.

Keeping in sight possible extentions of this work, as suggested above (i.e., total energy and pressure calculation), we employed the new version of BNDPKG. The band widths and exchange splittings discussed quantitatively described the variations of the electronic states in BCC and FCC iron as the lattice constant changes. The decrease or increase of the band width or the exchange splitting as the lattice parameter increases is explained by the competition between the kinetic and exchange energies. Several features of the electronic structures of iron have been reported here for the first time. In particular the reordering of representations in the band structure of BCC and FCC iron was described. This reordering, which occurs for both structures around R_s = 2.6616 a.u. is accompanied by changes of branching of the band to avoid forbidden crossings.This branch switching is suspected of being a contributing factor to the difference between the results of Madsen and Andersen[29] and Poulsen et al.[30]

While ferromagnetism in BCC iron was found to possess an atomic origin due to characteristically flat portions of the d bands, the results for FCC iron are mixed. We explained, using ab-initio self-consistent band structures, the abrupt jump in the magnetic moment of FCC iron when R_s varies from 6.5516 to 7.0 a.u. This jump is found to be the result of the establishment of strong ferromagnetism in FCC iron. We emphasized the increased flatness of the top d bands in FCC iron for R_s values above the transition point (R_s = 2.71 a.u.). For very large lattice constants we found the moment in both structures to behave similarly. We found in BCC iron, at lattice constants above 9.0 a.u., the crystal field splitting to be larger than the overlap effects. The forms factors we obtained as well as their locally

quadratic dependence on the lattice constant could be of use in the analysis of experimental works. BCC cobalt has been predicted to behave, as far as the moment variation with R_s is concerned, like iron. The reasons for this were given in terms of the band structure. We indicated the usefulness of our results in a complete understanding of iron alloys in general and the invar alloys in particular. We mentioned few of the many possible future works, experimental or theoretical, for which the results of this work, presented or available,[91] could play a role of reference material.

REFERENCES

1. R. A. Tawil and J. Callaway, Phys. Rev. B7, 4242 (1973).
2. J. Callaway and C. S. Wang, Phys. Rev. B16, 2095 (1977).
3. J. Callaway, Institute of Physics Conf. Ser. 55, 1 (1981).
4. E. P. Wohlfarth, Ferromagnetic Materials, Vol. 1, 1 (1980). Edited by E. P. Wohlfarth, North-Holland Publishing Co., Inc.
5. D. E. Eastman, J. F. Janak, A. R. Williams, R. V. Coleman, and G. Wendin, J. Appl. Phys. 50, 7426 (1979).
6. V. L. Moruzzi, J. F. Janak, and A. R. Williams, Calculated Electronic Properties of Metals, (1978). Pergamon Press, Inc.
7. H. Danan, A. Herr, and A. J. P. Meyer, J. Appl. Phys. 39, 669 (1968).
8. P. Heiman and H. Neddermeyer, Phys. Rev. B18, 3537 (1978).
9. A. M. Turner and J. L. Erskine, Phys. Rev. B25, 1983 (1982).
10. I. V. Svechkarev and A. S. Panfilov, Phys. Stat. Sol. (B)63, 11 (1974).
11. L. Kaufman, E. V. Clougherty, and R. J. Weiss, Acta Metallurgica, 11, 323 (1963).
12. L. Vinokurova, Soviet Phys. JETP 49(5), 834 (1979).
13. L. Vinokurova, and E. Kulatov, J. MMM 15-18, 1205 (1980).
14. L. G. Liu and W. A. Bassett, J. Geoph. Res. 80, 3777 (1975).
15. H. M. Strong, R. E. Tuft, and R. E. Hanneman, Met. Trans. 4, 2657 (1973).
16. F. P. Bundy, J. Appl. Phys. 36, 616 (1965).

17. P. J. Brown, H. Capellman, J. Deportes, D. Givord, and K. R. A. Ziebeck, J. MMM 31-34, 295 (1983).

18. W. B. Pearson, Handbook of Lattice Spacings, Pergamon Press, London (1959).

19. K. J. Tauer and R. J. Weiss, Bull. Amer. Phys. Soc. 6, 125 (1961).

20. R. J. Weiss, Proc. Phys. Soc 82, 281 (1963).

21. J. Kaspar and D. R. Salahub, Phys. Rev. Lett. 47, 54 (1981).

22. J. G. Wright, Philo. Mag. 24, 217 (1971).

23. U. Gradmann, N. Kummerle, and P. Tillmanns, Thin Solid Films 34, 249 (1976).

24. W. Keune, R. Halbauer, J. Gonser, J. Lauer, and D. L. Williamson, J. Appl. Phys. 48, 2976 (1977).

25. U. Gonser, K. Krischel, and S. Nasu, J. MMM 15-18, 1145 (1980).

26. J. H. Wood, Phys. Rev. 126, 517 (1962).

27. R. A. Deegan, Phys. Rev. 171, 659 (1968).

28. N. W. Dalton, J. Phys. C: Solid State Phys. Vol. 3, 1912 (1970).

29. J. Madsen and O. K. Andersen, AIP Conf. Proceed. 29, 327 (1975).

30. U. K. Poulsen, J. Kollar and O. K. Andersen, J. Phys. F: Metal Phys. Vol. 6, No. 9, L241 (1976).

31. O. K. Andersen, J. Madsen, U. K. Poulsen, O. Jepsen, and J. Kollar, Physica 86-88B, 249 (1977).

32. J. Kubler, Phys. Lett. 81A, 81 (1981).

33. A. R. Williams, J. Kubler and C. D. Gelatt, Jr., Phys. Rev. B19, 6094 (1979).

34. D. M. Roy and D. G. Pettifor, J. Phys. F: Metal Phys. Vol. 7, No. 7, L183, (1977).

35. E. C. Stoner, Pro. Roy. Soc. A169, 339 (1939).

36. H. Hasegawa and D. G. Pettifor, Phys. Rev. Lett. 50, 130 (1983).

37. H. Hasegawa, J. Phys. Soc. Japan 46, 1504 (1979) and 49, 963 (1980).

38. J. Hubbard, Phys. Rev. B19, 2626 (1979) and 23 5974 (1981).

39. W. Kohn and L. J. Sham, Phys. Rev. A140, 1133 (1965).

40. L. J. Sham and W. Kohn, Phys. Rev. 145, 561 (1966).

41. Hohenberg and W. Kohn, Phys. Rev. B136 (1964).

42. U. von Barth and L. Hedin, J. Phys. C5, 1629 (1972).

43. J. Callaway, Quantum Theory of the Solid State, Academic Press, N.Y. (1976).

44. F. Bloch, Zeit Physik 52, 555 (1928).

45. C. S. Wang and J. Callaway, Comput. Phys. Commun. 14, 327 (1978). The program package CNDPKG is available from comput. phys. commun. program library.

46. A. K. Rajagopal, S. P. Singhal, and J. Kimball (unpublished), as quoted by A. K. Rajagopal, in "Advances in Chemical Physics," edited by G. I. Prigogine and S. A. Rice (Wiley, New York, 1979), Vol. 41, p. 59.

47. J. Callaway and N. H. March, Solid State Physics, edited by H. Ehrenreich, F. Seitz, and D. Turnbull, Academic Press, N.Y., to be published.

48. A. R. Williams and U. von Barth, Applications of Density Functional Theory to Atoms, Molecules, and Solids.

49. J. Callaway, Xianwu Zou, and D. Bagayoko, Phys. Lett. A89, 86 (1982).

50. J. Callaway, Xianwu Zou, and D. Bagayoko, Phys. Rev. B27, 631 (1983).

51. C. S. Wang, J. MMM 31-34, 95 (1983).

52. O. Gunnarson, M. Jonson, and B. I. Lunquist, Phys Rev. B20, 3136 (1979). See also O. Gunnarson and R. O. Jones, Phys. Sci. 21, 394 (1980).

53. S. H. Vosko, L. Wilk, and M. Nusaiy, Can. J. Phys., 1200 (1980).

54. C. S. Wang and J. Callaway, Phys. Rev. B15, 298 (1977).

55. J. P. Perdew and M. R. Norman, Phys. Rev. B26, 5445 (1982).

56. J. D. Pack, H. J. Monkhorst, and D. L. Freeman, Solid State Commun. 29, 723 (1979).

57. J. Boettcher, private communication.

58. E. E. Lafon and C. C. Lin, Phys. Rev. 152, 579 (1966).

59. S. F. Boys, Proc. Roy. Soc. (London), A200, 542 (1950).

60. I. Shavitt and M. Karplus, J. Chem. Phys. 36, 550 (1962).

61. R. C. Chaney and F. Dorman, Int. J. Quantum Chem. 8, 465 (1974).

62. D. Bagayoko, D. G. Laurent, S. P. Singhal, and J. Callaway, Phys. Lett. 76A, 2 (1980).

63. A. J. H. Wachters, J. Chem. Phys. 52, 1033 (1970).

64. A. Veillard, Theorit. Chim. Acta (Berl.), 12, 405 (1968).

65. E. Clementi and D. A. Davis, J. Comput. Phys. 1, 223 (1966).

66. S. Huzinaga and Y. Sakai, J. Chem. Phys. 50, 1371 (1969).

67. T. H. Basch, C. T. Hornback, and J. W. Moskowitz, J. Chem. Phys. 50, 1311 (1969).

68. R. F. Steward, J. Chem Phys. 50, 2485 (1969).

69. C. Salez and A. Veillard, Theorit. Chem. Acta (Berl.), 11, 441 (1968).

70. W. Kutzelnigg and W. H. E. Schwarz, Phys. Rev. A26, 2361 (1982).

71. D. Bagayoko, Int. J. Quant. Chem. Proceed. 1983 Sanibel Conf., in press.

72. B. Roos, A. Veillard and G. Vinot, Theorit. Chem. Acta (Berl.), 20, 1 (1971).

73. D. Bagayoko, unpublished. Resulting bands are available upon request.

74. B. Van Laar, F. Maniawski, S, Kaprzyk, and L. Dobrzynski, J. MMM 14, 94 (1979).

75. D. Bagayoko and J. Callaway, Phys. Rev. B, to be published.

76. R. Walmsley, J. Thompson, D. Friedman, R. M. White, and Th. H. Geballe, (at Stanford University), to be published.

77. D. Bagayoko, A. Ziegler, and J. Callaway, Phys. Rev. B27, 7046 (1983).

78. F. Weling and J. Callaway, Phys. Rev. B26, 710 (1982).

79. W. Eberhardt and E. W. Plummer, Phys. Rev. B21, 3245 (1980).

80. A. R. Williams, V. L. Moruzzi, C. D. Gelatt, Jr., and J. Kubler, J. MMM 31-34, 88 (1983).

81. O. Yamada, F. Ono, I. Nakai, H. Maruyama, K. Ohta, and M. Suzuki, J. MMM 31-34, 105 (1983).

82. G. Gavoille, J. MMM 13, 255 (1979).

83. T. M. Hattox, J. B. Conklin, Jr., J. C. Slater, and S. B. Trickey, J. Phys. Chem. Solids 34, 1627 (1973).

84. M. Shiga, J. Phys. Soc. of Japan 22, 539 (1967).

85. J. F. Janak, Phys. Rev. B9, 3985 (1974).

86. C. C. Matthai, P. J. Grout and N. M. March Int. J. of Quant. Chem. Symp. 12, 443 (1978).

87. N. M. March to be published.

88. M. B. Stearns, AIP conf. proceed. 29, 286(1975). See also Physica 91b, 37 (1977).

89. A. Ziegler, Phys. Rev. Lett. 48, 695 (1982).

90. J. Callaway and A. J. Hughes, Phys. Rev., 156, 860 (1967).

91. Supplementary data available upon request from D. Bagayoko or J. Callaway.

APPENDIX A

APPENDIX A.1: New Version of PROGRAM FCOF

```
                                   DSN=PHBAGA.DIOLA.FCOF
------------------------------------------------------------------------
//FEF1B160 JOB (1103,72121,20,2),'PH.DIOLA',MSGLEVEL=1,
//       NOTIFY=PHBAGA
/*AFTER    FEF1B060
/*JOBPARM SHIFT=N
/*ROUTE PRINT PHYSICS
//A EXEC FORTHCLG,PARM.FORT='NOSOURCE,LANGLVL(66),OPT(2)',
//       PARM.LNED=NOXREF,REGION=1200K,TIME=999
//FORT.SYSIN DD *
C
C                                PROGRAM FCOF
C                              THE FIRST PART OF
C
C      A GENERAL PROGRAM TO CALCULATE SELF-CONSISTANT ENERGY BANDS
C
C          USING THE MODIFIED TIGHT BINDING OR LCGC METHOD
C
C                                     BY
C
C                          C.S. WANG AND J. CALLAWAY
C                    EXTENSION FOR TOTAL ENERGY CALCULATIONS
C                                     BY
C                      J. CALLAWAY,X. ZOU,AND D. BAGAYOKO
C
C                             DEPARTMENT OF PHYSICS
C
C                           LOUISIANA STATE UNIVERSITY
C
C                           BATON ROUGE LOUISIANA 70803
C
C
C
C               COMMON BLOCKS OCCURING IN FCOF
C
C               ROUTINES USED IN FCOF
C                           FOR TOTAL ENERGY CALCULATION
C      ATDENS                            ATDEN1
C      CPHYGF
C      COULOM
C      FILON                             FILO1
C      GBZPT
C      GINDPK
C      GMIS
C      GPEBRK
C      GRADPT
C      OPEWAD
C      POEXCH                            POEXC1
C      SPHWT
C      TELECT
C
C                                        VXCRS1
C
C
C
C      COMM. STS, ROUTINES IN WHICH THEY ARE USED
C
C      CHARGE    ATDENS,FCOF,OPEWAD,POEXCH
C      CONST     ATDENS,COULOM,FCOF,OPEWAD,POEXCH
C      END       FCOF,OPEWAD
```

```
                                    DSN=PHBAGA.DIOLA.FCOF
C     EXCH      FCOF,POEXCH
C     LCA       FCOF
C     LCB       FCOF
C     VK0       ATDENS,COULOM,FCOF,OPENAD,POEXCH
C
C
C
C
C               INPUT/OUTPUT CHANELS USED IN FCOF
C
C     FT01F001 FOURIER COEFFICIENTS FOR (K**2.LE.MAXK2)
C              USED IN ESINT,SCF1 AND SCF2.
C     FT01F002 FOURIER COEFFICIENTS FOR (K**2.GT.MAXK2) USED IN ESINT
C     FT02F001 FOURIER COEFFICIENTS OF W FOR (K**2.LE.MAXK2)
C     FT02F002 FOURIER COEFFICIENTS OF W FOR (K**2.GT.MAXK2)
C                   THIS IS NOT GENERALLY NEEDED
C     FT10F001 AND FT11F001 CONTAIN DATA IN FT01F002 AND FT02F002
C              PLUS ADDITIONAL ONES.
C     FT05F001 CARD READER
C     FT06F001 LINE PRINTER
C     FT07F001 CARD PUNCHER
C
C
C
C
C
C     FOURIER COEFFICIENTS OF THE COULOMB AND EXCHANGE POTENTIAL.
C     GAUSSIAN TYPE WAVE FUNCTIONS ARE USED IN THIS PROGRAM.
C     THE FOURIER COEFFICIENTS OF THE COULOMB POTENTIAL ARE EVALUATED
C     ANALYTICALLY.
C
C     THE EXCHANGE POTENTIAL IS EVALUATED IN THE FOLLOWING WAY.
C     EACH ATOM IS SURROUNDED BY TWO SPHERES OF RADIUS ROGAUS AND ROSPH.
C     IF(R.LT.ROGAUS), THE CHARGE DENSITY IS SPHERICALLY SYMMETRIC.
C     ITS FOURIER COEFFICIENTS ARE OBTAINED  BY FILON'S RULE AT NRPNT
C     POINTS.
C     IF(ROGAUS.LT.R.LE.ROSPH), THE CHARGE DENSITY IS EXPANED IN KUBIC
C     HARMONICS.
C     THE EXPANSION COEFFICIENTS ARE OBTAINED FROM CHARGE DENSITY ALONG
C     (DIRX,DIRY,DIRZ) DIRECTIONS.
C     THE FOURIER COEFFICIENTS OF THE EXCHANGE POTENTIAL ARE OBTAINED
C     BY THE FILON'S INTEGRATION METHOD BASED ON NFILON POINTS BETWEEEN
C     TWO SPHERES.
C     THE CONTRIBUTIONS FROM REGION BETWEEN NEIGHBORING SPHERES ARE AS
C     FOLLOWS:
C     THE REGION IS DIVIDED INTO CUBES OF LENGTH A/(2*IRCELD).
C     DENSITY**1/3 IS EXTRAPOLATED LINEARLY INSIDE EACH CUBE WHEN
C     THE FOURIER COEFFICIENTS ARE EVALUATED.
C     IF(IGRLV.EQ.0) THE CHARGE DENSITY IS APPROXIMATED BY  ITS
C     SPHERICAL AVERAGE AND IS INTEGRATED UP TO THE RADIUS OF THE WIGNER
C     SEITZ SPHERE.
C
C     EXP(I K.R)=((4*PI*I**L*JL(K*R)*KLM(K)*KLM(R),M=-L,L),L=0,INFINITE)
C     JL(KR) IS THE SPHERICAL BESSEL FUNCTION OF ORDER L.
C     KLM(K) IS THE CUBIC HARMONIC OF ORDER L TYPE M.
C
C
C
```

DSN=PRPAGA.DIOLA.FCOF

```
C       DIMENSION RESTRICTIONS.
C      KKX(NKPT),KKY(NKPT),KKZ(NKPT),NB(NKPT),RSQ(NKPT).
C      AX(IDIM),AY(IDIM),AZ(IDIM),NPN(I,1,1) WHERE I.EQ.IRCELD+2.
C      SINE(J,K),COSINE(J,K) WHERE J.GE.IRCELD+1, K.GE.SQRT(MAXK2)+2.
C      IRX(N),IRY(N),IRZ(N),IPT(6,N),WT(N), WHERE N=NO OF INDEPENDENT
C      POINTS IN 1/48TH OF THE UNIT CELL GENERATED BY IRCELD.
C      RHORMF(L*M) WHERE L IS NO OF PCINTS INVOLED IN CALCULATING THE
C      GRADIENTS.
C      R(NRPNT),RHOR(NRPNT*M),RFILON(NFILON),FLRHOR(NFILON*M*NDIRC)
C      RWGSIZ(NWGSIZ),WSRHOR(NWGSIZ*M), M=3 AND 9 IF NSPIN=1 AND 2.
C
C
C      ==========================================================
C
C                          NEW FEATURES
C
C           IVXCR=2,IW=1,IDO=2  OR 0 :GET V(K) ONLY
C
C           IVXCR=2,IW=2,IDO=1 OR 2 :GET W(K) ONLY
C
C
C      ==========================================================
C
C
C * * * * * * * * * * * * * * * * * * * * * * * * * * * * * * * *
      IMPLICIT REAL*8(A-F,H,C-Z)
      INTEGER*2 KKX(8000),KKY(8000),KKZ(8000),NB(8000),KX,KY,KZ,NNB
      INTEGER*2 NPN(34,34,34),IPT(6,1785),IRX(1785),IRY(1785),IRZ(1785)
      DIMENSION SINE(33,100),COSINE(33,100)
      DIMENSION RHORMF(14000),WT(1785),RHORV1(1505)
      DIMENSION ARO(36),BRO(9),CRO(9),CUBIC(4)
      DIMENSION AX(500),AY(500),AZ(500)
      DIMENSION R(201),RHOR(1809),RFILON(201),FLRHOR(7236),RWGSIZ(101),
     &WSRHOR(0909)
      DIMENSION RSQ(8000)
      COMMON/XCHARG/CHARGE(7),CHARUP(7),CHARDN(7)
      COMMON/VKO/C(7,14),EX(7,14),FACTO(10),IB(7),NORB(7),NSTA
      COMMON/EXCH/DIRX(4),DIRY(4),DIRZ(4),CNO01,CNO41,CNO61,CNO81,
     &CMAT(4,4)
      COMMON/EWD/OMEGA,AKR2,FACT,CG1,CEWD,ELECT,MAXK2
      COMMON/XCONST/A,PI,SIXPI,ONETHD,TWTHIV,IPON,IGAUS
      COMMON/LCB/SINE,COSINE,WT,IRX,IRY,IRZ,IPT
      COMMON/LCA/RSQ,KKX,KKY,KKZ,NB
      COMMON/TOTLE/IW
      EQUIVALENCE(RSQ(1),NPN(1,1,1))
      PI=3.14159265358979300
      ONETHD=1.D0/3.D0
      TWTHIV=-2.D0/3.D0
      FACTO(1)=1.D0
      DO 10 I=2,10
   10 FACTO(I)=FACTO(I-1)*DFLOAT(I)
C
C     A=LATTICE CONSTANT (IN A. U. )
C     ROGAUS=RADIUS OF THE SMALLER SPHERE.
C
      READ(5,20)A,ROGAUS
   20 FORMAT(8F10.5)
C
```

```
C     ================================================================
C
      VEKSUM=0.D0
      VCKSUM=0.D0
      VEKPSM=0.D0
      VCKPSM=0.D0
      VXCPSM=0.D0
      WPUPSM=0.D0
      WPDNSM=0.D0
      WPUDSM=0.D0
      WXCPSM=0.D0
C
C     SC  IDCUB=1,  BCC  IDCUB=2,  FCC  IDCUB=4
C     NKPT IS THE NUMBER    OF THE R.L.V. (KKX,KKY,KKZ)
C     MAXK2=THE SQUARE OF THE MAXIMUM MAGNITUDE OF THE R.L.V. GENERATED.
C     IDIM IS THE NUMBER    OF THE D.L.V. (AX,AY,AZ)
C     MAXR2=THE SQUARE OF THE MAXIMUM MAGNITUDE OF THE D.L.V.
C     NSPIN=1 FOR PARAMAGNETIC,  NSPIN=2 FOR FERROMAGNETIC.
C     ISYM=NUMBER OF ANGULAR SYMMETRIES CONSIDERED.
C     IF(IGENVO.EQ.0) NO R.L.V. IS GENERATED.
C     IF(ISORT.NE.0) R.L.V. IS SORTED IN ORDER OF INCREASING MAGNITUDE.
C     IF(IPUN.NE.0) CHARGE DENSITY WILL BE PUNCHED.
C     IRCELD=DIVISION IN THE UNIT CELL.
C     NRPNT= DIVISION FOR 0.LE.R.LE.ROGAUS.
C     NPILON DIVISION FOR ROGAUS.LE.R.LE.RCSPH (RADIUS OF JUST TOUCHING
C     SPHERE).
C     NWGSIZ= DIVISION FOR ROSPH.LE.R.LE.RADIUS OF WIGNER SEITZ SPHERE.
C     IF(IGAUS.NE.0) CHARGE DENSITIES ARE CALCULATED AT EQUALLY SPACED
C     POINTS AS DETERMINED BY IRCELD.  V(K) IS NOT GENERATED.
C     ================================================================
C
C     IVXCR=0,NO CALCULATION OF V(KS) FOR THE TOTAL ENERGY AND X-ALPHA
C     POTENTIAL USED ONLY.
C     IVXCR=1,CALCULATE VXC(KS) AND W(KS),USING X-ALPHA POTENTIAL.
C     IVXCR=2,CALCULATE VXC(KS) AND W(KS),USING VBH POTENTIAL.
C
C     ================================================================
      READ(5,30)IDCUB,NKPT,MAXK2,IDIM,MAXR2,NSPIN,ISYM,IGENVO,ISORT,
     1IPUN,IRCELD,NRPNT,NPILON,NWGSIZ,IGAUS
      READ(5,30)IVXCR,IN,IDC
   30 FORMAT(16I5)
      IRCM=IRCELD*2
      DO 32 I=1,IRCM
      DO 32 J=1,IRCM
      DO 32 K=1,IRCM
   32 NPN(I,J,K)=0
      AAA=A*A*A
      AKB=2.D0*PI/A
      AKB2=AKB*AKB
      OMEGA=AAA/DFLOAT(IDCUB)
      AHALF=A/2.D0
      COR=AHALF/DFLOAT(IRCELD)
   40 FORMAT(2X,A8,2I5,8F7.4)
   50 FORMAT(5F16.6)
   60 FORMAT(1X,'EXP=',F20.6,3X,'COEF=',4F16.6)
   70 FORMAT(1X,//,1X,A6,5X,'NO OF ORBITALS=',I4,5X,'ELECTRONS UP=',
     &F8.3,5X,'ELECTRONS DOWN=',F8.3,5X,'TOTAL ELECTRONS=',F8.3,/)
C
```

```
C      READ IN GAUSSIAN TYPE ORBITALS AND DEFINE THE NORMALIZATION
C      CONSTANT.
C      NSYM IS THE NO. OF TYPE OF OCCUPIED STATES OF A GIVEN ANGULAR
C      SYMMETRY.
C      CHARGE(I) IS THE NUMBER OF ELECTRONS IN THE I'TH STATE.
C       C(I,J) IS THE J'TH COEFFICIENT OF THE I'TH WAVE FUNCTION
C      EX(I,J) IS THE J'TH EXPONENTS OF THE I'TH WAVE FUNCTION
C      NN=NORB(I) IS THE NUMBER OF ORBITALS IN THE I'TH WAVE FUNCTION.
C
       ELEUP=0.D0
       ELEDN=0.D0
       IEND=0
       A0=4.D0/DSQRT(PI)
       DO 100 IJ=1,ISYM
       A1=0.5+IJ
       READ(5,40) Z1,NSYM,NN,(CHARUP(J+IEND),CHARDN(J+IEND),J=1,NSYM)
       IST=IEND+1
       IEND=IEND+NSYM
       DO 80 I=IST,IEND
       ELEUP=ELEUP+CHARUP(I)
       ELEDN=ELEDN+CHARDN(I)
       CHARGE(I)=CHARUP(I)+CHARDN(I)
       NORB(I)=NN
       IB(I)=IJ
    80 WRITE(6,70) Z1,NORB(I),CHARUP(I),CHARDN(I),CHARGE(I)
       DO 90 J=1,NN
       READ(5,50) ALPH,(C(I,J),I=IST,IEND)
       WRITE(6,60) ALPH,(C(I,J),I=IST,IEND)
       DO 90 I=IST,IEND
       EX(I,J)=ALPH
       C(I,J)=C(I,J)*DSQRT(A0*(2.D0*ALPH)**A1)
    90 CONTINUE
       A0=A0/A1
   100 CONTINUE
       NSTA=IEND
       ELECT=ELEUP+ELEDN
       EMAG=ELEUP-ELEDN
       IF(IDCUB.EQ.1)  RC=A/2.D0
       IF(IDCUB.EQ.2)  RC=AHALF*DSQRT(3.D0)/2.D0
       IF(IDCUB.EQ.4)  RC=AHALF*DSQRT(2.D0)/2.D0
       ROSPH=RC
       RONGSZ=(3.D0*OMEGA/(4.D0*PI))**ONETHI
       WRITE(6,600) A,RC,ELECT,EMAG,IDCUB,NRPT,MAXK2,IDIM,MAXE2,NSTA,IGRLV
      &0,ISORT,IRCELD
       IDC=8/IDCUB
       IF(IDCUB.EQ.1)  IDC=1
C
C      READ IN DIRECTIONS ALONG WHICH CHARGE DENSITIES ARE CALCULATED.
C      IF(IRDDIR.EQ.0) DIRECTIONS ARE GENERATED IN THE PROGRAM.
C      NDIRC=NO. OF DIRECTIONS USED.      (MAXIMUM=4).
C
  110 FORMAT(2I4,12F6.3)
       READ(5,110) IRDDIR,NDIRC,(DIRX(I),DIRY(I),DIRZ(I),I=1,NDIRC)
       IF(IRDDIR.NE.0)  GO TO 180
       I2=12
  120 IDIMC=IDIM
       CALL GINDPR(KKX,KKY,KKZ,KSQ,IDIMC,IDC,I2,NE,0,1,0)
       DO 130 I=1,IDIMC
```

```
      AX(I)=RKX(I)
      AY(I)=RKY(I)
  130 AZ(I)=RKZ(I)
      DIRX(1)=AX(2)
      DIRY(1)=AY(2)
      DIRZ(1)=AZ(2)
      IF(NDIRC.EQ.1) GO TO 170
      IST=3
      DO 160 ND=2,NDIRC
      NDM=ND-1
      ISCL=IST
      DO 150 I=ISCL,IDIMC
      DO 140 ID=1,NDM
      IF(AY(I)*DIRZ(ID)-AZ(I)*DIRY(ID).EQ.0.0.AND.
     &   AZ(I)*DIRX(ID)-AX(I)*DIRZ(ID).EQ.0.0.AND.
     &   AX(I)*DIRY(ID)-AY(I)*DIRX(ID).EQ.0.0) GO TO 150
  140 CONTINUE
      DIRX(ND)=AX(I)
      DIRY(ND)=AY(I)
      DIRZ(ND)=AZ(I)
      IS1=I+1
      IF(IST.LE.IDIMC) GO TO 160
  150 CONTINUE
      I2=I2+5
      GO TO 120
  160 CONTINUE
  170 CONTINUE
  180 CONTINUE
C
C     GENERATE PERMUTED DIRECT LATTICE VECTORS
C
      CALL GPERMK(RKX,RKY,RKZ,KSQ,IDIM,IDC,MAXR2,1,0)
      IF(IDCUB.EQ.1) AHALF=A
      DO 190 II=1,IDIM
      AX(II)=AHALF*RKX(II)
      AY(II)=AHALF*RKY(II)
  190 AZ(II)=AHALF*RKZ(II)
      CO1=ELECT*PI*8.D0/OMEGA
      FACT=1.D0/OMEGA
      CNC01=1.D0/DSQRT(4.D0*PI)
      BNC41=1.25D0*DSQRT(21.D0)
      BNC61=231.D0*DSQRT(26.D0)/8.D0
      BNC81=65.D0*DSQRT(561.D0)/16.D0
      CNC41=BNC41*CNC01
      CNC61=BNC61*CNC01
      CNC81=BNC81*CNC01
      SIXPI=-6.D0*(3.D0/(4.D0*PI))**ONETHD
      CDENS=4.D0*PI/OMEGA*CNC01
      CEXPE=CDENS
      CEXPA=CEXPE
      CEND=2.D0*PI/OMEGA
      III=IRCELD+1
      NFIDIM=NFILON*NDIRC
C
C     GENERATE OR READ IN THE PARAMETERS IN THE EWALD TYPE POTENTIAL.
C     V(R)=-(2*Z+ALPHA)*EXP(-BETA1*R**2)/R+ALPHA*EXP(-BETA2*R**2)/R
C     IF(IEWALD.EQ.0) THE PARAMETERS ARE GENERATED IN SUBROUTINE OPEWAD.
C
```

```
      READ(5,200) IEWALD,ALPHA,BETA1,BETA2
  200 FORMAT(I10,3F15.4)
      R2=(AX(2)*AX(2)+AY(2)*AY(2)+AZ(2)*AZ(2))/4.D0
      IF(IEWALD.NE.0) GO TO 210
      CALL OPEWAD(ALPHA,BETA1,BETA2,R2,5.D-1,2.D-1,50)
      GO TO 102
  210 CONTINUE
      VPT1=-(2.D0*ELECT*ALPHA)*DEXP(-BETA1*R2)/DSQRT(R2)
      VPT2=ALPHA*DEXP(-BETA2*R2)/DSQRT(R2)
      VRTST=VPT1+VPT2
      WRITE(6,101) IEWALD,ALPHA,BETA1,BETA2,VRTST
  101 FORMAT(//,2X,'IEWALD=',I10,'ALPHA=',F15.4,'BETA1=',F15.4,
     1'BETA1=',F15.4,'V(R)=',E20.5,//)
  102 CONTINUE
      IF(IGRLVO.EQ.0) GO TO 300
C
C     DEFINES EQUALLY SPACED POINTS IN 1/48TH OF THE UNIT CELL.
C
      CALL GRZPT(KKX,KKY,KKZ,RHORMF,NSPNT,IDC,III,SUMW,1,0,1)
C
C     MODIFY THE WEIGHTING FACTOR FOR THE CUBES THAT ARE INTERCEPTED BY
C     THE SPHERE.
C
      CALL SPHWT(KKX,KKY,KKZ,NSPNT,RHORMF,ROSPH,COR,SUMW,OMEGA)
      NFTIN=NSPNT
      WRITE(6,600) A,RO,ELECT,EMAG,IDCUB,NKPT,MAXK2,IDIM,MAXR2,NSTA,IGRLV
     60,ISORT,IRCELD,NSPNT,NFTIN,NFPNT
      IF(IGAUS.NE.0) GO TO 300
      CORHAF=COR/2.D0
C
C     SELECT POINTS THAT ARE INVOLVED IN CALCULATING THE GRADIENTS.
C
      J=0
      DO 230 I=1,NSPNT
      RX=COR*KKX(I)+CORHAF+COR
      RY=COR*KKY(I)+CORHAF+COR
      RZ=COR*KKZ(I)+CORHAF+COR
      IF(RX*RX+RY*RY+RZ*RZ.LT.ROSPH*ROSPH) GO TO 220
      J=J+1
      NB(I)=1
      GO TO 230
  220 NB(I)=0
  230 CONTINUE
      NFTIN=J
      I1=0
      I2=NFTIN
      DO 260 I=1,NSPNT
      IF(NB(I).EQ.0) GO TO 240
      I1=I1+1
      J=I1
      GO TO 250
  240 I2=I2+1
      J=I2
  250 CONTINUE
      IRX(J)=KKX(I)
      IRY(J)=KKY(I)
      IRZ(J)=KKZ(I)
      WT(J)=RHORMF(I)
```

DSN=PHBAGA.DIOLA.FCOF

```
  260 CONTINUE
      IDVDIM=III+1
      CALL GRADPT(NPN,IRX,IRY,IRZ,IPT,IDVDIM,NSPNT,IDC)
       KK=SQRT(FLOAT(MAXK2))+2
      RK=0
      DO 270 I=1,III
      SINE(I,1)=0.D0
  270 COSINE(I,1)=1.D0
      RK=0.D0
      DO 280 K=2,KK
      RK=RK+AKR
      AK=AK*CORRAF
      SINE(1,K)=0.D0
  280 COSINE(1,K)=DSIN(AK)/AK
      RK=0.D0
      DO 290 K=2,KK
      RK=AK+AKR
      AK=RK*CORRAF
      SIA=DSIN(AK)/AK
      COA=(DCOS(AK)-SIA)/(4.D0*AK)
      RA=0.D0
      DO 290 I=2,III
      RA=RA+COR
      RARK=RA*RK
      SINE(I,K)=DSIN(RARK)*CCA
  290 COSINE(I,K)=DCOS(RARK)*SIA
      CHFTIN=1.D0/(SUMW*CDENS*6.D0)
  300 CONTINUE
C     IF IW=2,VXCRS1 IS USED TO CALCULATE W(RS)
  305 READ(5,30,END=610) KST,KEND,KINCM,IGRIV,KPTPRT
  307 CONTINUE
C
C     CALCULATE THE CHARGE DENSITY.
C
      CALL ATDEN1(AX,AY,AZ,IDIM,IRX,IRY,IRZ,CCR,RFTIN,RHCRMF,WT,NSPIN,
     &CHFTIN,IVXCR,RHCRV1)
  310 CONTINUE
      DRGAUS=ROGAUS/DFLOAT(NRPNT-1)
      RF=0.D0
      DO 320I=1,NRPNT
      R(I)=RF
      RF=RF+DRGAUS
  320 CONTINUE
      CALL POEXC1(AX,AY,AZ,IDIM,NRPNT,R,RHCR,1,NDIRC,1,NSPIN,IVXCR)
      DRFILN=(ROSPH-ROGAUS)/DFLOAT(NFILON-1)
      RF=ROGAUS
      DO 330 I=1,NFILON
      RFILON(I)=RF
      RF=RF+DRFILN
  330 CONTINUE
      CALL POEXC1(AX,AY,AZ,IDIM,NFILON,RFILON,FLRHCR,NDIRC,NDIRC,0,
     &NSPIN,IVXCR)
      DRWGSZ=(ROWGSZ-ROSPH)/DFLOAT(NWGSIZ-1)
      RF=ROSPH
      DO 340 I=1,NWGSIZ
      RWGSIZ(I)=RF
      RF=RF+DRWGSZ
  340 CONTINUE
```

```
      CALL PCEXC1(AX,AY,AZ,IDIM,NWGSIZ,RWGSIZ,WSRHOR,1,NDIRC,0,NSPIN,
     &IVXCR)
      WRITE(6,600)A,BO,ELECT,EMAG,IDCUB,NKPT,MAXK2,IDIM,MAXR2,NSTA,
     &IGRLV0,ISORT,IRCELL,NSPNT,NPTIN,NRPNT,NDIRC,NFILCN
      IF(IGAUS.NE.0) STOP
C
C     GENERATE INDEPENDENT RECIPROCAL LATTICE VECTORS.
C
      IF(IGRLV0.NE.0)
     &CALL GINDPK(KKX,KKY,KKZ,RSQ,NKPT,IDCUB,MAXK2,NB,1,ISORT,0)
C
C     KPTPRT IS THE NO OF V(K) TO BE PRINTED.
C     GENERATES V(K) FROM KST TO KEND IN STEP KINCM.
C     IGRLV=0, V(K) IS GENERATED IN ORDER OF INCREASING K**2
C     IGRLV=1, V(K) IS GENERATED IN ORDER OF K VECTORS.
C
      IF(IGRLV.NE.0.AND.NSPIN.EQ.1) KIND=3
      IF(IGRLV.NE.0.AND.NSPIN.EQ.2) KIND=9
      IF(IGRLV.EQ.0) KIND=2*NSPIN
      WRITE(6,360)
      IF(KEND.EQ.0) KEND=NKPT
      IF(KST.EQ.0.AND.IGRLV.EQ.0) KST=KSQ(NKPT)+KINCR+1
  360 FORMAT(1H1)
      IF(IGRLV.EQ.0.AND.NSPIN.EQ.1.AND.IW.EQ.1) WRITE(6,370)
      IF(IGRLV.EQ.0.AND.NSPIN.EQ.1.AND.IW.EQ.2) WRITE(6,375)
  370 FORMAT(2X,'K2',1X,'COULOMB(K)',2X,'EWALD(K)',1X,'EXCHANGE(K)',1X,
     &'DENSITY(K)',2X,'CHECK DENS',1X,'SUM VEK',2X,'SUM VEKPK',2X,
     &'SUM VCKPK',2X,'SUM VXCKPK',/)
  375 FORMAT(2X,'K2',1X,'COULOMB(K)',2X,'EWALD(K)',4X,'W(K)',4X,
     &'DENSITY(K)',2X,'CHECK DENS',3X,'SUM VCK',3X,'SUM WXCKPK',/)
      IF(IGRLV.EQ.0.AND.NSPIN.EQ.2.AND.IW.EQ.1) WRITE(6,380)
      IF(IGRLV.EQ.0.AND.NSPIN.EQ.2.AND.IW.EQ.2) WRITE(6,385)
  380 FORMAT(2X,'K2',1X,'COULOMB',2X,'EWALD',3X,'EXCHANGE',3X,'EXCH UP'
     &,3X,'EXCH DOWN',2X,'DENSITY',3X,'CHECK DENS',/)
  385 FORMAT(2X,'K2',1X,'COULOMB',2X,'EWALD',6X,'W',8X,'W UP'
     &,6X,'W DOWN',4X,'DENSITY',3X,'CHECK DENS',/)
      IF(IGRLV.NE.0.AND.NSPIN.EQ.1.AND.IW.EQ.1) WRITE(6,390)
      IF(IGRLV.NE.0.AND.NSPIN.EQ.1.AND.IW.EQ.2) WRITE(6,395)
  390 FORMAT(2X,'K2',1X,'COULOMB(K)',2X,'EWALD(K)',1X,'EXCHANGE(K)',1X,
     2'DEN**(-2/3)',2X,'DENSITY(K)',1X,'KX',1X,'KY',1X,'KZ',1X,'NC',1X,
     3'CHECK DENS',2X,'SUM VEK',2X,'SUB VEKPK',2X,'SUM VCKPK',2X,
     4'SUM WXCKPK',/)
  395 FORMAT(2X,'K2',1X,'COULOMB(K)',2X,'EWALD(K)',4X,'W(K)',7X,
     2'DNDP(K)',4X,'DENSITY(K)',1X,'KX',1X,'KY',1X,'KZ',1X,'NO',3X,
     3'CHECK DENS',2X,'SUM VCK',4X,'SUM WXCKPK',/)
      IF(IGRLV.NE.0.AND.NSPIN.EQ.2.AND.IW.EQ.1) WRITE(6,400)
      IF(IGRLV.NE.0.AND.NSPIN.EQ.2.AND.IW.EQ.1) WRITE(6,402)
      IF(IGRLV.NE.0.AND.NSPIN.EQ.2.AND.IW.EQ.2) WRITE(6,405)
      IF(IGRLV.NE.0.AND.NSPIN.EQ.2.AND.IW.EQ.2) WRITE(6,403)
  400 FORMAT(3X,'K2',1X,'COULOMB',2X,'EWALD',2X,'EXCHANGE',4X,'EXCH UP'
     1,2X,'EXCH DOWN',4X,'D0',9X,'D1',9X,'D2',7X,
     2'DEN UP',5X,'DEN DOWN',3X,'KX',1X,'KY',1X,'KZ',1X,'NO',1X,
     3'CHECK DENS',/)
  402 FORMAT(72X,'D3',9X,'D4',7X,'SUM VEK',3X,'SUM VEKPK',3X
     &,'SUM VCKPK')
  403 FORMAT(72X,'D3',9X,'D4',9X,'SUM WKPK')
  405 FORMAT(3X,'K2',1X,'COULOMB',2X,'EWALD',5X,'W',9X,'W UP'
     1,5X,'W DOWN',6X,'D0',9X,'D1',9X,'D2',7X,
```

```
     2'DEN UP',5X,'DEN DOWN',3X,'KX',1X,'KY',1X,'KZ',1X,'NO',1X,
     3'CHECK DENS',/)
      KS2=-1
      DO 570 NPT=KST,KEND,KINCM
      IF(IGRLV.EQ.0) GO TO 410
      KX=KKX(NPT)
      KY=KKY(NPT)
      KZ=KKZ(NPT)
      NNB=NB(NPT)
      K2=KSQ(NPT)
      GO TO 420
  410 K2=NPT-1
  420 CONTINUE
      IF(K2.NE.0) GO TO 450
C
C     CALCULATE THE FOURIER COEFFICIENT V(K=0)
C
      BK=0.D0
      GEWLD=CEWD*((-2.D0*ELECT-ALPHA)/BETA1+ALPHA/BETA2)
      CALL FILO1(CRO,1,NRPNT,BK,DRGAUS,RHOR,R,0,NRPNT,KIND,CR1)
      CALL FILC1(CRO,1,NFILON,BK,DRFILN,FLRHOR,RFILOR,1,NFLDIM,KIND,CR1)
      DO 425 I=1,NPTIN
      IF(WT(I).LE.0.D0) GO TO425
      CO=6.D0*WT(I)
      II=I
      CR1=CR1+RHORV1(II)*CO
      II=II+NPTIN
  425 CONTINUE
      GCOUL=CR1*CDENS*(-4.D0*PI/3.D0)
      IF(IGRIV.EQ.0) GO TO 440
      GUMUP=ELEUP/OMEGA
      GUMDN=ELEDN/OMEGA
      DO 430 I=1,NPTIN
      IF(WT(I).LE.0.D0) GO TO430
      CO=6.D0*WT(I)
      II=I
      DO 429 K=1,KIND
      CRC(K)=CRO(K)+RHORMF(II)*CO
      II=II+NPTIN
  429 CONTINUE
  430 CONTINUE
      GO TO 550
  440 CONTINUE
      SUM=ELECT/OMEGA
      CALL FILC1 (CRC,1,NWGSIZ,BK,DRWGSZ,WSRHOR,RWGSIZ,1,NWGSIZ,KIND,
     &CR1)
      GO TO 460
C
C     CALCULATE THE FOURIER COEFFICIENTS (K.GT.0)
C
C     CALCULATE THE FOURIER COEFFICIENTS OF THE EXCHANGE POTENTIAL
C
  450 CONTINUE
      RK2=DFLOAT(K2)
      BS=RK2*AKB2
      BK=DSQRT(BS)
      IF(IGRLV.NE.0) GO TO 480
C
```

DSN=PHBAGA.DIOLA.FCOF

```
C      FOURIER COEFFICIENTS ARE GENERATED AS FUNCTION OF K**2.
C      CHARGE DENSITY**1/3 IS ASSUMED TO BE SPHERICALLY SYMMETRIC.
C      INTEGRATE FROM R=0 TO THE RADIUS OF THE WIGNER-SEITZ SPHERE.
C
       CALL FILON(CRO,1,NRPNT,RK,LRGAUS,RHOR,R,0,NRPNT,KIND)
       CALL FILON(CRO,1,NFILON,RK,DRFILN,FLRHOR,RFILON,1,NFLDIM,KIND)
       CALL FILON (CRO,1,NWGSIZ,RK,DRWGSZ,WSRHOR,RWGSIZ,1,NWGSIZ,KIND)
C
C      CALCULATE THE FOURIER COEFFICIENTS OF THE COULOMB POTENTIAL.
C
C
C              GET RO(K) UP  AND RO(K) DN THEN V(K) FOR THE
C              COULOM POTENTIAL
       CALL CCOLOM(CHARUP,SUMUP,RS,FACT)
       GUMUP=SUMUP
       IF(NSPIN.EQ.1) GO TO 451
       CALL COULOM(CHARDN,SUMDN,RS,FACT)
       GUMDN=SUMDN
       SUM=SUMUP+SUMDN
       GUM=SUM
       GO TO 452
  451  SUM=2.D0*SUMUP
       GUM=SUM
  452  CONTINUE
       GCOUL=(SUM*8.D0*PI-CO1)/RS
       GCOUEL=SUM*8.D0*PI/RS
       X=-RS/(4.D0*BETA2)
       CALL CFHYGF(1.D0,1.5D0,X,CFHYG,1.D-10)
       EW=CFHYG*ALPHA/BETA2
       X=-RS/(4.D0*BETA1)
       CALL CFHYGF(1.D0,1.5D0,X,CFHYG,1.D-10)
       EW=EW+CFHYG*(-2.D0*ELECT-ALPHA)/BETA1
       GEWLD=CEWD*EW
   460 CONTINUE
       NNNB=NNB
       ANNB=DFLOAT(NNNB)
       IF(NSPIN.EQ.1) GO TO 470
       RHOK=CRO(1)*CDENS
       GEXCH=CRO(2)*CEXPA
       GEXUP=CRO(3)*CEXFE
       GEXDN=CRO(4)*CEXFE
       IF(NPT.LE.KPTPRT.OR.(K2/200)*200.EQ.K2)
      &WRITE(6,580)K2,GCOUL,GEWLD,GEXCH,GEXUP,GEXDN,SUM,RHOK
C
C      WHEN IW.EQ.1, GEXCH(KS)=VXC(KS)
C
       IF(IW.EQ.2) GO TO 462
       WRITE(1) K2,GCOUL,GEWLD,GEXCH,GEXUP,GEXDN
       WRITE(10)K2,GCOUL,GEWLD,GEXCH,GEXUP,GEXDN,GUMUP,GUMDN,GUM
       VEKSUM=VEKSUM+GCOUEL
       VEKPSM=VEKPSM+GCOUEL*SUM
       VCKSUM=VCKSUM+GCOUL
       VCKPSM=VCKPSM+GCOUL*SUM
       IF(NPT.EQ.619.OR.NPT.EQ.620.OR.(K2/500)*500.EQ.K2)
      &WRITE(6,464) VEKSUM,VEKPSM,VCKSUM,VCKPSM
   462 CONTINUE
   464 FORMAT(05X,5F11.6)
C
```

DSN=PHBAGA.DIOLA.FCOP

```
C      FILE 2 IS USED FOR CALCULATION OF THE TOTAL ENERGY USING VBH
C      POTENTIAL ONLY
C
C      WHEN IW.EQ.2, GEXCH(KS)=W(KS)
C
       IF(IW.EQ.1) GO TO 570
       WRITE(2) K2,GCOUL,GEWLD,GEXCH,GEXUP,GEXDN
       WRITE(11)K2,GCOUL,GEWLD,GEXCH,GEXUP,GEXDN,GUMUP,GUMDN,GUM
       WPUPSM=WPUPSM+GEXUP*SUMUP
       WPDNSM=WPDNSM+GEXDN*SUMDN
       WPUDSM=WPUDSM+WPUPSM+WPDNSM
       IF(NPT.EQ.619.OR.NPT.EQ.620.OR.(K2/500)*500.EQ.K2)
      &WRITE(6,466) WPUPSM,WPDNSM,WPUDSM,GUM
       GO TO 570
  466  FORMAT(76X,4F11.6)
  470  CONTINUE
       RHOK=CRO(1)*CDENS
       GEXCH=CRO(2)*CEXPE
       IF(IW.EQ.2) GO TO 473
       WRITE(1) K2,GCOUL,GEWLD,GEXCH
       WRITE(10)K2,GCOUL,GEWLD,GEXCH,GUM
C      CACULATE SUMS OF VE(KS),VE(KS)*P(KS),VC(KS)*P(KS),VXC(KS)*P(KS)
C      AND W(KS)*P(KS) FOR PARAMAG. ONLY
       VEKSUM=VEKSUM+GCOUEL
       VEKPSM=VEKPSM+GCOUEL*SUM
       VCKSUM=VCKSUM+GCOUL
       VCKPSM=VCKPSM+GCOUL*SUM
       VXCPSM=VXCPSM+GEXCH*SUM
       IF(NPT.LE.KPTPRT.OR.(K2/200)*200.EQ.K2)
      &WRITE(6,475)K2,GCOUL,GEWLD,GEXCH,SUM,RHOK,VEKSUM,VEKPSM,
      &VCKSUM,VCKPSM
  473  CONTINUE
  475  FORMAT(1X,I5,10F11.7)
       IF(IW.EQ.1) GO TO 477
       WRITE(2) K2,GCOUL,GEWLD,GEXCH
       WRITE(11) K2,GCOUL,GEWLD,GEXCH,GUM
       VCKSUM=VCKSUM+GCOUL
       VXCPSM=VXCPSM+GEXCH*SUM
       IF(NPT.LE.KPTPRT.OR.(K2/200)*200.EQ.K2)
      &WRITE(6,475)K2,GCOUL,GEWLD,GEXCH,SUM,RHOK,VCKSUM,VXCPSM
  477  CONTINUE
       GO TO 570
  480  CONTINUE
C
C      FOURIER COEFFICIENTS ARE GENERATED AS FUNCTION OF K VECTORS.
C
C
C      INTEGRATE FROM 0 TO ROGAUS.
C
       IF(KS2.NE.K2)CALL FILON(BSC,1,NRPNT,SK,DRGAUS,RHOR,R,0,NRPM1,KIND)
       DO 490 K=1,KIND
  490  CRO(K)=BRO(K)
C
C      CALCULATE THE CONTRIBUTION FROM REGION BETWEEN NEIGHBORING SPHERES
C      TO THE EXCHANGE POTENTIAL.
C
       N1=KK+1
       N2=KY+1
```

```
      N3=KZ+1
      DO 510  IR=1,NPTIN
      IF(WT(IR).LE.0.D0) GO TO 510
      I1=IRX(IR)+1
      I2=IRY(IR)+1
      I3=IRZ(IR)+1
      C1=COSINE(I1,N1)
      C2=COSINE(I1,N2)
      C3=COSINE(I1,N3)
      C4=COSINE(I2,N1)
      C5=COSINE(I2,N2)
      C6=COSINE(I2,N3)
      C7=COSINE(I3,N1)
      C8=COSINE(I3,N2)
      C9=COSINE(I3,N3)
      S1=SINE(I1,N1)
      S2=SINE(I1,N2)
      S3=SINE(I1,N3)
      S4=SINE(I2,N1)
      S5=SINE(I2,N2)
      S6=SINE(I2,N3)
      S7=SINE(I3,N1)
      S8=SINE(I3,N2)
      S9=SINE(I3,N3)
      C0=(C1*(C5*C9+C6*C8)+C2*(C4*C9+C6*C7)+C3*(C4*C8+C5*C7))*WT(IR)
      D1=(S1*(C5*C9+C6*C8)+S2*(C4*C9+C6*C7)+S3*(C4*C8+C5*C7))*WT(IR)
      D2=(S4*(C2*C9+C3*C8)+S5*(C1*C9+C3*C7)+S6*(C1*C8+C2*C7))*WT(IR)
      D3=(S7*(C2*C6+C3*C5)+S8*(C1*C6+C3*C4)+S9*(C1*C5+C2*C4))*WT(IR)
      IXP=IPT(1,IR)
      IXM=IPT(2,IR)
      IYP=IPT(3,IR)
      IYM=IPT(4,IR)
      IZP=IPT(5,IR)
      IZM=IPT(6,IR)
      II=IR
      DO 500 K=1,KIND
      CBO(K)=CBO(K)+C0*RHORHF(II)+D1*(RHORHF(IXP)-RHCRHF(IXM))
     &      +D2*(RHORHF(IYP)-RHCRHF(IYM))+D3*(RHCRHF(IZP)-RHORHF(IZM))
      II=II+NPTIN
      IXP=IXP+NPTIN
      IYP=IYP+NPTIN
      IZP=IZP+NPTIN
      IXM=IXM+NPTIN
      IYM=IYM+NPTIN
      IZM=IZM+NPTIN
  500 CONTINUE
  510 CONTINUE
C
C     INTEGRATE FROM ROGAUS TO  THE RADIUS OF TOUCHING SPHERE AND SUM
C     OVER THE KUBIC HARMONIC EXPANSION.
C
      IF(KS2.NE.K2)
     &CALL FILON(AHO,NDIRC,NFILON,RK,DRFILN,FLRHOE,RFILOW,0,NFLDIM,KIND)
      RKX=AKR*KX
      RKY=AKR*KY
      RKZ=AKR*KZ
      X2=(RKX/RK)**2
      Y2=(RKY/RK)**2
```

```
      Z2=(BK2/BK)**2
      X4=X2*X2
      Y4=Y2*Y2
      Z4=Z2*Z2
      C41=X4+Y4+Z4-0.6D0
      C61=X2*Y2*Z2+C41/22.D0-1.D0/105.D0
      C81=X4*X4+Y4*Y4+Z4*Z4-5.6D0*C61-21C.E0*C41/143.D0-1.D0/3.D0
      CUBIC(1)=1.D0
      CUBIC(2)=C41*BNO41
C
C     '-' SIGN COMES FROM I**6.
C
      CUBIC(3)=-C61*BNC61
      CUBIC(4)=C81*BNO81
      DO 520 ND=1,NDIRC
      II=ND
      DO 520 K=1,KIND
      CRO(K)=CRO(K)+ARO(II)*CUBIC(ND)
      II=II+NDIRC
  520 CONTINUE
C
C     CALCULATE THE FOURIER COEFFICIENTS OF THE CHARGE DENSITIES FOR
C     BOTH SPINS .
C
      IF(KS2.EQ.K2) GO TO 540
      KS2=K2
      X=-RS/(4.D0*BETA2)
      CALL CFHYGF(1.D0,1.5D0,X,CFHYG,1.D-10)
      EW=CFHYG*ALPHA/BETA2
      X=-RS/(4.D0*BETA1)
      CALL CFHYGF(1.D0,1.5D0,X,CFHYG,1.D-10)
      EW=EW+CFHYG*(-2.D0*ELECT-ALPHA)/BETA1
      GEWLD=CEND*EW
      CALL CCULOB(CHARUP,SUMUP,RS,FACT)
      GUMUP=SUMUP
      IF(NSPIN.EQ.1) GO TO 530
      CALL CCULOB(CHARDN,SUMDN,RS,FACT)
      GUMDN=SUMDN
      GCOUL=((SUMUP+SUMDN)*8.D0*PI-CC1)/RS
      GCOUEL=(SUMUP+SUMDN)*8.D0*PI/RS
      GO TO 540
  530 GUMDN=GUMUP
      GCCUL=(2.D0*SUMUP*8.D0*PI-CC1)/RS
      GCOUEL=2.D0*SUMUP*8.D0*PI/RS
  540 CONTINUE
  550 CONTINUE
      IF(NSPIN.EQ.1) GO TO 560
      RHOK=CRO(1)*CDENS
      GEXCH=CRO(2)*CEXFA
      GEXUP=CRO(3)*CEXFE
      GEXDN=CRO(4)*CEXFE
      GDSPA=CRO(5)*CEXFE
      GDSUP=CRO(6)*CEXFE
      GDSDN=CRO(7)*CEXFE
      GDSUD=CRO(8)*CEXFE
      GDSDU=CRO(9)*CEXFE
      NNNB=NNB
      ANNB=DFLOAT(NNNB)
```

DSN=PHBAGA.DIOLA.FCOF

```
      IF (NPT.LE.KPTPRT.OR. (K2/100) *100.EQ.K2)
     1WRITE(6,580)K2,GCOUL,GEWLD,GEXCH,GEXUP,GEXDN,GDSPA,GDSUP,GDSDN,
     2GUMUP,GUMDN,KX,KY,KZ,NNB,RHOK
      IF (NPT.LE.40)
     &WRITE(6,584) GDSUD,GDSDU
      IF (IW.EQ.2) GO TC 552
      WRITE(1) K2,GCOUL,GEWLD,GEXCH,GEXUP,GEXDN,GDSPA,GDSUP,GDSDN,GDSUD,
     &GDSDU,GUMUP,GUMDN,KX,KY,KZ,NNB
      IF (K2.EQ.0) GO TC 552
      VEKSUM=VEKSUM+GCOUEL*ANNB
      VEKPSM=VEKPSM+GCOUEL*(SUMUP+SUMDN)*ANNB
      VCKPSM=VCKPSM+GCOUL*(SUMUP+SUMDN)*ANNB
      IF(K2.EQ.0.OR.NPT.EQ.2.OR.NPT.EQ.619.OR. (K2/500) *500.EQ.K2)
     &WRITE(6,586) VEKSUM,VEKPSM,VCKPSM
  552 CONTINUE
      IF(IW.EQ.1) GO TC 570
      WRITE(2) K2,GCOUL,GEWLD,GEXCH,GEXUP,GEXDN,GDSPA,GDSUP,GDSDN,GDSUD,
     &GDSDU,GUMUP,GUMDN,KX,KY,KZ,NNB
      IF (K2.NE.0)
     &WKPKSM=WKPKSM+ (GEXUP*SUMUP+GEXDN*SUMDN) *ANNB
      IF(K2.EQ.0.OR.NPT.EQ.2.OR.NPT.EQ.619.OR. (K2/500) *500.EQ.K2)
     &WRITE(6,586) WKPKSM
      GO TO 570
  584 FORMAT(71X,E10.4,2X,E10.4)
  586 FORMAT(90X,3F11.6)
  560 GUM=GUMUP+GUMDN
      RHOK=CHO(1)*CDENS
      GEXCH=CHO(2)*CEXFE
      GDSPA=CHO(3)*CEXFE
      NNNB=NNB
      ANNB=DFLOAT(NNNB)
      IF(IW.EQ.2) GO TO 565
      WRITE(1) K2,GCOUL,GEWLD,GEXCH,GDSPA,GUM,KX,KY,KZ,NNB
      IF(K2.EQ.0) GO TO 563
      VEKSUM=VEKSUM+GCOUEL*ANNB
      VEKPSM=VEKPSM+GCOUEL*2.D0*SUMUP*ANNE
      VCKPSM=VCKPSM+GCOUL*2.D0*SUMUP*ANNE
      VXCPSM=VXCPSM+GEXCH*2.D0*SUMUP*ANNE
  563 CONTINUE
      IF(NPT.LE.KPTPRT.OR. (K2/100) *100.EQ.K2)
     1WRITE(6,590)K2,GCOUL,GEWLD,GEXCH,GDSPA,GDE,KX,KY,KZ,NNB,RHCK,
     2VEKSUM,VEKPSM,VCKPSM,VXCPSM
  565 CONTINUE
      IF(IW.EQ.1) GO TC 570
      IF(K2.EQ.0) GO TC 568
      VCKSUM=VCKSUM+GCOUL*ANNB
      WXCPSM=WXCPSM+GEXCH*2.D0*SUMUP*ANNE
  568 CONTINUE
      WRITE(2) K2,GCOUL,GEWLD,GEXCH,GDSPA,GUM,KX,KY,KZ,NNB
      IF(NPT.LE.KPTPRT.OR. (K2/100) *100.EQ.K2)
     1WRITE(6,590)K2,GCOUL,GEWLD,GEXCH,GDSPA,GUM,KX,KY,KZ,NNB,RHOK,
     2VCKSUM,WXCPSM
  570 CONTINUE
  580 FORMAT(1X,I5,2F8.4,8(1X,E10.4),4I3,1X,E10.4)
  590 FORMAT(1X,I4,5F11.7,2X,4I3,1X,6F11.7)
      WRITE(6,600)A,RC,ELECT,EMAG,IDCUE,NKPT,MAXK2,IDIM,MAXB2,NSTA,IGRLV
     &,ISORT,IRCELD,NSPNT,NPTIN,NBPNT,NDIRC,NFILON,NSGSI2
  600 FORMAT(1X,//,1X,'LATTICE CONST=',F10.5,3X,'R=',F10.5,3X,'ELECT NO=
```

```
     1',F7.2,3X,'MAG NO=',F7.4,3X,'IDCUB=',I5,//,1X,
     2'K NO=',I8,3X,'K2 MAX=',I5,3X,'R NO=',I8,3X,'R2 MAX=',I5,3X,'ORBIT
     3ALS NO=',I5,3X,'GEN RLV=',I2,3X,'SORT=',I2,//,1X,'R DIV=',I5,
     43X,' R PTS=',I5,3X,'NONSPHERICAL PTS=',I5,3X,'GAUS PTS=',I5,5X,
     6'DIRECTION=',I5,3X,'EPSILON=',I6,3X,'NWGSIZ=',I5,/,1H1)
      IF(IW.EQ.2) GO TO 603
      END FILE 1
      IF(IVXCH.EQ.2) IW=IW+IDO
      IF(IW.EQ.2) GO TO 307
      GO TO 300
  603 CONTINUE
      END FILE 2
      GO TO 300
  610 STOP
      END
      SUBROUTINE VXCRS1(UP,DN,DENS,EXPA,EXUP,EXDN,DVUDRU,DVNDRN,DVUDRN,
     1DVNDRU,DVPADR,DVUDRH,DVNDRH,DVUDM,DVNDM,DELO,DVI,DVIA)
C     REVISION OF SUBROUTINE EXBATH, DECEMBER 1979
      IMPLICIT REAL*8(A-H,O-Z)
      COMMON/TOTLE/IW
      F(Z)=(1.D0+Z**3)*DLOG(1.D0+1.D0/Z)+Z/2.D0-Z*Z-1.D0/3.D0
      DENS=UP+DN
      PI=3.14159265358979300
      ONETHD=1.D0/3.D0
      AA=1.D0/2.D0**ONETHD
      COEP=4.D0*AA/(3.D0*(1.D0-AA))
      ONEPOR=1.D0/4.D0
      FORTHD=4.D0/3.D0
      CP=0.04612D0
      BP=39.7D0
      CF=.02628D0
      BF=70.6D0
      RS=(3.D0/(4.D0*PI*DENS))**ONETHD
      UPX=-2.D0*((9.D0*PI/4.D0)**ONETHD)/(PI*RS)
      ECP=-CP*F(RS/BP)
      ECF=-CF*F(RS/BF)
      UNC=COEP*(ECP-ECF)
      UCP=-CP*DLOG(1.D0+BP/RS)
      UCF=-CF*DLOG(1.D0+BF/RS)
      A=UPX+UNC
      TC=UCP-UCF-FORTHD*(ECF-ECP)
      B=(UCP-AA*UCF)/(1.D0-AA)
      C=TC/(1.D0-AA)
      XUP=UP/DENS
      XDN=DN/DENS
      IF(IW.EQ.2) GO TO 10
      X4=XUP**FORTHD+XDN**FORTHD
      CQ=B+C*X4
      QA=(2.D0*XUP)**ONETHD
      QB=(2.D0*XDN)**ONETHD
      QC=AA*QA
      QD=AA*QB
      EXUP=CQ+A*QA
      EXDN=CQ+A*QB
      EXPA=A+B+AA*C
      FLX=(X4-AA)/(1.D0-AA)
      DVT=28.D0*ONETHD*(ECF-ECP-6.D0*(UCF-UCP)/7.D0)*(FLX+AA/(1.D0-AA))
      DVI = DVT-CF*BF*FLX/(BF+RS)-CP*BP*(1.D0-FLX)/(BP+RS)
```

```
      DVT=ONETHD*DVT/DENS
      DVUDRU=DVT+ONETHD*A*QA/UP+8.D0*ONETHD*C*QC/DENS
      DVNDRN=DVT+ONETHD*A*QB/DN+8.D0*ONETHD*C*QD/DENS
      DVUDRN=DVT+FORTHD*C*(QC+QD)/DENS
      DVNDRU=DVUDRN
      DVPADR=DVT+8.D0*ONETHD*C*AA/DENS+ONETHD*A/DENS
      DVUDRH=0.5D0*(DVUDRU+DVUDRN)
      DVNDRH=0.5D0*(DVNDRU+DVNDRN)
      DVUDM=0.5D0*(DVUDRU-DVUDRN)
      DVNDM=-0.5D0*(DVNDRN-DVUDRN)
      DEL0=0.5D0*(DVUDRH+DVNDRH)
      DEL1=0.5D0*(DVUDRH-DVNDRH)
      DEL2=0.5D0*(DVUDM-DVNDM)
      RETURN
   10 CONTINUE
      GR=AA*(UCP-UCP-7.D0*ONETHD*(ECP-ECP))/(1.D0-AA)
      PR=(ONEFOR*UPX+UAC+GR)/AA
      QR=UCP-ECP-UNC-GR
      WUP=PR*XUP**ONETHD+QR
      WDN=PR*XDN**ONETHD+QR
      WPA=PR*AA+QR
      DGDRS=AA*(CP*RP/(RS+RP)-CP*RP/(RS+RP)-7.D0*(ECP-ECP-UCP+UCP))/
     &(1.D0-AA)/RS
      DPDRS=-UPX/(4.D0*AA*RS)+4.D0*(ECP-ECP-UCP+UCP)/(1.D0-AA)/RS+
     &DGDRS/AA
      DQDRS=CP*RP/RS/(RS+RP)-3.D0*(ECP-UCP)/RS-4.D0*AA*(ECP-ECP-UCP+UCP)
     &/(1.D0-AA)/RS-DGDRS
      DVD1=-(DPDRS*XUP**ONETHD+DQDRS)*RS*ONETHD/DENS
      DVD2=-(DPDRS*XDN**ONETHD+DQDRS)*RS*ONETHD/DENS
      DWUDRU=DVD1+PR*XDN*XUP**(-2.D0*ONETHD)*ONETHD/DENS
      DWNDRN=DVD2+PR*XUP*XDN**(-2.D0*ONETHD)*ONETHD/DENS
      DWUDRN=DVD1-PR*XUP**ONETHD*ONETHD/DENS
      DWNDRU=DVD2-PR*XDN**ONETHD*ONETHD/DENS
      DWPADR=-(DPDRS*AA+DQDRS)*RS*ONETHD/DENS
      EXPA=WPA
      EXUP=WUP
      EXDN=WDN
      DVUDRU=DWUDRU
      DVNDRN=DWNDRN
      DVUDRN=DWUDRN
      DVNDRU=DWNDRU
      DVPADR=DWPADR
      DVT=DVD1
      DVTA=DVD2
      RETURN
      END
      SUBROUTINE POEXC1(AX,AY,AZ,IDIM,NRPNT,R,RHOR,NDIRC,NDTOL,IGMAT,
     &NSFIN,IVICM)
C
C     CALCULATE THE CUBIC HARMONICS EXPANSION COEFFICIENTS OF THE
C     FUNCTIONS OF THE CHARGE DENSITIES.
C     GAUSSIAN TYPE ORBITALS ARE USED.
C
C * * * * * * * * * * * * * * * * * * * * * * * * * * * * * * * * * * * *
      IMPLICIT REAL*8(A-F,H,O-Z)
      DIMENSION AX(IDIM),AY(IDIM),AZ(IDIM),RHOR(1),R(1)
      DIMENSION CC(4,4),D(4)
      COMMON/VKO/C(7,14),EX(7,14),FACTO(10),IB(7),NORB(7),NSTA
```

DSN=PHBAGA.DIOLA.FCOP

```
      COMMON/EXCH/BX(4),BY(4),BZ(4),CNC01,CNO41,CNO61,CNO81,CMAT(4,4)
      COMMON/XCHARG/CHARGE(7),CHARUP(7),CHARDN(7)
      COMMON/XCONST/A,PI,SIXPI,ONETHD,TWTHIV,IPUN,IGAUS
C
C     CALCULATE THE KUBIC HARMONICS ALONG EACH DIRECTIONS.
C
      SIXPA=SIXPI/2.D0**ONETHD
      CONST=1.D0/(4.D0*PI)
      IF(IGMAT.EQ.0) GO TO 50
      DO 10I=1,NDTOL
      RR=BX(I)*BX(I)+BY(I)*BY(I)+BZ(I)*BZ(I)
      RA=DSQRT(RR)
      BX(I)=BX(I)/RA
      BY(I)=BY(I)/RA
      BZ(I)=BZ(I)/RA
      X2=BX(I)*BX(I)
      Y2=BY(I)*BY(I)
      Z2=BZ(I)*BZ(I)
      X4=X2*X2
      Y4=Y2*Y2
      Z4=Z2*Z2
      C41=X4+Y4+Z4-0.6D0
      C61=X2*Y2*Z2+C41/22.D0-1.D0/105.D0
      C81=X4*X4+Y4*Y4+Z4*Z4-5.6D0*C61-210.D0*C41/143.D0-1.D0/3.D0
      CMAT(I,1)=CNO01
      CMAT(I,2)=C41*CNC41
      CMAT(I,3)=C61*CNO61
      CMAT(I,4)=C81*CNO81
      WRITE(6,40)BX(I),BY(I),BZ(I),(CMAT(I,J),J=1,NDTOL)
   10 CONTINUE
C
C     CALCULATE THE INVERSE OF THE MATRIX.
C
      CALL GMIS(NDTOI,CMAT,CC,D,DET,4)
      DO 20I=1,NDTOL
   20 WRITE(6,30)BX(I),BY(I),BZ(I),(CMAT(I,J),J=1,NDTOL)
   30 FORMAT(1X,'A=(',3F10.5,')',4F15.5)
   40 FORMAT(1X,'A=(',3F10.5,')',5X,'K01=',F10.5,5X,'K41=',F10.5,3X,'K61
     &=',F10.5,3X,'K81=',F15.5)
   50 CONTINUE
C
C     CALCULATE THE DENSITY ALONG EACH DIRECTIONS (BX(I),BY(I),BZ(I))
C     AND THE KUBIC HARMONIC EXPANSION COEFFICIENTS.
C
      WRITE(6,60 )
   60 FORMAT(1X,//,14X,'F',9X,'DENSITY',10X,'KUBIC HARM. COEF. FOR THE P
     &ARAMAGNETIC EXCHANGE POTENTIAL',/)
      IKRT=NRPNT*NDIRC
      IF(NSPIN.EQ.1) GO TO 170
C
C     FERROMAGNETIC
C
      IKRTOL=IKRT*9
      DO 70  I=1,IKRTOL
   70 RHOK(I)=0.D0
      DO 160 KR=1,NRPNT
      DO 140 ND=1,NDTOL
      DENSUP=0.D0
```

```
      DENSDN=0.D0
      X=R(KB)*RX(ND)
      Y=R(KB)*RY(ND)
      Z=R(KB)*RZ(ND)
      DO 120I=1,NSTA
      IBE=IB(I)-1
      SUM=0.D0
      N=NORB(I)
      DO 110JJ=1,IDIM
      PSI=0.D0
      RA2=(AX(JJ)-X)**2+(AY(JJ)-Y)**2+(AZ(JJ)-Z)**2
      RA=DSQRT(RA2)
      IF(RA.LE.0.0) GO TO 90
      DO 80 J=1,N
      EAX=RA2*EX(I,J)
      IF(EAX.GT.25.D0)GO TO 80
      REX=C(I,J)*RA**IEB*DEXP(-EAX)
      PSI=PSI+REX
   80 CONTINUE
      GO TO 110
   90 IF(IEB.NE.0) GO TO 110
      DO 100J=1,N
      PSI=PSI+C(I,J)
  100 CONTINUE
  110 SUM=SUM+PSI*PSI
      DENSUP=DENSUP+SUM*CHARUP(I)*CONST
      DENSDN=DENSDN+SUM*CHARDN(I)*CONST
  120 CONTINUE
         IF(IVXCR.EQ.2) GO TO  123
       DENS=DENSUP+DENSDN
      CX=DENS**ONETHD*SIXPA
      UP=DENSUP**ONETHD*SIXPI
      DN=DENSDN**ONETHD*SIXPI
      D0=DENS**TWTHIV*SIXPA/3.D0
      D1=DENSUP**TWTHIV*SIXPI/3.D0
      D2=DENSDN**TWTHIV*SIXPI/3.D0
         GO TO 127
  123 CALL VXCBS1(DENSUP,DENSDN,DENS,CX,UP,DN,D1,D2,D3,D4,D0,CA,CB,CE,
     &CF,DELO,DVT,DVTA)
  127 CONTINUE
      DO 130 I=1,NDIBC
      IKB=(I-1)*NBPNT+KB
      I2=IKB+IKBT
      I3=I2+IKBT
      I4=I3+IKBT
      I5=I4+IKBT
      I6=I5+IKBT
      I7=I6+IKBT
      I8=I7+IKBT
      I9=I8+IKBT
      RHOR(IKB)=RHOR(IKB)+CMAT(I,ND)*DENS
      RHOR(I2)=RHOR(I2)+CMAT(I,ND)*CX
      RHOR(I3)=RHOR(I3)+CMAT(I,ND)*UP
      RHOR(I4)=RHOR(I4)+CMAT(I,ND)*DN
      RHOR(I5)=RHOR(I5)+CMAT(I,ND)*D0
      RHOR(I6)=RHOR(I6)+CMAT(I,ND)*D1
      RHOR(I7)=RHOR(I7)+CMAT(I,ND)*D2
      RHOR(I8)=RHOR(I8)+CMAT(I,ND)*D3
```

```
      RHOR(19)=RHOR(19)+CMAT(I,ND)*D4
  130 CONTINUE
  140 CONTINUE
      DENS=RHOR(KR)*CNO01
      WRITE(6,150) KR,R(KR),DENS,CX,UP,DN,D0,D1,D2,D3,D4,DVT,DVTA
  150 FORMAT(1X,I4,F7.3,9(1X,E10.4),2(1X,E9.3))
  160 CONTINUE
      RETURN
  170 CONTINUE
C
C     PARAMAGENTIC.
C
      IKRTOL=IKRT*3
      DO 180 I=1,IKRTOL
  180 RHOR(I)=0.D0
      DO 270 KR=1,NRPNT
      DO 250 ND=1,NDTOL
      DENSUP=0.D0
      X=R(KR)*RX(ND)
      Y=R(KR)*RY(ND)
      Z=R(KR)*RZ(ND)
      DO 230I=1,NSTA
      IBB=IB(I)-1
      SUM=0.D0
      N=NORB(I)
      DO 220 JJ=1,IDIM
      PSI=0.D0
      RA2=(AX(JJ)-X)**2+(AY(JJ)-Y)**2+(AZ(JJ)-Z)**2
      RA=DSQRT(RA2)
      IF(RA.LE.0.0) GO TO 200
      DO 190 J=1,N
      EAX=RA2*EX(I,J)
      IF(EAX.GT.25.D0)GO TO 190
      REX=C(I,J)*RA**IBB*DEXP(-EAX)
      PSI=PSI+REX
  190 CONTINUE
      GO TO 220
  200 IF(IBB.NE.0) GO TO 220
      DO 210J=1,N
      PSI=PSI+C(I,J)
  210 CONTINUE
  220 SUM=SUM+PSI*PSI
      DENSUP=DENSUP+SUM*CHARUP(I)*CONST
  230 CONTINUE
         IF(IVXCR.EQ.2) GO TO 233
       DENS=DENSUP*2.D0
      UP=DENSUP**ONETHD*SIXPI
      DO=DENS**TWTHIV*SIXPA/3.D0
         GO TO 237
  233 CALL VXCRS1(DENSUP,DENSUP,DENS,CX,UP,DN,D1,D2,D3,D4,DO,CA,CB,CE,
     &CF,DEIO,DEL1,DEI2)
  237 CONTINUE
      DO 240 I=1,NDIRC
      IKR=(I-1)*NRPNT+KR
      I2=IKR+IKRT
      I3=I2+IKRT
      RHOR(IKR)=RHOR(IKR)+CMAT(I,ND)*DENS
      RHOR(I2)=RHOR(I2)+CMAT(I,ND)*UP
```

```
      RHOR(I3)=RHOR(I3)+CMAT(I,ND)*DO
  240 CONTINUE
  250 CONTINUE
      DENS=RHOR(KR)*CNOO1
      WRITE(6,150)  KR,R(KR),DENS,UP,DO
  270 CONTINUE
      RETURN
      END
      SUBROUTINE ATDEN1(AX,AY,AZ,IDIM,IRX,IRY,IRZ,COR,NRPNT,RHOR,WT,
     &NSPIN,CMFTIN,IVXCR,RHORV1)
C
C     CALCULATE CHARGE DENSITIES AT POINTS (IRX,IRY,IRZ)  BY
C     SUPERPOSITION OF NEUTRAL ATOM CHARGE DENSITY.
C     GAUSSIAN TYPE ORBITALS ARE USED.
C
C * * * * * * * * * * * * * * * * * * * * * * * * * * * * * * * * * * * *
      IMPLICIT REAL*8(A-F,H,O-Z)
      INTEGER*2 IRX(NRPNT),IRY(NRPNT),IRZ(NRPNT)
      DIMENSION RHOR(1),WT(1),RHORV1(1)
      DIMENSION AX(IDIM),AY(IDIM),AZ(IDIM)
      COMMON/VKO/C(7,14),EX(7,14),FACTO(10),IB(7),NORB(7),NSTA
      COMMON/XCHARG/CHARGE(7),CHARUP(7),CHARDN(7)
      COMMON/XCONST/A,PI,SIXPI,ONETHD,TWTHIV,IPUN,IGAUS
      SIXPA=SIXPI/2.D0**ONETHD
      CONST=1.D0/(4.D0*PI)
      IF(NSPIN.EQ.1)  GO TO 110
C
C     FERROMAGNETIC
C
      IF(IGAUS.NE.0)  WRITE(6,10 )
   10 FORMAT(//,6X,'R',10X,'X',10X,'Y',10X,'Z',16X,'DENSITY',14X,'DENSIT
     &Y  UP',14X,'DENSITY DN',//)
      DO 100 KR=1,NRPNT
      DENSUP=0.D0
      DENSDN=0.D0
      X=IRX(KR)*COR
      Y=IRY(KR)*COR
      Z=IRZ(KR)*COR
      R2=X*X+Y*Y+Z*Z
      DO 60 I=1,NSTA
      IBB=IB(I)-1
      SUM=0.D0
      N=NORB(I)
      DO 50 JJ=1,IDIM
      PSI=0.D0
      RA2=(AX(JJ)-X)**2+(AY(JJ)-Y)**2+(AZ(JJ)-Z)**2
      RA=DSQRT(RA2)
      IF(RA.LE.0.0)  GO TO 30
      DO 20 J=1,N
      EAX=RA2*EX(I,J)
      IF(EAX.GT.25.D0)GO TO 20
      REX=C(I,J)*RA**IBB*DEXP(-EAX)
      PSI=PSI+REX
   20 CONTINUE
      GO TO 50
   30 IF(IBB.NE.0)  GO TO 50
      DO 40 J=1,N
      PSI=PSI+C(I,J)
```

```
   40 CONTINUE
   50 SUM=SUM+PSI*PSI
      DRUP=SUM*CHARUP(I)*CONST
      DRDN=SUM*CHARDN(I)*CONST
      DENSUP=DENSUP+DRUP
      DENSDN=DENSDN+DRDN
      IF(IGAUS.EQ.0) GO TO 60
      DRP=DRUP+DRDNP
      WRITE(6,70 ) DRP,DRUP,DRDN,I
   60 CONTINUE
   70 FORMAT(41X,3F20.5,I5)
      DENS=DENSUP+DENSDN
      IF(IGAUS.NE.0)
     &WRITE(6,90 ) R2,X,Y,Z,DENS,DENSUP,DENSDN,WT(KR)
      IF(IPUN.NE.0)
     &WRITE(7,80 ) X,Y,Z,DENS,DENSUP,DENSDN,WT(KR)
   80 FORMAT(3F9.7,1X,4F13.7)
   90 FORMAT(1X,4F10.5,4F20.6,I5)
      IF(IVXCR.NE.0) GO TO 93
      CX=DENS**ONETHD*SIXPA
      UP=DENSUP**ONETHD*SIXPI
      DN=DENSDN**ONETHD*SIXPI
      D0=DENS**TWTHIV*SIXPA/3.D0
      D1=DENSUP**TWTHIV*SIXPI/3.D0
      D2=DENSDN**TWTHIV*SIXPI/3.D0
      GO TO 97
   93 CALL VXCRS1(DENSUP,DENSDN,DENS,CX,UP,DN,D1,D2,D3,D4,D0,CA,CB,CE,
     &CP,DE10,DEL1,DEL2)
   97 CONTINUE
      RHORV1(KR)=CNFTIN*DENS*R2
      RHOR(KR)=CNFTIN*DENS
      RHOR(KR+NRPNT)=CNFTIN*CX
      RHOR(KR+2*NRPNT)=CNFTIN*UP
      RHOR(KR+3*NRPNT)=CNFTIN*DN
      RHOR(KR+4*NRPNT)=CNFTIN*D0
      RHOR(KR+5*NRPNT)=CNFTIN*D1
      RHOR(KR+6*NRPNT)=CNFTIN*D2
      RHOR(KR+7*NRPNT)=CNFTIN*D3
      RHOR(KR+8*NRPNT)=CNFTIN*D4
  100 CONTINUE
      RETURN
  110 CONTINUE
C
C     PARAMAGENTIC.
C
      IF(IGAUS.NE.0) WRITE(6,120)
  120 FORMAT(//,6X,'R',10X,'X',10X,'Y',10X,'Z',18X,'DENSITY',//)
      DO 190 KR=1,NRPNT
      DENSUP=0.D0
      X=IRX(KR)*COR
      Y=IRY(KR)*COR
      Z=IRZ(KR)*COR
      R2=X*X+Y*Y+Z*Z
      DO 1701=1,NSTA
      IBB=IB(I)-1
      SUM=0.D0
      N=NORB(I)
      DO 160 JJ=1,IDIM
```

DSN=PHBAGA.DIOLA.FCOF

```
      PSI=0.D0
      RA2=(AX(JJ)-X)**2+(AY(JJ)-Y)**2+(AZ(JJ)-Z)**2
      RA=DSQRT(RA2)
      IF(RA.LE.0.0) GO TC 140
      DO 130 J=1,N
      EAX=RA2*EX(I,J)
      IF(EAX.GT.25.D0)GO TO 130
      REX=C(I,J)*RA**IEB*DEXP(-EAX)
      PSI=PSI+REX
  130 CONTINUE
      GO TC 160
  140 IF(IEB.NE.0) GO TO 160
      DO 150J=1,N
      PSI=PSI+C(I,J)
  150 CONTINUE
  160 SUM=SUM+PSI*PSI
      DRUP=SUM*CHARUP(I)*CONST
      DENSUP=DENSUP+DRUP
      IF(IGAUS.EQ.0) GO TO 170
      WRITE(6,180)DRUP,I
  170 CONTINUE
  180 FORMAT(41X,F20.5,I5)
      IF(IGAUS.NE.0)
     &WRITE(6,90 ) R2,X,Y,Z,DENSUP,WT(KR)
      IF(IPUN.NE.0)
     &WRITE(7,80 ) X,Y,Z,DENSUP,WT(KR)
      IF(IVXCR.NE.0) GO TO 183
      DENS=DENSUP*2.D0
      UP=DENSUP**ONETHD*SIXPI
      DN=DENS**TWTHIV*SIXPA/3.D0
      GO TO 187
  183 CALL VXCRS1(DENSUP,DENSUP,DENS,CX,UP,DN,D1,D2,D3,D4,D0,CA,CB,CE,
     &CF,DEL0,DEL1,DEL2)
  187 CONTINUE
      RHOBV1(KR)=CMPTIN*DENS*R2
      RHOA(KR)=CMPTIN*DENS
      RHOB(KR+NRPNT)=CMPTIN*UP
      RHOB(KR+2*NRPNT)=CMPTIN*DN
  190 CONTINUE
      RETURN
      END
      SUBROUTINE FILC1(ABC,NDIBC,NRPNT,RK,DRFILN,RHOB,RFILON,NZERC,NDIM,
     &KIND,AB1)
C
C     INTEGRATE F(R)*J1(KR)*R**2 OV R BY FILON INTEGRATION METHCD.
C     J1(KR) IS THE SPHERICAL BESSEL FUNCTION OF ORDER 1.
C     5 POINTS BODE'S RULE IS USED IF K=0.
C
C * * * * * * * * * * * * * * * * * * * * * * * * * * * * * * * * * * * *
      IMPLICIT REAL*8(A-F,H,C-Z)
      COMPLEX*16 TPBELS,TPEB2,TPBB4
      DIMENSION ABC(1),RHOB(1),RFILON(1)
      PI=3.14159265358SDC
      IF(NZERO.NE.0) GC TO 20
      NT=NDIBC*KIND
      AB1=0.D0
      DO 10  I=1,NT
      ABC(I)=0.D0
```

DSN=PHDAGA.DIOLA.FCOF

```
   10 CONTINUE
   20 CONTINUE
      IF(RK.LT.1.D-5) GO TO 120
      TH=RK*DRFILN
      TH2=TH*TH
      IF(TH.LT.1.D-4) GO TO 30
      SIN1=DSIN(TH)
      COS1=DCOS(TH)
      SIN2=2.D0*SIN1*COS1
      ALPHA=(1.D0+SIN2/(2.D0*TH)-2.D0*SIN1*SIN1/TH2)/TH
      BETA=2.D0*(1+COS1*COS1-SIN2/TH)/TH2
      AGAMA=4.D0*(SIN1/TH-COS1)/TH2
      GO TO 40
   30 CONTINUE
      TH3=TH2*TH
      TH4=TH2*TH2
      ALPHA=2.D0*TH3*(1.D0/45.D0-TH2/315.D0+TH4/4725.D0)
      BETA=2.D0*(1.D0/3.D0+TH2/15.D0-2.D0*TH4/105.D0+TH4*TH2/567.D0)
      AGAMA=4.D0/3.D0-2.D0*TH2/15.D0+TH4/210.D0-TH4*TH2/11340.D0
   40 CONTINUE
      IF(NDIRC.EQ.1) GO TO 100
      DO 90  I=1,NRPNT
      RAK=RK*RFILON(I)
      CR0=1.D0/(RAK*RAK)
      CR1=3.D0/(RK*RAK)
      CR2=DSIN(RAK)/RK
      CR3=DCOS(RAK)/RK
      SPBELS=CR2*RFILON(I)
      SPBM2=CR1*CR2-SPBELS-3.D0*CR3/RK
      SPBM4=SPBELS
      IF(I.NE.1.AND.I.NE.NRPNT) GO TO 50
      APBELS=CR3*RFILON(I)
      TPBELS=APBELS
      TPBM2=DCMPLX(CR1*CR3-APBELS,-3.D0*CR2/RK)
      TPBM4=TPBELS
   50 DO 90  ND=1,NDIRC
      IF(ND.EQ.1) GO TO 60
      CL=DFLOAT(2*ND)
      C1=2.D0*CL-1.D0
      C3=C1-2.D0
      C5=C3-2.D0
      C6=4.D0*CL-6.D0
      SPBELS=(C3*C1*CR0-C6/C5)*SPBM2-C1/C5*SPBM4
      SPBM4=SPBM2
      SPBM2=SPBELS
      IF(I.NE.1.AND.I.NE.NRPNT) GO TO 60
      TPBELS=(C3*C1*CR0-C6/C5)*TPBM2-C1/C5*TPBM4
      TPBM4=TPBM2
      TPBM2=TPBELS
   60 CONTINUE
      IF((I/2)*2.EQ.I) SPBELS=SPBELS*AGAMA
      IF((I/2)*2.NE.I) SPBELS=SPBELS*BETA
      IF(I.NE.1.AND.I.NE.NRPNT) GO TO 70
      BELS=TPBELS*(1.D0,1.D0)
      IF(I.EQ.1) SPBELS=SPBELS/2.D0+ALPHA*BELS
      IF(I.EQ.NRPNT) SPBELS=SPBELS/2.D0-ALPHA*BELS
   70 CONTINUE
      SPBELS=SPBELS*DRFILN
```

DSN=PHBAGA.DIOLA.FCOF

```
      IND=(ND-1)*NRPNT+I
      KD=ND
      DO 80 K=1,KIND
      ARO(KD)=ARO(KD)+RHOR(IND)*SPBELS
      IND=IND+NDIM
      KD=KD+NDIRC
   80 CONTINUE
   90 CONTINUE
      RETURN
  100 CONTINUE
      DO 110 I=1,NRPNT
      RAK=RK*RFILON(I)
      SPBELS=DSIN(RAK)*RFILON(1)/RK
      IF((1/2)*2.EQ.I) SPBELS=SPBELS*AGAMA
      IF((1/2)*2.NE.I) SPBELS=SPBELS*BETA
      IF(I.EQ.1) SPBELS=SPBELS/2.D0+ALPHA*DCOS(RAK)*RFILON(I)/RK
      IF(I.EQ.NRPNT) SPBELS=SPBELS/2.D0-ALPHA*DCOS(RAK)*RFILON(I)/RK
      SPBELS=SPBELS*DRFILN
      II=I
      DO 110 K=1,KIND
      ARO(K)=ARO(K)+RHOR(II)*SPBELS
      II=II+NDIM
  110 CONTINUE
      RETURN
  120 CONTINUE
C
C     K=0
C
      DO 130 I=1,NRPNT,4
      II=I
      CC1=RFILON(I)**4*DRFILN*14.D0/45.D0
      IF(I.NE.1.AND.I.NE.NRPNT) CC1=CC1*2.D0
      AR1=AR1+RHOR(II)*CC1
      CO=RFILON(I)**2*DRFILN*14.D0/45.D0
      IF(I.NE.1.AND.I.NE.NRPNT) CO=CO*2.D0
      DO 130 K=1,KIND
      ARO(K)=ARO(K)+RHOR(II)*CO
      II=II+NDIM
  130 CONTINUE
      NRP2=NRPNT-2
      DO 140 I=3,NRP2,4
      II=I
      CC1=RFILON(I)**4*DRFILN*24.D0/45.D0
      AR1=AR1+RHOR(II)*CC1
      CO=RFILON(I)**2*DRFILN*24.D0/45.D0
      DO 140 K=1,KIND
      ARO(K)=ARO(K)+RHOR(II)*CO
      II=II+NDIM
  140 CONTINUE
      NRP1=NRPNT-1
      DO 150 I=2,NRP1,2
      II=I
      CC1=RFILON(I)**4*DRFILN*64.D0/45.D0
      AR1=AR1+RHOR(II)*CC1
      CO=RFILON(I)**2*DRFILN*64.D0/45.D0
      DO 150 K=1,KIND
      ARO(K)=ARO(K)+RHOR(II)*CO
      II=II+NDIM
```

DSN=PHBAGA.DIOLA.FCOF

```
  150 CONTINUE
      RETURN
      END
//LKED.SYSLIB  DD DSN=D1103.CALLAWAY.BVCMPLIB,DISP=SHR
//     DD DSN=D1103.CALLAWAY.BNDPKG.SUBLIB.COMPL,DISP=SHR
//      DD DSN=SYS1.VFORTLIB,DISP=SHR
//      DD DSN=SYS2.FORTLIB,DISP=SHR
//      DD DSN=SYS2.SSP.LIB,DISP=SHR
//      DD DSN=SYS2.PLOT.LIB,DISP=SHR
//GO.FT01F001 DD UNIT=3380,VOL=SER=USER77,DISP=(NEW,CATLG),
//       SPACE=(TRK,(10,10),RLSE),
//      DCB=(BLKSIZE=06404,RECFM=VBS,LRECL=64),
//             DSNAME=PHBAGA.DIOLA.FEF5P4.BCC.VK1
//GO.FT01F002 DD UNIT=3380,VOL=SER=USER77,DISP=(NEW,CATLG),
//       SPACE=(TRK,(10,10),RLSE),
//      DCB=(BLKSIZE=02804,RECFM=VBS,LRECL=28),
//             DSNAME=PHBAGA.DIOLA.FEF5P4.BCC.VK2
//*GO.FT02F001 DD UNIT=3380,VOL=SER=USER77,DISP=(NEW,CATLG),
//*       SPACE=(TRK,(10,10),RLSE),
//*      DCB=(BLKSIZE=06404,RECFM=VBS,LRECL=64),
//*             DSNAME=PHBAGA.DIOLA.FEF5P4.BCC.VK3
//*GO.FT02F002 DD UNIT=3380,VOL=SER=USER77,DISP=(NEW,CATLG),
//*       SPACE=(TRK,(10,10),RLSE),
//*      DCB=(BLKSIZE=02804,RECFM=VBS,LRECL=28),
//*             DSNAME=PHBAGA.DIOLA.FEF5P4.BCC.VK4
//GO.FT10F001 DD UNIT=3380,VOL=SER=USER77,DISP=(NEW,CATLG),
//         SPACE=(TRK,(30,10),RLSE),
//      DCB=(BLKSIZE=6000,RECFM=VBS,LRECL=40),
//       DSNAME=PHBAGA.DIOLA.FEF5P4.BCC.VKL
//*GO.FT11F001 DD UNIT=3380,VOL=SER=USER77,DISP=(NEW,CATLG),
//*         SPACE=(TRK,(30,10),RLSE),
//*      DCB=(BLKSIZE=6000,RECFM=VBS,LRECL=40),
//*       DSNAME=PHBAGA.DIOLA.FEF5P4.BCC.VKL
//GO.SYSIN DD *
   5.4057    1.0
    2 8000 2000   400    25    2    3    1    1    0   24  201  201  101    0
    2    1    0
     IBON      4   14 1.00   1.00   1.00   1.00   1.00   1.00   0.50   0.50
  257539.000000        0.000290       -0.000090        0.000030       -0.000010
   38636.900000        0.002260       -0.000680        0.000250       -0.000050
    8891.440000        0.011520       -0.003540        0.001310       -0.000270
    2544.010000        0.045660       -0.014150        0.005290       -0.001120
     844.777000        0.140350       -0.046880        0.017380       -0.003660
     312.527000        0.314200       -0.117530        0.045270       -0.009630
     125.593000        0.408780       -0.219620        0.085050       -0.017940
      53.498700        0.211630       -0.126610        0.058570       -0.012940
      17.715100        0.017650        0.517710       -0.304220        0.068870
       7.376770       -0.002920        0.604690       -0.495030        0.114380
       2.018470        0.000860        0.054560        0.671410       -0.192220
       0.779935       -0.000410       -0.009560        0.593010       -0.303710
       0.114220        0.000110        0.002290        0.011490        0.579850
       0.041889       -0.000050       -0.001060       -0.003120        0.558820
     IBON      2    9 3.00   3.00   3.00   3.00
    1678.400000        0.002490       -0.000900
     396.392000        0.020150       -0.007350
     126.586000        0.091990       -0.034720
      49.115800        0.259910       -0.101890
      20.503500        0.426870       -0.183100
```

```
                                    ESN=PHBAGA.DIOLA.FCOF
        8.987120          0.326910         -0.104200
        3.682490          0.062750          0.321950
        1.521750         -0.001610          0.569250
        0.592684          0.001220          0.268630
   IRON      1     5 4.6     2.4
       41.452600          0.025110
       11.540300          0.136260
        3.885430          0.353230
        1.323800          0.468670
        0.416680          0.343950
 0    4
      0
  1    0     1    1  100
  0 8001     1    0  100
//
```

APPENDIX A.2: New Version of PROGRAM SCF2

```
                                   DSN=PHBAGA.DIOLA.SCF
------------------------------------------------------------------------
//PHBAGA01 JOB (1103,60245,010,3),'PH.DIOLA',MSGCLASS=S,
//       NOTIFY=PHBAGA
/*AFTER     PHBAGA00
/*JOBPARM SHIFT=N
/*ROUTE PRINT PHYSICS
// EXEC FORTHCLG,PARM.FORT='NOSOURCE,LANGLVL(66),OPT(2)',
//       PARM.LKED=NOXREF,REGION=1200K,TIME=999
//FORT.SYSIN DD *
C
C
C                                PROGRAM SCF2
C                      THE FIFTH PART (FERROMAGNET) OF
C
C     A GENERAL PROGRAM TO CALCULATE SELF-CONSISTANT ENERGY BANDS
C
C         USING THE MODIFIED TIGHT BINDING OR LCGC METHOD
C
C                                    BY
C
C                        C.S. WANG AND J. CALLAWAY
C
C
C                          TOTAL ENERGY FEATURES
C                                    BY
C                   J. CALLAWAY,X. ZOU, AND D. BAGAYOKO
C
C
C                             DEPARTMENT OF PHYSICS
C
C                           LOUISIANA STATE UNIVERSITY
C
C                           BATON ROUGE LOUISIANA 70803
C
C
C
C
C               ROUTINES USED IN SCF2
C
C     DIAGHS    (FROM PROGRAM BND)
C     DIGEN     (FROM PROGRAM BND)
C     DMFSD     FROM IBM S.S.P.   (NOT INCLUDED IN THIS PACKAGE)
C     DMTDS     FROM IBM S.S.P.   (NOT INCLUDED IN THIS PACKAGE)
C     FERMIE    (FROM PROGRAM SCF1)
C     GBZPT     (FROM PROGRAM FCOF)
C     GPERMK    (FROM PROGRAM FCOF)
C     PETMAT    (FROM PROGRAM BND)
C     SUMOVK    (FROM PROGRAM SCF1)
C     TDBZPT    (FROM PROGRAM SCF1)
C     TDVL      (FROM PROGRAM SCF1)
C     TELECT    (FROM PROGRAM FCOF)
C
C
C               COMMON BLOCKS OCCURING IN SCF2
C
C               ROUTINES IN WHICH THEY ARE USED
C
C     LCA       SCF2
C     LCB       SCF2
```

DSN=PHRAGA.DIOLA.SCF

```
C     SPACE    SCF2
C
C
C
C
C              INPUT/OUTPUT CHANNELS USED IN SCF2
C
C     FT01F001 GENERALIZED OVERLAP MATRIX.
C              (OUTPUT CHANNEL FT03F001 OF PROGRAM INVSIJ)
C     FT02F001 ENERGIES AND WAVE FUNCTIONS OF THE CORE AND BAND STATES.
C              (DOUBLE PRECISION VARIABLES)
C     FT04F001 THE NON-SELF-CONSISTENT COULOMB, EXCHANGE, KINETIC AND
C              OVERLAP MATRICES.
C              (OUTPUT CHANNEL FT10F001 OF PROGRAM CCBBH)
C     FT05F001 CARD READER.
C     FT06F001 LINE PRINTER.
C     FT07F001 CARD PUNCHER
C     FT08F001 NON-SELF-CONSISTENT FOURIER COEFFICIENTS OF THE POTENTIAL
C              (OUTPUT CHANNEL FT01F001 OF PROGRAM FCCF)
C     FT10F001 ENERGIES AND WAVE FUNCTIONS OF ALL STATES.
C              (SINGLE PRECISION VARIABLES)
C     FT19F001 SELF-CONSISTENT CORRECTION TO THE FOURIER COEFFICIENTS
C              OF THE POTENTIAL.
C
C
C
C
C     CALCULATE THE SELF-CONSISTENT POTENTIAL AND ENERGY BANDS FOR
C     FERROMAGNETIC MATERIAL.
C
C
C
C
C
C     DIMENSION RESTRICTIONS.
C     IPT(4,IPTOL) WHERE IPTOL IS THE NUMBER OF TETRAHEDRONS IN 1/48'TH
C     OF THE B.Z.
C     NKBZPT, DIMENSION OF KBX,KBY,KBZ,WT
C     NKP(I,I,I), I.GT.2*SQRT(K2MAXM)+1
C     NKPRT, DIMENSION OF KPERMX,KPERMY,KPERMZ,KASIGP,KSQU.
C     NKPT=NUMBER OF INDEPENDENT R.L.V. WITH K**2.LE.4*K2MAXM.
C     NKPT, DIMESNION OF KSX,KSY,KSZ,KNB,ALAMUP,ALAMDN,ALAMPA
C     FUP(NBFERM,NB),FDN(NBFERM,NE),
C     RHOUP(NKPTRM,NBFERM,NKBZPT),BHCDN(NKPTRM,NBFERM,NB),EUP(NBFERM,
C     NKBZPT)
C     EDN(NBFERM,NKZBPT)
C     NBTRI=NB*(NB+1)/2, DIMENSION OF SIJ,HUP,HDN,OV
C     GXUP(NB),GXDN(NB),XUP(NB,NB),XDN(NB,NB)
C
C
C
C * * * * * * * * * * * * * * * * * * * * * * * * * * * * * * * * * * * *
      IMPLICIT REAL*8(A-F,H,O-Z)
      REAL*4 RHOUP,RHODN
      REAL*4 SIJ(0946)
      INTEGER*2 IPT(4,500),KBX(140),KBY(140),KBZ(140),
     &NKP(24,24,24),KPERMX(3000),KPERMY(3000),KPERMZ(3000),KASIGP(3000)
      INTEGER*2 KSX(900),KSY(900),KSZ(900),KNB(900),KS2(900)
```

DSN=PHBAGA.DIOLA.SCF

```
      DIMENSION KSQU(3000)
      DIMENSION FUP(15,91),EUP(15,91),EHOUP(40,15,91),ALAMUP(900),
     &DWDPUP(900), WT(91)
      DIMENSION FDN(15,91),EDN(15,91),EHODN(40,15,91),ALAMDN(900),
     &DWDPDN(900), ALAMPA(900),DWDPPA(900),
     &ALAMUD(900), ALAMDU(900),DWDPUD(900),DWDPDU(900)
      DIMENSION HUP(0946),OV(0946),XUP(43,43),GXUP(43)
      DIMENSION HDN(0946),XDN(43,43),GXDN(43)
C
C     THE FOLLOWING ARRAIES MUST BE DIMENSIONED AT LEAST NKPTRN.
C
      DIMENSION VKO(40),WUPO(40),WDNO(40),VXUPO(40),CVKOD(40),CVKNW(40),
     1CXUPNW(40),DKUPO(40),DKUPOD(40),DKUPNW(40),DCOKUP(40),DVAKUP(40)
     2,CXUPOD(40),DWUP(40)
      DIMENSION DKDNO(40),DKDNOD(40),DKDNNW(40),DCOKDN(40),DVAKDN(40)
     1,CXDNOD(40),DWDN(40),VXDNO(40),CXDKNW(40)
      COMMON/LCA/HUP,OV
      COMMON/LCB/EHODN
      COMMON/SPACE/ FUP,FDN
      EQUIVALENCE(FUP(1,1),SIJ(1))
     &           ,(HUP(1),EHOUP(1,1,1))
     &           ,(HDN(1),EHODN(1,1,1))
      PI=3.141592653589793
C
C     ACONST=LATTICE CONSTANT (IN A. U.)
C     ALPHA=THE EXCHANGE PARAMETER
C     ELECT=NUMBER OF ELECTRONS PER ATOM
C
      READ(5,10)ACONST,ALPHA,ELECT
   10 FORMAT(6F12.8)
C
C     SC  IDCUB=1,  BCC  IDCUB=2,  FCC  IDCUB=4
C     K2MAXM=MAXIMUM MAGNITUDE OF (K*ACONST/2/PI)**2
C     NB,DIMENSION OF THE HAMILTONIAN AND OVERLAP ARE NB*NB
C     KBZDIV=DIVISION ALONG (1,0,0) DIRECTION IN THE B.Z.
C     IF(KBZHAF.NE.0) POINTS BELONGING TO THE DOUBLE DIVISION ARE SORTED
C     TO APPEAR FIRST.
C     NKPRT.GE.NUMBER OF PERMUTED R.L.V. WITH K**2.LE.K2MAXM.
C     NBCORE=NUMBER OF THE CORE STATES FOR EACH SPIN.
C     NBFERM=NUMBER OF BAND STATES FOR EACH SPIN.
C     NKPTRN=NUMBER OF NEW DENSITY(K) CONSIDERED IN EACH ITERATION.
C     NKPICL=NUMBER OF CORRECTIONS TO V(K) INCLUDED WHEN CONSTRUCTING
C            THE NEW HAMILTONIAN.
C     ================================================================
C     IF(IETCTL.EQ.0) THE FUNCTION IS THE SAME AS THE FUNCTION OF SCF1
C     IETOTL=1 ,FOR THE VBH POTENTIAL AND CALCULATION OF THE TOTAL
C                ENERGY
C     IETOTL=2 ,FOR ALPHA=2/3 POTENTIAL AND CALCULATION OF THE TOTAL
C                ENERGY
C     ================================================================
      READ(5,20)IDCUB,K2MAXM,NB,KBZDIV,KBZHAF,NKPRT
     1,NBCORE,NBFERM,NKPTRN,NKPICL,IETCTL
   20 FORMAT(2015)
      OMEGA=ACONST**3/DFLOAT(IDCUB)
      AKB=2.D0*PI/ACONST
      AKB2=AKB*AKB
      AKBBZ=AKB/DFLOAT(KBZDIV)
      IF(IDCUB.EQ.1) AKBBZ=AKBBZ/2.D0
```

DSN=PHBAGA.DIOLA.SCF

```
      ONETHD=1.D0/3.D0
      NBTRI=NB*(NB+1)/2
      RO=(OMEGA*3.D0/(4.D0*PI))**ONETHD
      CODK1=-16.D0*PI*PI/(3.D0*OMEGA)
      IF(IDCUB.NE.1) AHALF=ACONST/2.D0
      IF(IDCUB.EQ.1) AHALF=ACONST
C
C     GENERATE EQUALLY SPACED POINTS AND THE CORNERS OF THE TETRAHEDRONS
C     IN 1/48TH OF THE INDEPENDENT BRILLIOUIN ZONE
C
      KL=KBZDIV+1
      CALL GBZPT(KBX,KBY,KBZ,WT,NKBZPT,IDCUB,KL,SUMW,1,0,KBZHAF)
      COEF0=OMEGA*(AKBBZ/PI)**3
      COEF1=COEF0/OMEGA
      COEFK=1.D0/(OMEGA*SUMW)
      CALL TDBZPT(IPT,NKP,KL,IPTOL,KBX,KBY,KBZ,NKBZPT,IDCUB)
       NBTOL=NBCORE+NBFERM
       NBST=NB-NBTOL+1
      NBEND=NBST+NBFERM-1
      NCST=NBEND+1
      NBNO=NBFERM
      CALL GPERMK(KPERMX,KPERMY,KPERMZ,KSQU,NKPBT,IDCUB,K2MAXM,1,0)
C
C     READ IN THE NON-SELF-CONSISTENT FOURIER COEFFICIENTS OF THE
C     COULOMB, AND EXCHANGE POTENTIAL.
C
      J=0
   30 CONTINUE
      J=J+1
      READ(8) KS,GCOUL,GEWAD,GEXCH,GEXUP,GEXDN,GAPA,GAUP,GADN,GAUD,
     &GALU,GDU,GDD,KSX(J),KSY(J),KSZ(J),KNB(J)
      IF(IETOTL.EQ.1)
     &READ(9) KS,GCOUL,GEWAD,GW,GWUP,GWDN,GBPA,GBUP,GBDN,GBUD,GBDU,
     &GDU,GDD,KSX(J),KSY(J),KSZ(J),KNB(J)
      IF(KS.GT.4*K2MAXM) GO TO 50
      ALAMPA(J)=GAPA
      ALAMUP(J)=GAUP
      ALAMDN(J)=GADN
      ALAMUD(J)=GAUD
      ALAMDU(J)=GADU
      IF(IETOTL.NE.1) GO TO 35
      DELPPA(J)=GBPA
      DELPUP(J)=GBUP
      DELPDN(J)=GBDN
      DELPUD(J)=GBUD
      DELPDU(J)=GBDU
   35 CONTINUE
      II=KSX(J)+1
      JJ=KSY(J)+1
      KK=KSZ(J)+1
      NKP(II,JJ,KK)=J
      NKP(II,KK,JJ)=J
      NKP(JJ,KK,II)=J
      NKP(JJ,II,KK)=J
      NKP(KK,II,JJ)=J
      NKP(KK,JJ,II)=J
      IF(J.GT.NKPTBN) GO TO 30
      KSQU(J)=KS
```

```
      DKUPO(J)=GDD
      DKDNO(J)=GDD
      IF(KS.EQ.0) GO TO 40
      AA=AKR2*DFLOAT(KS)
      AA=8.D0*PI/AA
      VXDNO(J)=GEXDN
      VXUPO(J)=GEXUP
      IF(IETOTL.EQ.1) WUPO(J)=GWUP
      IF(IETOTL.EQ.1) WDNO(J)=GWDN
      VKO(J)=GCOUL+AA*ELECT/OMEGA
      GO TO 30
   40 VXUPO(J)=GEXUP
      VXDNO(J)=GEXDN
      IF(IETOTL.EQ.1) WUPO(J)=GWUP
      IF(IETOTL.EQ.1) WDNO(J)=GWDN
      VKO(J)=GCOUL
      GO TO 30
   50 NKPT=J-1
      WRITE(6,60 ) ACCNST,ALPHA,ELECT,NKPT,NKPTRN,NKPRT,IDCUB,KBZDIV,
     &KBZHAF,NB,IPTOL,NKPICL
   60 FORMAT(1X,'LATTICE CONST=',F10.5,2X,'EXCH PARA=',F10.5,2X,
     1'ELECT NO=',F8.2,2X,'NKPT=',I5,2X,'K STAR=',I5,2X,'K NO=',I5,//,
     21X,'ATOMS/CUBE=',I5,2X,'B.Z.DIV=',I5,2X,'KBZHAF=',I5,2X,'3D NO=',
     3I5,2X,'TEDRONS NO=',I5,2X,'INCLUDED K=',I5,//)
      DO 70  J=1,NKPRT
      II=KPERMX(J)
      JJ=KPERMY(J)
      KK=KPERMZ(J)
      II=IABS(II)+1
      JJ=IABS(JJ)+1
      KK=IABS(KK)+1
   70 KASIGP(J)=NKP(II,JJ,KK)
      REWIND 8
      IF(IETOTL.EQ.1)
     &REWIND 9
      DO 80  IRLV=1,NKPTRN
      DKUPCD(IRLV)=0.D0
      DKDNOD(IRLV)=0.D0
      CVKOD(IRLV)=0.D0
      CXUPCD(IRLV)=0.D0
      CXDNOD(IRLV)=0.D0
   80 CONTINUE
C
C     FACTOO,FACTO, AND FACT ARE PARAMETERS USED TO MODIFY THE POTENTIAL
C     IN ORDER TO SPEED UP THE ITERATIVE PROCEDURE.
C     FACTOO IS THE FACTO USED IN ITERATION ITEROD.
C     FACTO MODIFIES THE POTENTIAL OBTAINED IN ITERATION ITEROD BEFORE
C     CONSTRUCTIONG THE NEW HAMILTONIAN FOR ITERATION ITEROD+1.
C     FACT MODIFIES THE NEW POTENTIAL OBTAINED IN ITERATIONS ITEROD+1 TO
C     ITERNM.
C     PERFORM ITERATION NUMBER ITEROD+1 TO ITERNM.
C     IF(NPART.EQ.0)  PERFORM THE COMPLETE CALCULATION.
C     IF(NPART.GT.0)  ENERGY BAND HAS ALREADY BEEN CALCULATED
C     IF(NPART.EQ.1)  CALCULATE DENSITY(K) AND EXCH(K)
C     IF(NPART.EQ.2)  CALCULATE EXCH(K) ONLY.
C     IF(NPART.EQ.3)  CALCULATE DENSITY(K) ONLY.
C     IF(NPART.LT.0.AND.NKBZST.EQ.0) B.Z. POINTS NKBZST AND NKBZED ARE
C     DETERMINED AUTOMATICALLY.
```

```
                                DSN=PHBAGA.DIOLA.SCF
------------------------------------------------------------------------------
C      IF(NPART.EQ.-1) CALCULATE BANDS FROM NKBZST TO NKBZED ONLY.
C      IF(NPART.EQ.-2) CALCULATE BANDS FROM NKBZST TO NKBZED AND DENSITY.
C      IF(NPART.EQ.-3) CALCULATE BANDS FROM NKBZST TO NKBZED ,DENSITY,
C      AND EXCH(K).
C      IF(NPART.EQ.-4) CALCULATE BANDS AT NKBZST+1 AND NKBZED ONLY.
C      IF(IPUN.NE.0) PUNCH THE CHARGE DENSITY AND THEIR FOURIER COEFFICIE
C      IF(IBDFNL.NE.0) ENERGIES AND WAVE FUNCTIONS OF ALL NB STATES ARE
C      SAVED IN OUTPUT CHANNEL FT10F001  (IN SINGLE PRESISION)
C
   90 READ(5,100,END=780) FACT00,FACT0,FACT1,ITEROD,ITEBNW,NPART,
     &NKBZST,NKBZED,IPUN,IBDFNL
  100 FORMAT(3F10.5,1015)
  110 CONTINUE
      IF(NPART.EQ.0) GO TO 160
      IF(NPART.LT.0) GO TO 130
C
C     TEST THE NUMBER OF B.Z. POINTS AT WHICH ENERGIES AND WAVE
C     FUNCTIONS HAVE BEEN CALCULATED.
C
      DO 120 NM=1,NKBZPT
      DO 120 II=1,NBTOL
      READ(2) ENGU,(XUP(JJ,II),JJ=1,NB)
     &       ,ENGD,(XDN(JJ,II),JJ=1,NB)
      IF(II.GT.NBPERM) GO TO 120
      EUP(II,NM)=ENGU
      EDN(II,NM)=ENGD
  120 CONTINUE
      REWIND 2
      GO TO 170
  130 IF(NKBZST.NE.0) GO TO 170
      DO 140 NM=1,NKBZPT
      NKBZST=NM
      DO 140 II=1,NBTOL
      READ(2,END=150) ENG,(XUP(JJ,II),JJ=1,NB),ENGD,(XDN(JJ,II),JJ=1,NB)
  140 CONTINUE
      REWIND 2
      NPART=1
      GO TO 110
  150 CONTINUE
      REWIND 2
      NKBZED=NKBZPT
      GO TO 170
  160 CONTINUE
      NKBZST=1
      NKBZED=NKBZPT
  170 CONTINUE
      IF(ITEROD.EQ.0) GO TO 240
C
C     READ THE CORECTIONS DUE TO SELF-CONSISTANCY IN THE PREVIOUS
C     ITERATION AND MODIFY THEM WITH FACT0 BEFORE CONSTRUCTING THE
C     NEW POTENTIAL.
C
      DO 220 I=1,ITEROD
      READ(19,END=250) (DCOKUP(J),DVAKUP(J),DCOKDN(J),DVAKDN(J),J=1,
     &NKPTBN)
      READ(19,END=260) (CVKNW(J),CXUPNW(J),CXDNNW(J),DKUPNW(J),DKDNNW(J),
     &J=1,NKPTBN)
      IF(I.NE.ITEROD-2) GO TO 190
```

```
      DO 180 J=1,NKPTBA
      CVKOD(J)=CVKNW(J)
      CXUPOD(J)=CXUPNW(J)
      CXDNOD(J)=CXDNNW(J)
      DKUPOD(J)=DKUPNW(J)
      DKDNOD(J)=DKDNNW(J)
  180 CONTINUE
  190 CONTINUE
      IF(I.NE.ITEROD-1) GO TO 210
      DO 200 KN=1,NKPTRN
      DKUPOD(KN)=FACT00*DKUPNW(KN)+(1.D0-FACT00)*DKUPOD(KN)
      DKDNOD(KN)=FACT00*DKDNNW(KN)+(1.D0-FACT00)*DKDNOD(KN)
      CVKOD(KN)=FACT00*CVKNW(KN)+(1.D0-FACT00)*CVKOD(KN)
      CXUPOD(KN)=FACT00*CXUPNW(KN)+(1.D0-FACT00)*CXUPOD(KN)
      CXDNOD(KN)=FACT00*CXDNNW(KN)+(1.D0-FACT00)*CXDNOD(KN)
  200 CONTINUE
  210 CONTINUE
  220 CONTINUE
      DO 230 KN=1,NKPTRN
      DKUPOD(KN)=FACT0*DKUPNW(KN)+(1.D0-FACT0)*DKUPOD(KN)
      DKDNOD(KN)=FACT0*DKDNNW(KN)+(1.D0-FACT0)*DKDNOD(KN)
      CVKOD(KN)=FACT0*CVKNW(KN)+(1.D0-FACT0)*CVKOD(KN)
      CXUPOD(KN)=FACT0*CXUPNW(KN)+(1.D0-FACT0)*CXUPOD(KN)
      CXDNOD(KN)=FACT0*CXDNNW(KN)+(1.D0-FACT0)*CXDNOD(KN)
  230 CONTINUE
  240 CONTINUE
      GO TO 270
  250 ITEROD=I-1
      NPART=0
      FACT0=1.D0
      FACT00=1.D0
      GO TO 160
  260 ITEROD=I
      NPART=2
      FACT00=1.D0
      FACT0=1.D0
      GO TO 110
  270 ITERST=ITEROD+1
      WRITE(6,280 ) ITERST,FACT00,FACT0,NPART
  280 FORMAT(1H1,1X,'ITERATION=',I3,5X,'FACT00=',F6.3,5X,'FACT0=',F6.3,
     &5X,'NPART=',I5,//)
      DO 770    ITER=ITERST,ITERNW
      IF(NPART.GT.0.AND.ITER.EQ.ITERST) GO TO 490
  290 CONTINUE
      DO 460    NM=1,NKBZED
      WRITE(6,300) KBX(NM),KBY(NM),KBZ(NM),NM
  300 FORMAT(/,30X,3HK=(,3I4,1H),5X,'NM=',I5,/)
      IF(NM.LT.NKBZST.AND.ITER.EQ.ITERST) GO TO 410
      IF(NPART.EQ.-4.AND.NM.BE.NKBZST+1.AND.NM.NE.NKBZED) GO TO 410
  310 FORMAT(6A4)
C
C     READ THE ORIGINAL COULOMB, KINETIC, EXCHANGE, AND OVERLAP MATRICES
C
      DO 320 IJ=1,NBTRI
      READ(4,310 ) GC,GX,GU,GD,GK,GO
      HUP(IJ)=GC+GK+GU*ALPHA
      HDN(IJ)=GC+GK+GD*ALPHA
      OV(IJ)=GO
```

```
  320 CONTINUE
      IF(ITER.EQ.1) GO TO 350
C
C     CALCULATE THE HAMILTONIAN OBTAINED FROM LAST ITERATION BY THE
C     GENERALIZED OVERLAP MATRICES.
C
      DO 340 IRLV=1,NKPTRN
      READ(1) KS,KT,SIJ
      IF(IRLV.GT.NKPICL) GO TO 340
      AA=CVKOD(IRLV)+CXUPCD(IPLV)*ALPHA
      BB=CVKOD(IRLV)+CXDNOD(IRLV)*ALPHA
      DO 330 IJ=1,NBTRI
      HUP(IJ)=HUP(IJ)+AA*SIJ(IJ)
      HDN(IJ)=HDN(IJ)+BB*SIJ(IJ)
  330 CONTINUE
  340 CONTINUE
  350 CONTINUE
      KX=KBX(NM)
      KY=KBY(NM)
      KZ=KBZ(NM)
C
C     DIAGONALIZE THE HAMILTONIAN
C
      CALL DIAGHS(HUP,OV,XUP,NB,1,IPUN,0,1,KX,KY,KZ,0,0,NBST,NBEND)
      CALL DIAGHS(HDN,OV,XDN,NB,2,IPUN,0,0,KX,KY,KZ,0,0,NBST,NBEND)
      IF(NPART.EQ.-4) GO TO 460
      DO 360 II=NBST,NB
      WRITE(2) HUP(II),(XUP(JJ,II),JJ=1,NB)
     &        ,HDN(II),(XDN(JJ,II),JJ=1,NB)
      I=II-NBST+1
      IF(I.GT.NBPERM) GO TO 360
      EUP(I,NM)=HUP(II)
      EDN(I,NM)=HDN(II)
  360 CONTINUE
      IF(IBDFNL.EQ.0) GO TO 460
      DO 380 II=1,NB
      GEUP=HUP(II)
      DO 370 JJ=1,NB
  370 GXUP(JJ)=XUP(JJ,II)
  380 WRITE(10) GEUP,GXUP
      DO 400 II=1,NB
      GEDN=HDN(II)
      DO 390 JJ=1,NB
  390 GXDN(JJ)=XDN(JJ,II)
  400 WRITE(10) GEDN,GXDN
      GO TO 460
  410 DO 420 IJ=1,NBTRI
  420 READ(4,410) GC,GX,GU,GD,GK,GO
      DO 430 IRLV=1,NKPTRN
  430 READ(1) KS,KT,SIJ
      DO 440 II=1,NBTOL
      READ(2) ENGU,(XUP(JJ,1),JJ=1,NB),ENGL,(XDN(JJ,1),JJ=1,NB)
      IF(II.GT.NBPERM) GO TO 440
      EUP(II,NM)=ENGU
      EDN(II,NM)=ENGD
  440 CONTINUE
      IF(IBDFNL.EQ.0) GO TO 460
      DO 450 KSP=1,2
```

```
      DO 450 II=1,NB
  450 READ(10,END=470) GEUP,GXUP
  460 CONTINUE
      GO TO 480
  470 NKBZST=NM
      REWIND 1
      REWIND 2
      REWIND 4
      REWIND 10
      GO TO 290
  480 IF(NPART.EQ.-1.OR.NPART.EQ.-4) STOP
      REWIND 1
      REWIND 2
      REWIND 4
      REWIND 10
C
C     DETERMINE THE FERMI ENERGY
C
  490 IF(NBFERM.EQ.0) GO TO 500
      NSPIN=2
      ELE=ELECT-2*NBCORE
      CALL FERMIE(EUP,EDN,NEFERM,NKBZPT,IPT,IPTOL,COEFO,ELE,NSPIN,FERMI)
  500 CONTINUE
      IF(NPART.GT.1.AND.ITER.EQ.ITERST) GO TO 650
C
C     CALCULATE FOURIER TRANSFORM OF CHARGE DENSITY
C     THE B.Z. INTEGRATION FOR THE CORE STATES ARE OBTAINED BY HISTOGRAM
C     METHOD AND THE BAND STATES BY ANALYTICAL TETRAHEDRON METHOD.
C
      DO 510 IRLV=1,NKPTRN
      DCOKUP(IRLV)=0.D0
      DCOKDN(IRLV)=0.D0
  510 CONTINUE
      DO 570 NM=1,NKBZPT
      DO 520 II=1,NBTOL
      READ(2) ENGU,(XUP(JJ,II),JJ=1,NB)
     &       ,ENGD,(XDN(JJ,II),JJ=1,NB)
  520 CONTINUE
      DO 570 IRLV=1,NKPTRN
      READ(1) KS,KT,SIJ
      DO 560 IN=1,NBTOL
      AA=0.D0
      BB=0.D0
      IJ=0
      DO 540 I1=1,NB
      DO 540 I2=1,I1
      IJ=IJ+1
      AC=XUP(I1,IN)*SIJ(IJ)*XUP(I2,IN)
      BC=XDN(I1,IN)*SIJ(IJ)*XDN(I2,IN)
      IF(I1.EQ.I2) GO TO 530
      AC=AC*2.D0
      BC=BC*2.D0
  530 AA=AA+AC
      BB=BB+BC
  540 CONTINUE
      IF(IN.LE.NBFERM)GO TO 550
      DCOKUP(IRLV)=DCOKUP(IRLV)+AA*WT(NM)
      DCOKDN(IRLV)=DCOKDN(IRLV)+BB*WT(NM)
```

```
      GO TO 560
  550 RHOUP(IRLV,IN,NM)=AA
      RHODN(IRLV,IN,NM)=BB
  560 CONTINUE
  570 CONTINUE
      WRITE(6,580)
  580 FORMAT(1H1,7X,'KX',3X,'KY',3X,'KZ',3X,'DENSITY UP',4X,'NEW DEN UP'
     &,5X,'COND',8X,'CORE',7X,'DENSITY DN',3X,'NEW DEN DN',
     &5X,'COND',9X,'CORE',/)
      SUMUP=0.D0
      SUMDN=0.D0
      DO 630 IRLV=1,NKPTRN
      AA=1.D0/KNB(IRLV)
      IF(NBNO.EQ.0) GO TO 600
      DO 590 NK=1,NBNO
      DO 590 KPT=1,NKBZPT
      FDN(NK,KPT)=RHODN(IRLV,NK,KPT)
  590 FUP(NK,KPT)=RHOUP(IRLV,NK,KPT)
      CALL SUMOVK(EUP,IPT,IPTOL,KBX,KBY,KBZ,FUP,NKBZPT,SUMUP,COEF1,FERMI
     &,NBNO)
      CALL SUMOVK(EDN,IPT,IPTOL,KBX,KIY,KBZ,FDN,NKBZPT,SUMDN,COEF1,FERMI
     &,NBNO)
      SUMUP=SUMUP*AA
      SUMDN=SUMDN*AA
  600 CONTINUE
      DVAKUP(IRLV)=SUMUP
      DVAKDN(IRLV)=SUMDN
      CUMUP=DCOKUP(IRLV)*AA*COEFK
      CUMDN=DCOKDN(IRLV)*AA*COEFK
      DCOKUP(IRLV)=CUMUP
      DCOKDN(IRLV)=CUMDN
      SUP=SUMUP+CUMUP
      SDN=SUMDN+CUMDN
      WRITE(6,610)IRLV,KSX(IRLV),KSY(IRLV),KSZ(IRLV),DKUPO(IRLV),SUP,
     &SUMUP,CUMUP,DKDNO(IRLV),SDN,SUMDN,CUMDN
      IF(IPUN.NE.0)
     &WRITE(7,620)IRLV,KSX(IRLV),KSY(IRLV),KSZ(IRLV),SUMUP,CUMUP,
     &SUMDN,CUMDN
  610 FORMAT(4I5,8F13.6)
  620 FORMAT(4I5,4E15.8)
  630 CONTINUE
      WRITE(19) (DCOKUP(J),DVAKUP(J),DCOKDN(J),DVAKDN(J),J=1,NKPTRN)
      AELC=(DCOKUP(1)+DVAKUP(1)+DCOKDN(1)+DVAKDN(1))*OMEGA
      AMAG=(DCOKUP(1)+DVAKUP(1)-DCOKDN(1)-DVAKDN(1))*OMEGA
      WRITE(6,640) AELC,AMAG
  640 FORMAT(//,1X,'ELECT=',F10.6,5X,'MAGNETON NO=',F10.6)
      GO TO 660
  650 CONTINUE
      READ(19) (DCOKUP(J),DVAKUP(J),DCOKDN(J),DVAKDN(J),J=1,NKPTRN)
  660 CONTINUE
      IF(NPART.EQ.-2.OR.NPART.EQ.3) STOP
      REWIND 1
C
C
C     MODIFIED THE SELF-CONSISTENT CORRECTIONS TO IMPROVE CONVERGENCE.
C
      DO 670 KN=1,NKPTRN
      DKUPNW(KN)=DCOKUP(KN)+DVAKUP(KN)-DKUPO(KN)
```

```
      DKDNNW(KN)=DCOKDN(KN)+DVARDN(KN)-DKDNO(KN)
      DKUPNW(KN)=FACT*DKUPNW(KN)+(1.D0-FAC1)*DKUPOD(KN)
      DKDNNW(KN)=FACT*DKDNNW(KN)+(1.D0-FACT)*DKDNOD(KN)
  670 CONTINUE
C
C     CALCULATE THE CORRECTION TO THE EXCHANGE POTNETIAL.
C
      DO 690 KN=1,NKPTRN
      SUMUP=0.D0
      SUMDN=0.D0
      SUMWUP=0.D0
      SUMWDN=0.D0
      DO 680 J=1,NKPRT
      II=KSX(KN)-KPERMX(J)
      JJ=KSY(KN)-KPERMY(J)
      KK=KSZ(KN)-KPERMZ(J)
      II=IABS(II)+1
      JJ=IABS(JJ)+1
      KK=IABS(KK)+1
      KS=NKP(II,JJ,KK)
      KT=KASIGP(J)
      SUMUP=SUMUP+ALAMUP(KS)*DKUPNW(KT)+ALAMUD(KS)*DKDNNW(KT)
      SUMDN=SUMDN+ALAMDN(KS)*DKDNNW(KT)+ALAMDU(KS)*DKUPNW(KT)
      IF(IETOTL.EQ.1) SUMWUP=SUMWUP+DWDPUP(KS)*DKUPNW(KT)+DWDPUD(KS)*
     &DKDNNW(KT)
      IF(IETOTL.EQ.1) SUMWDN=SUMWDN+DWDPDN(KS)*DKDNNW(KT)+DWDPDU(KS)*
     &DKUPNW(KT)
  680 CONTINUE
      CXUPNW(KN)=SUMUP
      CXDNNW(KN)=SUMDN
      IF(IETOTL.EQ.1) DWUP(KN)=SUMWUP
      IF(IETOTL.EQ.1) DWDN(KN)=SUMWDN
  690 CONTINUE
C
C     CALCULATE THE CORRECTION TO THE  COULOMB PART OF V(K=0).
C
      AA=0.D0
      RO2=RO*RO
      RO3=RO*RO2
      DO 700 J=2,NKPTRN
      RK2=AK2*KSQU(J)
      RK1=DSQRT(RK2)
      RK3=RK1*RK2
      RK4=RK2*RK2
      ROK=RO*RK1
      CO=(DKUPNW(J)+DKDNNW(J))*KNE(J)
      AA=AA+CO/RK1*((3.D0*RO2/RK2-6.D0/RK4)*DSIN(ROK)+
     &              (6.D0*RO/RK3-RO3/RK1)*DCOS(ROK))
  700 CONTINUE
      CVANW(1)=CODK1*AA
C
C     PRINT FOURIER COEFFICIENTS OF THE NEW POTENTIAL.
C
  710 FORMAT(1H1,1X,'ITERATION=',I3,5X,'FACTO=',F6.3,5X,'FACT=',F6.3,5X,
     &'NPART=',I5,//)
      WRITE(6,710  ) ITER,FACTO,FACT,NPART
      WRITE(6,720  )
  720 FORMAT(2X,'KS',2X,'NUCLEAR',6X,'COUL',4X,'DEL NEW',4X,'DEL OLD'
```

```
     &,4X,'EXUP',4X,'DEL NEW',4X,'DEL OLD',4X,'EXDN'
     &,2X,'DEL NEW',3X,'DEL NEW')
      IF(IETOTL.EQ.1.AND.ITER.EQ.ITERNW) WRITE(6,725)
  725 FORMAT(52X,'WUP(KS)',3X,'DWUP(KS)',3X,'DWUP(KS)',
     &3X,'WDN(KS)',3X,'DWDN(KS)',//)
      ANUCLE=0.0
      DO 740  J=1,NKPTRN
      IF(J.EQ.1) GO TO 730
      RK2=AKR2*KSQU(J)
      AA=8.D0*PI/RK2
      ANUCLE=-AA*ELECT/OMEGA
      CVKNW(J)=AA*(DKUPNW(J)+DKDNNW(J))
  730 CONTINUE
      WRITE(6,750  ) KSX(J),KSY(J),KSZ(J),ANUCLE,VKO(J),CVKNW(J),CVKOD(J
     &),VXUPO(J),CXUPNW(J),CXUPOD(J),VXDNO(J),CXDNNW(J),CXDNOD(J)
      IF(IETOTL.EQ.1)
     &WRITE(6,735  ) KSX(J),KSY(J),KSZ(J),ANUCLE,VKO(J),CVKNW(J),CVKOD(J
     &),WUPO(J),DWUP(J),DWUP(J),WDNO(J),DWDN(J)
  735 FORMAT(1X,I2,2I1,4(1X,F9.6),5X,8(1X,F9.6))
      IF(IPUN.NE.0)
     &WRITE(7,620) J,KSX(J),KSY(J),KSZ(J),CVKNW(J),CXUPNW(J),CXDNNW(J)
      CVKOD(J)=CVKNW(J)
      DKUPOD(J)=DKUPNW(J)
      DKDNOD(J)=DKDNNW(J)
      CXUPOD(J)=CXUPNW(J)
      CXDNOD(J)=CXDNNW(J)
  740 CONTINUE
  750 FORMAT(1X,I2,2I1,12(1X,F9.6))
      WRITE(19) (CVKOD(J),CXUPOD(J),CXDNOD(J),DKUPOD(J),DKDNOD(J),
     &J=1,NKPTRN)
      WRITE (6,760)
  760 FORMAT(1H1)
      REWIND 2
  770 CONTINUE
      REWIND 19
      GO TO 90
  780 CONTINUE
      IF(IETOTL.EQ.0) GO TO 810
C     ==========================================================
C     OUTPUT DATA SETS  OF  FILE 17 ARE
C                 KS2(KS),NB(KS),VEO(KS),DVE(KS),
C                 VXUP(KS),DVXUP(KS),DPUP(KS)
C     OUTPUT DATA SETS  OF  FILE 37 ARE
C                 KS2(KS),NB(KS),DENSTDN(KS),DPDN(KS),
C                 VXDN(KS),DVXDN(KS),DPDN(KS)
C     IF(IETOTL.EQ.1) OUTPUT DATA SETS OF FILE  27  ARE
C                 KS2(KS),NB(KS),WDN(KS),DWDN(KS),
C                 WUP(KS),DWUP(KS),DENSTUP(KS)
C     ==========================================================
      DO 800 J=1,NKPTRN
      KS2(J)=KSX(J)*KSX(J)+KSY(J)*KSY(J)+KSZ(J)*KSZ(J)
  800 CONTINUE
      WRITE(17)  (KS2(J),KNB(J),VKO(J),CVKNW(J),
     &J=1,NKPTRN)
      WRITE(17)  (VXUPO(J),CXUPNW(J),DKUPNW(J),J=1,NKPTRN)
      WRITE(37)  (KS2(J),KNB(J),DKDNO(J),DKDNNW(J),
     &J=1,NKPTRN)
      WRITE(37)  (VXDNO(J),CXDNNW(J),DKDNNW(J),J=1,NKPTRN)
```

DSN=PHBAGA.DIOLA.SCF

```
      IF(IETCTL.NE.1) GO TO 810
      WRITE(27) (KS2(J),KNB(J),WDNO(J),DWDN(J),
     &J=1,NKPTBN)
      WRITE(27) (WUPO(J),DWUP(J),DKUPO(J),J=1,NKPTBN)
  810 STOP
      END
//LKED.SYSLIB  DD DSN=D1103.CALLAWAY.BVCMPLIB,DISP=SHR
//     DD DSN=D1103.CALLAWAY.ENDPKG.SUBLIB.COMPL,DISP=SHR
//      DD DSN=SYS1.VFORTLIB,DISP=SHR
//      DD DSN=SYS2.FORTLIB,DISP=SHR
//      DD DSN=SYS2.SSP.LIB,DISP=SHR
//      DD DSN=SYS2.PLOT.LIB,DISP=SHR
//GO.FT01F001 DD UNIT=3380,VOL=SER=USER77,DISP=SHR,
//      DCB=(BLKSIZE=07294,RECFM=VBS,LRECL=03624),
//             DSNAME=PHBAGA.DICLA.FEF5P4.ECC.INVSIJ
//GO.FT02F001 DD UNIT=3380,VOL=SER=USER77,DISP=(NEW,CATLG),
//           SPACE=(TRK,(30,20)),
//      DCB=(BLKSIZE=07294,RECFM=VBS,LRECL=176),
//        DSNAME=PHBAGA.DIOLA.FEF5P4.BCC.BAND91.REALS
//GO.FT04F001 DD UNIT=3380,VOL=SER=USER77,DISP=SHR,
//          DSNAME=PHBAGA.DIOLA.FEF5P4.BCC.CXKO91
//GO.FT08F001 DD UNIT=3380,VOL=SER=USER77,DISP=SHR,
//             DSNAME=PHBAGA.DIOLA.FEF5P4.BCC.VK1
//GO.FT09F001 DD UNIT=3380,VOL=SER=USER77,DISP=SHR,
//             DSNAME=PHBAGA.DIOLA.FEF5P4.BCC.VK3
//GO.FT10F001 DD UNIT=3380,VOL=SER=USER77,DISP=(NEW,CATLG),
//       SPACE=(TRK,(30,20)),
//      DCB=(BLKSIZE=07294,RECFM=VBS,LRECL=00176),
//          DSNAME=PHBAGA.DIOLA.FEF5P4.BCC.BAND1
//GO.FT19F001 DD UNIT=3380,VOL=SER=USER77,DISP=(NEW,CATLG),
//        SPACE=(TRK,(20,5)),
//        DCB=(BLKSIZE=488,RECFM=VBS,LRECL=484),
//        DSNAME=PHBAGA.DIOLA.FEF5P4.BCC.SELFVK
//GO.FT17F001 DD UNIT=3380,VOL=SER=USER77,DISP=(NEW,CATLG),
//        SPACE=(TRK,(3,2)),
//        DCB=(BLKSIZE=488,RECFM=VBS,LRECL=484),
//        DSNAME=PHBAGA.DIOLA.FEF5P4.BCC.SELFVX
//GO.FT27F001 DD UNIT=3380,VOL=SER=USER77,DISP=(NEW,CATLG),
//        SPACE=(TRK,(3,2)),
//        DCB=(BLKSIZE=488,RECFM=VBS,LRECL=484),
//        DSNAME=PHBAGA.DIOLA.FEF5P4.BCC.SELFWK
//GO.FT37F001 DD UNIT=3380,VOL=SER=USER77,DISP=(NEW,CATLG),
//        SPACE=(TRK,(3,2)),
//        DCB=(BLKSIZE=488,RECFM=VBS,LRECL=484),
//        DSNAME=PHBAGA.DIOLA.FEF5P4.BCC.SELFUD
//GO.SYSIN DD *
   5.4057    1.0000000       26.0
    2   62   43   10    1 1200    0   15   40   20    1
   1.0       1.0       0.3       00   01   00   00   00    0    1
//
```

APPENDIX A.3: New Version of PROGRAM DENST

```
                                   DSN=PHBAGA.DIOLA.DEN
-------------------------------------------------------------------------
//PHBAGA54 JOB (1103,60245,004,2),'PH.DIOLA',MSGCLASS=S,
//       NOTIFY=PHBAGA
/*AFTER FEF1B254
/*ROUTE PRINT PHYSICS
/*JOBPARM SHIFT=D
// EXEC FORTHCLG,PARM.FORT='NOSOURCE,LANGLVL(66),OPT(2)',
//      PARM.LKED=NOXREF,REGION=1200K,TIME=999
//FORT.SYSIN DD *
C
C                              PROGRAM DENST
C                          THE SIXTH PART OF
C
C      A GENERAL PROGRAM TO CALCULATE SELF-CONSISTANT ENERGY BANDS
C
C          USING THE MODIFIED TIGHT BINDING OR ICGC METHOD
C
C                                    BY
C
C                           C.S. WANG AND J. CALLAWAY
C
C                           TOTAL ENERGY CALCULATION
C                                    BY
C                      J. CALLAWAY,X. ZOU, AND D. BAGAYOKO
C
C                            DEPARTMENT OF PHYSICS
C
C                           LOUISIANA STATE UNIVERSITY
C
C                          BATON ROUGE LOUISIANA 70803
C
C
C
C
C                ROUTINES USED IN DENST
C
C      FERMIE    (FROM PROGRAM SCF1)
C      GBZPT     (FROM PROGRAM FCOF)
C      TDBZPT    (FROM PROGRAM SCF1)
C      TDENST
C      TDVL      (FROM PROGRAM SCF1)
C      TELECT    (FROM PROGRAM FCOF)
C
C
C
C                INPUT/OUTPUT CHANNELS USED IN DENST
C
C      FT01F001 ENERGIES AND WAVE FUNCTIONS.
C               (OUTPUT CHANNEL FT02F001 OF PROGRAM BND  OR
C               OUTPUT CHANNEL FT10F001 OF PROGRAM SCF1 OR SCF2)
C      FT05F001 CARD READER.
C      FT06F001 LINE PRINTER.
C
C
C
C
C      CALCULATE THE DENSITY OF STATES BY THE LINEAR ANALYTICAL
C      TETRAHEDRON METHOD.
C
```

DSN=PHBAGA.DICLA.DEN

```
C
C
C
C
C     DIMENSION RESTRICTIONS.
C     IPT(4,IPTOL) WHERE IPTOL IS THE NUMBER OF TETRAHEDRONS IN 1/48'TH
C     OF THE B.Z.
C     NKBZPT, DIMENSION OF KBX,KBY,KBZ
C     NP(I,I,I), I=KBZDIV+1
C     EUP(NBFERM,NB),EUP(NBFERM,NKBZPT),GX(NB)
C     NEMAX, DIMENSION OF EN,SWUP,SWDN,TWUP,TWDN.
C
C
C
C * * * * * * * * * * * * * * * * * * * * * * * * * * * * * * * * * * * * *
      IMPLICIT REAL*8(A-F,H,O-Z)
      INTEGER*2 KX1,KY1,KZ1,KNB
      INTEGER*2 IPT(4,2048),KBX(506),KBY(506),KBZ(506),NP(21,21,21),
     &KSX(40),KSY(40),KSZ(40),KNB(40),K2(40)
      REAL*4 SIJ(0946)
      DIMENSION EUP(15,506),EDN(15,506),GX(43),GX1(43)
      DIMENSION EN(1801),SWUP(1801),SWDN(1801),TWUP(1801),TWDN(1801),
     &ESINGU(1801),ESINGD(1801),SW(1801)
      DIMENSION CVKNW(40),DWUP(40),DPUP(40),VCKO(40),VXCUPO(40),
     &VKO(40),WUPO(40),DVXCUP(40),PUPO(40)
     &,DWDN(40),DPDN(40),VXCDNO(40),WDNO(40),DVXCDN(40),EDNO(40)
C
C     NEMAX=NUMBER OF DIVISION IN ENERGY AT WHICH THE DENSITY OF STATES
C     ARE CALCULATED.
C     KBZDIV=DIVISION ALONG (1,0,0) DIRECTION IN THE B.Z.
C     IF(KBZHAF.NE.0) POINTS BELONGING TO THE DOUBLE DIVISION ARE SORTED
C     TO APPEAR FIRST.
C     SC  IDCUB=1,  BCC  IDCUB=2,  FCC  IDCUB=4
C     NSPIN =1 AND 2 FOR PARAMAGNET AND FERROMAGNET RESPECTIVELY.
C     NBFERM=NUMBER OF BAND STATES FOR EACH SPIN.
C     NBCORE=NUMBER OF THE CORE STATES FOR EACH SPIN.
C     NB,DIMENSION OF THE HAMILTONIAN AND OVERLAP ARE NB*NB
C     IF(IDISC.NE.0) ENERGIES ARE READ FROM CHANNEL FT01F001.
C     IF(IDISC.EQ.0) ENERGIES ARE READ FROM CARDS.
C     ============================================================
C     IF(IETOTL.EQ.1) CALCULATE THE TOTAL ENERGY AND USE VBH POTENTIAL
C     IF(IETOTL.EQ.2) CALCULATE THE TOTAL ENERGY AND USE ALPHA=2/3 POT.
C     IF(IETOTL.EQ.0) THE FUNCTION IS THE SAME AS THE FUNCTION OF DENST
C       IF(NDENS.EQ.0) THE DENSITY OF STATES IS NOT CALCULATED
C     ============================================================
      READ(5,333) NDENS,IETOTL
  333 FORMAT(10I5)
      READ(5,10) NEMAX,KBZDIV,KBZHAF,IDCUB,NSPIN,NBFERM,NBCORE,NB,IDISC
     &,NKPTBH
   10 FORMAT(20I5)
C
C     EMIN=MINIMUM ENERGY CONSIDERED.
C     DE=STEPS IN THE ENERGY DIVISION.
C     ZERO, IF ENERGIES DIFFERENCE IS LESS THAN ZERO THAN ENERGIES ARE
C     CONSIDERED EQUAL.
C     ELECT=NUMBER OF BAND ELECTRONS PER ATOM
C
      READ(5,20) EMIN,DE,ZERO,ELECT,Z,ACONST
```

DSN=PHBAGA.DIOLA.DEN

```
C
C     ================================================================
C
      AAA=ACONST**3
      OMEGA=AAA/DFLOAT(IDCUB)
      PO=Z/OMEGA
      NBNO=NBFERM
      NBTOL=NBCORE+NBFERM
      NBST=NB-NBTOL+1
      NBEND=NBST+NBFERM-1
      NBTRI=NB*(NB+1)/2
   20 FORMAT(10F10.5)
      CONST=8.D0/DFLOAT(IDCUB*KBZDIV**3)
      IF(IDCUB.EQ.1) CONST=CONST/8.D0
      IF(NSPIN.EQ.1) CONST=CONST*2.D0
      COM=CONST*3.D0
      PI=3.1415926535897932
      KL=KBZDIV+1
      CALL GBZPT(KBX,KBY,KBZ,WT,NKBZPT,IDCUB,KL,SUMW,0,0,KIZHAF)
      IF(IDISC.NE.0) GO TO 50
      DO 30  K=1,NKBZPT
C
C     EUP=BAND STATES ENERGIES OF MAJORITY SPIN.
C     KX= X COMPONENTS OF K POINTS IN THE B.Z.
C     KY= Y COMPONENTS OF K POINTS IN THE B.Z.
C     KZ= Z COMPONENTS OF K POINTS IN THE B.Z.
C
      READ(5,40 ) (EUP(I,K),I=1,NBFERM),KX,KY,KZ
      KBX(K)=KX
      KBY(K)=KY
      KBZ(K)=KZ
      IF(NSPIN.EQ.1) GO TO 30
C
C     EDN=BAND STATES ENERGIES OF MINORITY SPIN.
C
      READ(5,40 ) (EDN(I,K),I=1,NBFERM)
   30 CONTINUE
   40 FORMAT(6F11.7,3I3,I5)
      GO TO 80
   50 CONTINUE
      DO 70  K=1,NKBZPT
      DO 60  NSP=1,NSPIN
      DO 60  J=1,NB
      READ(1) GENG,GX
      IF(J.LT.NBST.OR.J.GT.NBEND) GO TO 60
      IF(NSP.EQ.1) EUP(J-NBST+1,K)=GENG
      IF(NSP.EQ.2) EDN(J-NBST+1,K)=GENG
   60 CONTINUE
   70 CONTINUE
      REWIND 1
   80 CONTINUE
      KDIM=KBZDIV+1
      CALL TDBZPT(IPT,NP,KDIM,IPTOL,KBX,KBY,KBZ,NKBZPT,IDCUB)
      WRITE(6,810) IDCUB,KBZDIV,NEMAX,EMIN,DE,IPTOL,NKBZPT,NBCORE,
     &NBFERM,NB
  810 FORMAT(1X,'ATOM/CUBE=',I5,3X,'B.Z.DIV=',I5,3X,'NE=',I5,3X,
     &'EMIN=',F10.5,3X,'DE=',F10.5,3X,'TD NO=',I8,3X,
     2'B.Z.PT=',I5,/1X,'CORE=',I5,2X,'ENAD=',I5,2X,'NB=',I5,//)
```

DSN=PHBAGA.DIOLA.DEN

```
      CALL FERMIE(EUP,EDN,NBFEEN,NKPZPT,IPT,IPTCL,CONST,ELECT,NSPIN,
     &FERMI)
C
C     CALCULATE THE AVERAGE SINGLE ELECTRON ENERGY,D,U AND THE
C     EXCHANGE-CORRELATION ENERGY
C
      IF(IETOTL.EQ.0) GO TO 99
C
C     READ IN KS2*A/2PI AND THE NON-SELF-CONSISTENT FOURIER
C     COEFFICIENTS OF THE COULOMB AND EXCHANGE POTENTIALS.
C
      READ(17)  (K2(J),KNB(J),VKO(J),CVKNB(J),J=1,NKPTRN)
      READ(17) (VXCUPO(J),DVXCUP(J),DPUP(J),J=1,NKPTRN)
      IF(NSPIN.EQ.2) GO TO 814
      READ(27)  (K2(J),KNB(J),VKO(J),PUPO(J),J=1,NKPTRN)
      READ(27) (WUPO(J),DWUP(J),DPUP(J),J=1,NKPTRN)
  814 CONTINUE
      IF(NSPIN.EQ.1) GO TO 818
      READ(27)  (K2(J),KNB(J),WDNO(J),DWDN(J),J=1,NKPTRN)
      READ(27) (WUPO(J),DWUP(J),PUPO(J),J=1,NKPTRN)
      READ(37)  (K2(J),KNB(J),PDNO(J),DPDN(J),J=1,NKPTRN)
      READ(37) (VXCDNO(J),DVXCDN(J),DPDN(J),J=1,NKPTRN)
  818 CONTINUE
      WRITE(6,820)
  820 FORMAT(/,1X,'K2(J),J=1,NKPTRN')
      WRITE(6,10)  (K2(J),J=1,NKPTRN)
      WRITE(6,824)
  824 FORMAT(/,1X,'KNB(J),J=1,NKPTRN')
      WRITE(6,10)  (KNB(J),J=1,NKPTRN)
      WRITE(6,828)
  828 FORMAT(/,1X,'VKO(J),J=1,NKPTRN')
      WRITE(6,858)  (VKO(J),J=1,NKPTRN)
      VCKO(1)=VKO(1)
      DO 830 J=2,NKPTRN
      KK=K2(J)
      AKS2=(2.D0*PI/ACONST)**2*DFLOAT(KK)
      VCKO(J)=VKO(J)-8.D0*PI*Z/OMEGA/AKS2
  830 CONTINUE
      WRITE(6,834)
  834 FORMAT(/,1X,'CVKNB(J),J=1,NKPTRN')
      WRITE(6,858)  (CVKNB(J),J=1,NKPTRN)
      WRITE(6,838)
  838 FORMAT(/,1X,'VXCO(J) (PARAMAG) OR VXCUPO(J) (FERROMAG), J=1,NKPTRN')
      WRITE(6,858)  (VXCUPO(J),J=1,NKPTRN)
      WRITE(6,840)
  840 FORMAT(/,1X,'DVXC(J) (PARAMAG) OR DVXCUP(J) (FERROMAG), J=1,NKPTRN')
      WRITE(6,858)  (DVXCUP(J),J=1,NKPTRN)
      WRITE(6,844)
  844 FORMAT(/,1X,'WO(J) (PARAMAG) OR WUPO(J) (FERROMAG), J=1,NKPTRN')
      WRITE(6,858)  (WUPO(J),J=1,NKPTRN)
      WRITE(6,848)
  848 FORMAT(/,1X,'DW(J) (PARAMAG) OR DWUP(J) (FERROMAG), J=1,NKPTRN')
      WRITE(6,858)  (DWUP(J),J=1,NKPTRN)
      WRITE(6,850)
  850 FORMAT(/,1X,'DENS(J) (PARAMAG) OR DENSUP(J) (FERROMAG), J=1,NKPTRN')
      WRITE(6,858)  (PUPO(J),J=1,NKPTRN)
      WRITE(6,854)
  854 FORMAT(/,1X,'DP(J) (PARAMAG) OR DPUP(J) (FERROMAG), J=1,NKPTRN')
```

```
      WRITE(6,858) (DPUP(J),J=1,NKPTRN)
  858 FORMAT(1X,10F13.6)
      IF(NSPIN.EQ.1) GO TO 884
      WRITE(6,860)
  860 FORMAT(/,1X,'VXCDNC(J), J=1,NKPTRN')
      WRITE(6,858) (VXCDNO(J),J=1,NKPTRN)
      WRITE(6,864)
  864 FORMAT(/,1X,'DVXCDN(J), J=1,NKPTRN')
      WRITE(6,858) (DVXCDN(J),J=1,NKPTRN)
      WRITE(6,870)
  870 FORMAT(/,1X,'WDNO(J), J=1,NKPTRN')
      WRITE(6,858) (WDNO(J),J=1,NKPTRN)
      WRITE(6,874)
  874 FORMAT(/,1X,'DWDN(J), J=1,NKPTRN')
      WRITE(6,858) (DWDN(J),J=1,NKPTRN)
      WRITE(6,878)
  878 FORMAT(/,1X,'DENSDN(J), J=1,NKPTRN')
      WRITE(6,858) (FDNO(J),J=1,NKPTRN)
      WRITE(6,880)
  880 FORMAT(/,1X,'DDENSDN(J), J=1,NKPTRN')
      WRITE(6,858) (DPDN(J),J=1,NKPTRN)
  884 CONTINUE
C     IF(NSPIN.EQ.2) GO TO 888
C     IF(IETOTL.NE.2) GO TO 89
C     DO 89 J=1,NKPTRN
C     WUPO(J)=WUPO(J)*2.D0/3.D0
C     DWUP(J)=DWUP(J)*2.D0/3.D0
C  89 CONTINUE
C     IF(IETOTL.EQ.2) EEXCH=EEXCH/4.D0  ??
  888 CONTINUE
C
C     CALCULATE THE AVERAGE SINGLE ELECTRON ELECTRON ENERGY
C
      CALL  SUMOVK(EUP,IPT,IPTOL,KBX,KBY,KBZ,EUP,NKBZPT,ESNGEL,CONST,
     &FERMI,NSNO)
      IF(NSPIN.EQ.1) GO TO 890
      CALL  SUMOVK(EDN,IPT,IPTOL,KBX,KBY,KBZ,EDN,NKBZPT,ESNGED,CONST,
     &FERMI,NDNO)
      ESNGEL=ESNGEL+ESNGED
      PO=PUPO(1)+PDNO(1)+DPUP(1)+DPDN(1)
  890 CONTINUE
      WRITE (6,894) NKBZPT,NKPTRN,ND,IETOTL,ACONST,FERMI,ESNGEL,
     &PO,OMEGA
  894 FORMAT(///,1X,'NO. K=',I3,2X,'NO. KS=',I3,2X,'NB=',I3,2X,
     &'IETOTL=',I1,2X,'LATTICE. CONST.=',F7.4,2X,
     &'FERMI=',F9.6,2X,'SINGLE ELE. E=',F13.7,/,2X,
     &'DENST OF KO=',F9.7,2X,'CELL V=',F8.4,/)
C
C     CALCULATE D,U AND EXCHANGE-CCOPELATION ENERGY AND THE CORRECTIONS
C     BY CONSIDERING MORE KS POINTS.  AND CALCULATE THE TOTAL ENERGY.
C
      VP1=0.D0
      VP2=0.D0
      VXCP1=0.D0
      VXCPU1=0.D0
      VXCPD1=0.D0
      SP1=0.D0
      SPUP1=0.D0
```

```
      WPDN1=0.D0
      VCESUM=0.D0
      VTSUM=0.D0
      VEPSUM=0.D0
      VTPSUM=0.D0
      VXCPSM=0.D0
      VXCPUS=0.D0
      VXCPDS=0.D0
      WPSUM=0.D0
      WPUPSM=0.D0
      WPDNSM=0.D0
      NPT=0
  898 CONTINUE
      IF(NSPIN.EQ.1)  GO TO 900
      READ(11,END=934)  KSQ,GCOLT,GEWLD,GEXCH,GEXUP,GEXDN,GDSPA,GDSUP,
     &GDSDN,GDSUD,GDSDU,GUMUP,GUMDN,KX1,KY1,KZ1,NNB
      IF(NPT.EQ.0)
     &WRITE(6,904)  KSQ,GCOLT,GEWLD,GEXCH,GEXUP,GEXDN,GDSPA,GDSUP,
     &GDSDN,GDSUD,GDSDU,GUMUP,GUMDN,KX1,KY1,KZ1,NNB
      IF(IETOTL.NE.1)  GO TO 900
      READ(12,END=934)  KSQ,GCOLT,GEWLD,GW,GWUP,GWDN,GDSPA,GDSUP,
     &GDSDN,GDSUD,GDSDU,GUMUP,GUMDN,KX1,KY1,KZ1,NNB
      IF(NPT.EQ.0)
     &WRITE(6,904)  KSQ,GCOLT,GEWLD,GW,GWUP,GWDN,GDSPA,GDSUP,
     &GDSDN,GDSUD,GDSDU,GUMUP,GUMDN,KX1,KY1,KZ1,NNB
  900 CONTINUE
  904 FORMAT(1X,/,I5,12F9.5,4I4,/)
  905 FORMAT(1X,/,I5,5F9.5,4I4,/)
      IF(NSPIN.EQ.2)  GO TO 908
      READ(11,END=934)  KSQ,GCOLT,GEWLD,GEXCH,GDSPA,GUM,KX1,KY1,KZ1,NNB
      IF(NPT.EQ.0)
     &WRITE(6,905)      KSQ,GCOLT,GEWLD,GEXCH,GDSPA,GUM,KX1,KY1,KZ1,NNB
      IF(IETOTL.NE.1)  GO TO 908
      READ(12,END=934)  KSQ,GCOLT,GEWLD,GW,GDSPA,GUM,KX1,KY1,KZ1,NNB
      IF(NPT.EQ.0)
     &WRITE(6,905)      KSQ,GCOLT,GEWLD,GW,GDSPA,GUM,KX1,KY1,KZ1,NNB
C     GEXCH=GW
  908 CONTINUE
C     IF(IETOTL.EQ.2)  GEXCH=GEXCH*2.D0/3.D0
      NNBB=NNB
      ANNB=DFLOAT(NNBB)
      NPT=NPT+1
      AKS2=(2.D0*PI/ACONST)**2*DFLOAT(KSQ)
      IF(NPT.GT.NKPTRA.AND.NSPIN.EQ.2)  GUM=GUMUP+GUMDN
      IF(NPT.GT.NKPTPA)  GO TO 914
      GCOLT=VCK0(NPT)+CVKNW(NPT)
      IF(NSPIN.EQ.2)  GO TO 910
      GEXCH=GEXCH+DVXCUP(NPT)
      GW=GW+DWUP(NPT)
      GUM=GUM+DPUP(NPT)
      GO TO 914
  910 CONTINUE
      GEXUP=VXCUP0(NPT)+DVXCUP(NPT)
      GEXDN=VXCDN0(NPT)+DVXCDN(NPT)
      GWUP=WUP0(NPT)+DWUP(NPT)
      GWDN=WDN0(NPT)+DWDN(NPT)
      GUMUP=PUP0(NPT)+DPUP(NPT)
      GUMDN=PDN0(NPT)+DPDN(NPT)
```

```
      GUM=GUMUP+GUMDN
  914 CONTINUE
      IF(NPT.NE.1) GO TO 918
      GCOULT=GCOLT
      GCOUEL=GCOULT
      WRITE(6,858) GCOUEL,GCOULT,VKO(1)
  918 CONTINUE
      IF(NPT.EQ.1) GO TO 920
      GCOULT=GCOLT
      GCOUEL=GCOULT+2.D0*PI*Z/OMEGA/AKS2
  920 CONTINUE
      IF(NPT.EQ.1) WRITE(6,858) GCOUEL,GCOULT
      VCESUM=VCESUM+GCOUEL*ANNB
      VTSUM=VTSUM+GCOULT*ANNB
      VTPSUM=VTPSUM+GCOULT*GUM*ANNB
      VEPSUM=VEPSUM+GCOUEL*GUM*ANNB
      IF(NSPIN.EQ.2) GO TO 924
      VXCPSM=VXCPSM+GEXCH*GUM*ANNB
      VXCPUD=VXCPSM
      WPSUM=WPSUM+GW*GUM*ANNB
      WPUDS=WPSUM
  924 CONTINUE
      IF(NPT.LE.NKPTBN) GO TO 928
      VP1=VP1+GCOUEL*GUM*ANNB
      VP2=VP2+GCOULT*GUM*ANNB
      IF(NSPIN.EQ.2) GO TO 928
      VXCP1=VXCP1+GEXCH*GUM*ANNB
      VXCP2=VXCP1
      WP1=WP1+GW*GUM*ANNB
      WPUD2=WP1
  928 CONTINUE
      IF(NSPIN.EQ.1) GO TO 930
      VXCPUS=VXCPUS+GEXUP*GUMUP*ANNB
      VXCPDS=VXCPDS+GEXDN*GUMDN*ANNB
      VXCPUD=VXCPUS+VXCPDS
      WPUPSM=WPUPSM+GWUP*GUMUP*ANNB
      WPDNSM=WPDNSM+GWDN*GUMDN*ANNB
      WPUDS=WPUPSM+WPDNSM
      IF(NPT.LE.NKPTBN) GO TO 930
      VXCPU1=VXCPU1+GEXUP*GUMUP*ANNB
      VXCPD1=VXCPD1+GEXDN*GUMDN*ANNB
      VXCP2=VXCPU1+VXCPD1
      WPUP1=WPUP1+GWUP*GUMUP*ANNB
      WPDN1=WPDN1+GWDN*GUMDN*ANNB
      WPUD2=WPUP1+WPDN1
  930 CONTINUE
      IF(NPT.EQ.1) WRITE(6,948)
      IF(NPT.EQ.NKPTBN.OR.NPT.EQ.1.OR.NPT.EQ.2.OR.NPT.EQ.300.OR.
     &NPT.EQ.1000.OR.NPT.EQ.1500.OR.NPT.EQ.1800.OR.NPT.EQ.2000)
     &WRITE(6,950) NPT,VP1,VP2,VXCP2,WPUD2,VCESUM,VTSUM,VEPSUM,VTPSUM,
     &VXCPUD,WPUDS
      GO TO 898
  934 CONTINUE
      REWIND 11
      IF(IETCTL.NE.1) GO TO 938
      REWIND 12
  938 CONTINUE
      VP=VP1*OMEGA/2.DC
```

```
      VTP=VP2*OMEGA/2.D0
      VXP=VXCP2*OMEGA
      WP=WPDD2*OMEGA
C     IF(IFTOTL.EQ.2) WP=WP/4.D0
      C=-11.432877*2.D0*PI/ACONST
      UNUNU=Z**2*C/(2.D0*PI**2)
      D=-Z*VCESUM/2.D0+C*Z**2/2.D0/PI**2
      U=-VTPSUM*OMEGA/2.D0
      X=VXCPUD*OMEGA
      EVEPSM=VEPSUM*OMEGA/2.D0
      EVECSM=WPUDS*OMEGA
      IF(IETOTL.EQ.2) EVECSM=EVECSM/4.D0
C
C     CALCULATE THE TOTAL ENERGY
C
      ETOTH=ESNGEL+D+U-EVECSM
      EPOTEH=D-U
      EKINET=ESNGEL+2.D0*U-X
      PRESSH=(2.D0*EKINET+EPOTEH+3.D0*EVECSM)/(3.D0*OMEGA)
      IF(NSPIN.EQ.1)
     &WRITE(6,940)
      IF(NSPIN.EQ.2)
     &WRITE(6,944)
  940 FORMAT(//,2X,'NPT',2X,'ESMVEP FR40',2X,'ESMVCP FR40',2X,
     &'ESMWP FR40',2X,'C*2*PI/A',3X,'UNUC-NUC')
      IF(NSPIN.EQ.1)
     &WRITE(6,950) NPT,VP,VTP,WP,C,UNUNU
  944 FORMAT(//,1X,'NPT',2X,'ESMVEP FR40',2X,'ESMVCP FR40',2X,
     &'ESMWP FR40',2X,'C*2*PI/A',3X,'UNUC-NUC',4X,'SMWP*PP',4X,
     &'SMWUP*PUP',3X,'SMWDN*PDN')
      IF(NSPIN.EQ.2)
     &WRITE(6,950) NPT,VP,VTP,WP,C,UNUNU,WPSUM,WPUPSM,WPDNSM
  948 FORMAT(//,2X,'NPT',4X,'SMVEP FR40',2X,'SMVCP FR40',2X,
     &'SMVXP FR40',2X,'SMWP FR40',4X,'SMVEK',7X,'SMVCK',6X,
     &'SMVEK*PK',3X,'SMVCK*PK',3X,'SMVXK*PK',3X,'SMWK*PK',/)
  950 FORMAT(1X,I4,1X,6F12.7,4F11.7)
      WRITE(6,98)
      WRITE(6,954)EVEPSM,ESNGEL,U,D,EVECSM,ETOTH,EPOTEH,EKINET,X,PRESSH
   98 FORMAT(/,3X,'E1E CCUL',3X,'E SINGL.',7X,'U',11X,'D',8X,
     &'E EXCH.',4X,'E TOTAL',5X,'E POTENT.',4X,'E KINET.',8X,
     &'X',9X,'PRESSUE')
  954 FORMAT(1X,2F12.6,2F11.4,F9.5,F16.7,4F13.6)
C
C
C
C
C     CALCULATE THE DENSITY OF STATES
C
   99 CONTINUE
      IF(NDENS.EQ.0) GO TO 180
      EE=EMIN
      DO 100 NE=1,NEMAX
      EN(NE)=EE
      SWUP(NE)=0.D0
      SWDN(NE)=0.D0
      TWUP(NE)=0.D0
      TWDN(NE)=0.D0
      ESINGU(NE)=0.D0
```

```
      ESINGD(NE)=0.DC
      EE=EE+DE
      IF(EN(NE).GE.FERMI.OR.EE.LE.FERMI) GC TO 100
      EN(NE)=FERMI
  100 CONTINUE
      DO 118 IT=1,IPTOL
      I1=IPT(1,IT)
      I2=IPT(2,IT)
      I3=IPT(3,IT)
      I4=IPT(4,IT)
      DO 118 NB=1,NDFERM
      E1=EUP(NB,I1)
      E2=EUP(NB,I2)
      E3=EUP(NB,I3)
      E4=EUP(NB,I4)
C
C     FOLLLOWING STATEMENTS ARE USED FOR SUBROUTINE TDENST
C
      IF(E1.LE.E2) GO TO 102
  101 CONTINUE
      EE=E1
      E1=E2
      E2=EE
  102 IF(E2.LE.E3) GO TO 104
  103 CONTINUE
      EE=E2
      E2=E3
      E3=EE
      IF(E1.GT.E2) GO TO 101
  104 IF(E3.LT.E4) GO TO 105
      EE=E3
      E3=E4
      E4=EE
      IF(E2.GT.E3) GO TO 103
  105 CONTINUE
      D43=E4-E3
      IF(D43.LE.ZERO) E4=E4+ZERO
      D32=E3-E2
      IF(D32.LE.ZERO) E2=E2-ZERO
      D21=E2-E1
      IF(D21.EQ.ZERO) E1=E1-ZERO
      IF(D21.LT.ZERO) E1=E1-2.D0*ZERO
      D41=E4-E1
      IF(D41.LT.3.D0*ZERO) E4=E4+ZERO
C     IF(E4.LE.E3.OR.E3.LE.E2.OR.E2.LE.E1.OR.D41.LE.3.D0*ZERO)
C    &WRITE(6,140) ZERO,D41,E1,E2,E3,E4
      CALL TDENST(E1,E2,E3,E4,EN,SWUP,NEMAX,CCN,ZERO)
      CALL TELECT(E1,E2,E3,E4,CONST,EN,TWUP,NEMAX)
      CALL TELEC1(E1,E2,E3,E4,CONST,EN,ESINGU,NEMAX)
      IF(NSPIN.EQ.1) GO TO 118
      E1=EDN(NB,I1)
      E2=EDN(NB,I2)
      E3=EDN(NB,I3)
      E4=EDN(NB,I4)
      IF(E1.LE.E2) GO TO 112
  111 CONTINUE
      EE=E1
      E1=E2
```

```
      E2=EE
  112 IF(E2.LE.E3) GO TO 114
  113 CONTINUE
      EE=E2
      E2=E3
      E3=EE
      IF(E1.GT.E2) GO TO 111
  114 IF(E3.LT.E4) GO TO 115
      EE=E3
      E3=E4
      E4=EE
      IF(E2.GT.E3) GO TO 113
  115 CONTINUE
      D43=E4-E3
      IF(D43.LE.ZERO) E4=E4+ZERO
      D32=E3-E2
      IF(D32.LE.ZERO) E2=E2-ZERO
      D21=E2-E1
      IF(D21.EQ.ZERO) E1=E1-ZERO
      IF(D21.LT.ZERO) E1=E1-2.D0*ZERO
      D41=E4-E1
      IF(D41.LT.3.D0*ZERO) E4=E4+ZERO
C     IF(E4.LE.E3.OR.E3.LE.E2.OR.E2.LE.E1.OR.D41.LE.3.D0*ZERO)
C    &WRITE(6,140) ZERO,D41,E1,E2,E3,E4
      CALL TDENST(E1,E2,E3,E4,EN,SWDN,NEMAX,CON,ZERO)
      CALL TELECT(E1,E2,E3,E4,CONST,EN,TWDN,NEMAX)
      CALL TELEC1(E1,E2,E3,E4,CONST,EN,ESINGD,NEMAX)
  118 CONTINUE
      IF(NSPIN.EQ.1) GO TO 150
      WRITE(6,120)
  120 FORMAT(//,6X,'E',10X,'DEN UP',8X,'DEN DOWN',6X,'ELEC UP',7X,'ELEC
     &DOWN',5X,'TOTAL ELEC',7X,'MAG NO',7X,'ESINGL',/)
      DO 130 NE=1,NEMAX
      ENO=TWUP(NE)+TWDN(NE)
      EMAG=TWUP(NE)-TWDN(NE)
      ESINGE=ESINGD(NE)+ESINGD(NE)
      IF(DABS(SWUP(NE)).GT.ZERO.OR.DABS(SWDN(NE)).GT.ZERO)
     &WRITE(6,140) EN(NE),SWUP(NE),SWDN(NE),TWUP(NE),TWDN(NE),ENO,EMAG
     &,ESINGE
  130 CONTINUE
  140 FORMAT(1X,8F14.7)
      DO 143 NE=1,NEMAX
      GEN=EN(NE)
      GSWUP=SWUP(NE)
      GTWUP=TWUP(NE)
  143 WRITE(40,148) GEN,GSWUP,GTWUP
      DO 145 NE=1,NEMAX
      GEN=EN(NE)
      GSWDN=SWDN(NE)
      GTWDN=TWDN(NE)
  145 WRITE(41,148) GEN,GSWDN,GTWDN
  148 FORMAT(3F15.5)
      GO TO 180
  150 CONTINUE
      WRITE(6,160)
  160 FORMAT(//,11X,'E',10X,'DENSITY',7X,'ELEC NO',6X,'ESINGL',/)
      DO 170 NE=1,NEMAX
      IF(DABS(SWUP(NE)).GT.ZERO)
```

DSN=PHBAG&.DIOL&.DEN

```
      &WRITE(6,140) EN(NE),SWUP(NE),TWUP(NE),ESINGU(NE)
       GEN=EN(NE)
       GSWUP=SWUP(NE)
       GTWUP=TWUP(NE)
       WRITE(40,148) GEN,GSWUP,GTWUP
  170 CONTINUE
  180 CONTINUE
       STOP
       END
       SUBROUTINE TELEC1(E1,E2,E3,E4,CONST,EN,SW,NEMAX)
C
C      E1,E2,E3,E4 ARE E(K) AT FOUR CORNERS OF TETRAHEDRONS.
C      SW(NE)/EAVRG IS THE FRACTION OF THE VOLUME WITH E(K).LE.EN(NE).
C
C      TELEC1 IS USED FOR CALCULATION OF THE SINGLE ELECTRON ENERGY
C
       IMPLICIT REAL*8(A-F,H,O-Z)
       DIMENSION EN(NEMAX),SW(NEMAX)
       IF(E1.LE.E2) GO TO 20
   10 CONTINUE
       EE=E1
       E1=E2
       E2=EE
   20 IF(E2.LE.E3) GO TO 40
   30 CONTINUE
       EE=E2
       E2=E3
       E3=EE
       IF(E1.GT.E2) GO TO 10
   40 IF(E3.LE.E4) GO TO 50
       EE=E3
       E3=E4
       E4=EE
       IF(E2.GT.E3) GO TO 30
   50 CONTINUE
       IF(EN(NEMAX).LT.E1) RETURN
       D41=E4-E1
       IF(EN(1).LE.E4) GO TO 70
       EAVRG=(E1+E2+E3+E4)/4.D0
       DO 60 NE=1,NEMAX
   60 SW(NE)=SW(NE)+CONST*EAVRG
       RETURN
   70 CONTINUE
       D21=E2-E1
       D31=E3-E1
       D32=E3-E2
       D42=E4-E2
       D43=E4-E3
       IF(D21.GT.0.D0) CS1=1.D0/(D21*D31*D41)
   80 IF(D32.LE.0.D0) GO TO 90
       CS23=-(1.D0/D31+1.D0/D42)/(D41*D32)
       CS22=3.D0/(D31*D41)
       CS21=D21*CS22
       CS20=D21*CS21/3.D0
   90 IF(D43.GT.0.D0) CS4=1.D0/(D41*D42*D43)
       DO 140 NE=1,NEMAX
       EE=EN(NE)
       IF(EE.LT.E1) GO TO 140
```

DSN=PHBAGA.DIOLA.DEN

```
      IF(EE.GE.E4) GO TO 130
      IF(EE.LT.E2) GO TO 100
      IF(EE.LT.E3) GO TO 110
      DE4=EE-E4
      EAVRG=(E1+E2+E3+EE)/4.D0
      S=1.D0+CS4*DE4**3
      GO TO 120
  100 CONTINUE
      DE1=EE-E1
      EAVRG=(E1+3.D0*EE)/4.D0
      S=CS1*DE1**3
      GO TO 120
  110 CONTINUE
      DE2=EE-E2
      DE22=DE2*DE2
      DE23=DE22*DE2
      EAVRG=(E1+E2+2.D0*EE)/4.D0
      S=CS23*DE23+CS22*DE22+CS21*DE2+CS20
  120 SW(NE)=SW(NE)+S*CONST*EAVRG
      GO TO 140
  130 EAVRG=(E1+E2+E3+E4)/4.D0
      SW(NE)=SW(NE)+CONST*EAVRG
  140 CONTINUE
      RETURN
      END
//LKED.SYSLIB  DD DSN=D1103.CALLAWAY.RVCMPLIB,DISP=SHR
//      DD DSN=D1103.CALLAWAY.BNDPKG.SUBLIB.COMPL,DISP=SHR
//       DD DSN=SYS1.VFORTLIB,DISP=SHR
//       DD DSN=SYS2.FORTLIB,DISP=SHR
//       DD DSN=SYS2.SSP.LIB,DISP=SHR
//       DD DSN=SYS2.PLOT.LIB,DISP=SHR
//GO.FT01F001 DD UNIT=3380,VOL=SER=USER77,DISP=SHR,
//       DCB=(BLKSIZE=7294,RECFM=VSB,LRECL=00176),
//           DSNAME=PHBAGA.DIOLA.FEF5P4.BCC.BAND
//GO.FT11F001 DD UNIT=3380,VOL=SER=USER77,DISP=SHR,
//             DSNAME=PHBAGA.DIOLA.FEF5P4.BCC.VK1
//GO.FT12F001 DD UNIT=3380,VOL=SER=USER77,DISP=SHR,
//             DSNAME=PHBAGA.DIOLA.FEF5P4.BCC.VK3
//GO.FT40F001 DD UNIT=3380,VOL=SER=USER77,DISP=(NEW,CATLG),
//         SPACE=(TRK,(20,10),RLSE),
//       DCB=(BLKSIZE=4500,RECFM=FB,LRECL=0045),
//           DSNAME=PHBAGA.DIOLA.FEF5P4.BCC.DNSTUP3
//GO.FT41F001 DD UNIT=3380,VOL=SER=USER77,DISP=(NEW,CATLG),
//         SPACE=(TRK,(20,10),RLSE),
//       DCB=(BLKSIZE=4500,RECFM=FB,LRECL=0045),
//           DSNAME=PHBAGA.DIOLA.FEF5P4.BCC.DNSTDK3
//GO.FT17F001 DD UNIT=3380,VOL=SER=USER77,DISP=SHR,
//         DSNAME=PHBAGA.DIOLA.FEF5P4.BCC.SELFVX
//GO.FT27F001 DD UNIT=3380,VOL=SER=USER77,DISP=SHR,
//         DSNAME=PHBAGA.DIOLA.FEF5P4.BCC.SELFWK
//GO.FT37F001 DD UNIT=3380,VOL=SER=USER77,DISP=SHR,
//         DSNAME=PHBAGA.DIOLA.FEF5P4.BCC.SELFDD
//GO.SYSIN DD *
    1    1
  901   20     1    2    2   15    0   43    1   40    1
  -1.0        0.0025     0.00001  26.0       26.0       5.4057
//
```

APPENDIX B

Table B1. Valence band energies at high symmetry points of the Brillouin zone of BCC iron - in Rydbergs (Ry) - for up (↑) and down (↓) spins. The Lattice constant a = 5.2 a.u.

The Fermi energy E_F = -0.0398 Ry

Γ↑	Γ↓	P↑	P↓
-0.6971 (1)	-0.6811 (1)	-0.3071 (4)	-0.2186 (4)
-0.2267 (25')	-0.1069 (25')	-0.3071 (4)	-0.2186 (4)
-0.2267 (25')	-0.1069 (25')	-0.3071 (4)	-0.2186 (4)
-0.2267 (25')	-0.1069 (25')	-0.0905 (3)	0.0727 (3)
-0.1101 (12)	0.0484 (12)	-0.0905 (3)	0.0727 (3)
-0.1101 (12)	0.0484 (12)	0.6342 (4)	0.6999 (4)

N↑	N↓	H↑	H↓
-0.4429 (1)	-0.3635 (1)	-0.4354 (12)	-0.3300 (12)
-0.3185 (2)	-0.2107 (2)	-0.4354 (12)	-0.3300 (12)
-0.1078 (1)	0.0011 (1')	-0.0196 (25')	0.1198 (25')
-0.0935 (4)	0.0419 (1)	-0.0196 (25')	0.1198 (25')
-0.0153 (1')	0.0691 (4)	-0.0196 (25')	0.1198 (25')
0.0037 (3)	0.1455 (3)	0.7285 (15)	0.7515 (15)

Table B2. Valence band energies at high symmetry points of the Brillouin zone of BCC iron - in Rydbergs (Ry) - for up (↑) and down (↓) spins. The Lattice constant a = 5.4057 a.u.

The Fermi energy E_f = -0.1214 Ry

Γ↑	Γ↓	P↑	P↓
-0.7275 (1)	-0.7125 (1)	-0.3551 (4)	-0.2589 (4)
-0.2863 (25')	-0.1565 (25')	-0.3551 (4)	-0.2589 (4)
-0.2863 (25')	-0.1565 (25')	-0.3551 (4)	-0.2589 (4)
-0.2863 (25')	-0.1565 (25')	-0.1729 (3)	-0.0011 (3)
-0.1880 (12)	-0.0202 (12)	-0.1729 (3)	-0.0011 (3)
-0.1880 (12)	-0.0202 (12)	0.4931 (4)	0.5605 (4)

N↑	N↓	H↑	H↓
-0.4725 (1)	-0.3870 (1)	-0.4556 (12)	-0.3387 (12)
-0.3618 (2)	-0.2437 (2)	-0.4556 (12)	-0.3387 (12)
-0.1869 (1)	-0.0791 (1')	-0.1121 (25')	0.0378 (25')
-0.1752 (4)	-0.0276 (1)	-0.1121 (25')	0.0378 (25')
-0.0936 (3)	-0.0038 (4)	-0.1121 (25')	0.0378 (25')
-0.0927 (1')	0.0595 (3)	0.5863 (15)	0.6086 (15)

Table B3. Valence band energies at high symmetry points of the Brillouin zone of BCC iron - in Rydbergs (Ry) - for up (↑) and down (↓) spins. The Lattice constant a = 5.6 a.u.

The Fermi energy E_F = -0.1817 Ry

Γ↑	Γ↓	P↑	P↓
-0.7433 (1)	-0.7286 (1)	-0.3881 (4)	-0.2842 (4)
-0.3291 (25')	-0.1894 (25')	-0.3881 (4)	-0.2842 (4)
-0.3291 (25')	-0.1894 (25')	-0.3881 (4)	-0.2842 (4)
-0.3291 (25')	-0.1894 (25')	-0.2325 (3)	-0.0532 (3)
-0.2442 (12)	-.0683 (12)	-0.2325 (3)	-0.0532 (3)
-0.2442 (12)	-0.0683 (12)	0.3849 (4)	0.4540 (4)

N↑	N↓	H↑	H↓
-0.4908 (1)	-0.3992 (1)	-0.4647 (12)	-0.3355 (12)
-0.3917 (2)	-0.2631 (2)	-0.4647 (12)	-0.3355 (12)
-0.2442 (1)	0.1358 (1')	-0.1802 (25')	-0.0204 (25')
-0.2342 (4)	-0.0761 (1)	-0.1802 (25')	-0.0204 (25')
-0.1638 (3)	-0.0553 (4)	-0.1802 (25')	-0.0204 (25')
-0.1492 (1')	-0.0016 (3)	0.4761 (15)	0.4983 (15)

Table B.4. Valence band energies at high symmetry points of the Brillouin zone of FCC iron , in Rydberg (Ry),for up (↑) and down (↓) spins. The lattice constant is a = 6.5516 a.u. The Fermi energy is E_F = -0.0573 Ry

$\Gamma_\uparrow$	$\Gamma_\downarrow$		$X_\uparrow$	$X_\downarrow$		$W_\uparrow$	$W_\downarrow$		$L_\uparrow$	$L_\downarrow$	
-0.6912	-0.6982	(1)	-0.4402	-0.3906	(1)	-0.3630	-0.3095	(2')	-0.4302	-0.3897	(1)
-0.2143	-0.1357	(25')	-0.3911	-0.3316	(3)	-0.2756	-0.2162	(3)	-0.2234	-0.1436	(3)
-0.2143	-0.1357	(25')	-0.0379	+0.0614	(2)	-0.2756	-0.2162	(3)	-0.2234	-0.1436	(3)
-0.2143	-0.1357	(25')	-0.0096	+0.0871	(5)	-0.1183	-0.0302	(1)	-0.0458	-0.0531	(2')
-0.1111	-0.0178	(12)	-0.0096	+0.0871	(5)	-0.0095	+0.0873	(1')	-0.0317	+0.0651	(3)
-0.1111	-0.0178	(12)	+0.1759	+0.1713	(4')	+0.6171	+0.6439	(3)	-0.0317	+0.0651	(3)

$K_\uparrow$	$K_\downarrow$	
-0.3762	-0.3208	(1)
-0.3418	-0.2866	(1)
-0.1801	-0.1197	(3)
-0.0960	-0.0044	(4)
-0.0364	0.0580	(2)
0.4636	0.4952	(1)

Table B.5 Valence band energies at high symmetry points of the Brillouin zone of FCC iron , in Rydberg (Ry),for up (↑) and down (↓) spins. The lattice constant is a = 6.8107 a.u . The Fermi energy is E_F = -0.1283 Ry.

$\Gamma_\uparrow$	$\Gamma_\downarrow$		$X_\uparrow$	$X_\downarrow$		$W_\uparrow$	$W_\downarrow$		$L_\uparrow$	$L_\downarrow$	
-0.7239	-0.7210	(1)	-0.4645	-0.3921	(1)	-0.4004	-0.3244	(2')	-0.4639	-0.4059	(1)
-0.2738	-0.1718	(25')	-0.4213	-0.3395	(3)	-0.3262	-0.2461	(3)	-0.2823	-0.1776	(3)
-0.2738	-0.1718	(25')	-0.1287	-0.0029	(2)	-0.3262	-0.2461	(3)	-0.2823	-0.1776	(3)
-0.2738	-0.1718	(25')	-0.1022	+0.0188	(5)	-0.1951	-0.0812	(1)	-0.1227	-0.1205	(2')
-0.1900	-0.0705	(12)	-0.1022	+0.0188	(5)	-0.1021	+0.0189	(1')	-0.1217	+0.0001	(3)
-0.1900	-0.0705	(12)	+0.0767	+0.0816	(4')	+0.4736	+0.5135	(3)	-0.1217	+0.0001	(3)

$K_\uparrow$	$K_\downarrow$	
-0.4099	-0.3320	(1)
-0.3825	-0.3062	(1)
-0.2458	-0.1652	(3)
-0.1768	-0.0591	(4)
-0.1243	-0.0057	(2)
+0.3315	+0.3767	(1)

Table B. 6. Valence band energies at high symmetry points of the Brillouin zone for FCC iron , in Rydberg (*Ry*), for up (+) and down (+) spins. The lattice constant is a = 7.0 a.u. The Fermi energy is E_F = -0.1501 Ry.

$\Gamma_\uparrow$	$\Gamma_\downarrow$		$X_\uparrow$	$X_\downarrow$		$W_\uparrow$	$W_\downarrow$		$L_\uparrow$	$L_\downarrow$	
-0.7390	-0.7234	(1)	-0.4820	-0.3658	(1)	-0.4268	-0.3067	(2')	-0.4877	-0.3904	(1)
-0.3176	-0.1537	(25')	-0.4453	-0.3090	(3)	-0.3626	-0.2318	(3)	-0.3246	-0.1607	(3)
-0.3176	-0.1537	(25')	-0.1909	-0.0010	(2)	-0.3626	-0.2318	(3)	-0.3246	-0.1607	(3)
-0.3176	-0.1537	(25')	-0.1673	+0.0229	(5)	-0.2483	-0.0745	(1)	-0.1846 (3)	-0.1526	(2')
-0.2447	-0.0633	(12)	-0.1673	+0.0229	(5)	-0.1673	+0.0229	(1')	-0.1846 (3)	+0.0041	(3)
-0.2447	-0.0633	(12)	-0.0183	+0.0368	(4')	+0.3838	+0.4539	(3)	-0.1662 (2')	+0.0041	(3)

$K_\uparrow$	$K_\downarrow$	
-0.4343	-0.3118	(1)
-0.4123	-0.2850	(1)
-0.2915	-0.1615	(3)
-0.2326	-0.0537	(4)
-0.1865	+0.0005	(2)
-0.2492	+0.3278	(1)

Table B.7. Least square fit coefficients, as defined in section D of Chapter 4, for the charge form factors of BCC iron. The lattice constants used are 5.0, 5.4057, and 6.0 in atomic units (a.u.).

k	ℓ	m	$a^c_{0,k,\ell,m}$	$a^c_{1,k,\ell,m}$	$a^c_{2,k,\ell,m}$
1	1	0	3.58136484	3.82979289	-0.204981172
2	0	0	-0.53493592	3.91177317	-0.188461197
2	1	1	-2.02307672	3.65074480	-0.158685891
2	2	0	-1.40850876	2.94225321	-0.099150292
3	1	0	0.20577533	2.05663904	-0.029130822
2	2	2	0.86298061	1.65095044	-0.003977313
3	2	1	2.01638714	1.12533471	0.031469571
4	0	0	3.33933146	0.57493513	0.069487715
3	3	0	3.02149173	0.65213636	0.053233058
4	1	1	3.43664824	0.49926231	0.066621608
4	4	2	0.78131382	1.23413160	-0.039602873
6	0	0	1.40023291	1.01385793	-0.020968903

Table B.8. Least square fit coefficients, as defined in section D of Chapter 4, for the spin form factors of BCC iron. The lattice constants used are 5.0, 5.4057, and 6.0 in atomic units (a.u.).

k	ℓ	m	$a^s_{0,k,\ell,m}$	$a^s_{1,k,\ell,m}$	$a^s_{2,k,\ell,m}$
1	1	0	-0.92334553	0.47537670	-0.034361518
2	0	0	-0.61031707	0.28057959	-0.016707236
2	1	1	-0.83298532	0.28955795	-0.016196177
2	2	0	-0.60380824	0.18832302	-0.008220275
3	1	0	-0.01999695	-0.00250778	0.005973435
2	2	2	-0.61723276	0.16405534	-0.006977759
3	2	1	-0.26844538	0.05403997	0.000941820
4	0	0	0.46889063	-0.16349990	0.016636354
3	3	0	-0.13055622	0.00777395	0.003611459
4	1	1	0.23540831	-0.09688971	0.011253610
4	4	2	0.01297626	-0.02959130	0.004099209
6	0	0	0.41962568	-0.13630275	0.011227522

APPENDIX C

C.1. Evaluation of the Pressure for a Metal

The expression of the pressure P is, for a paramagnetic substance,[85]

$$3PV = 2E_{ki} + E_{PC} - 3 \int \rho \, (e_{xc} - V_{xc}) \, d^3r \qquad \text{C.1.1}$$

where

$$E_{ki} = \sum_n \int \Psi_n^*(\vec{k},\vec{r}) \, (-\nabla^2) \, \Psi_n(\vec{k},\vec{r}) \, d^3r, \qquad \text{C.1.2}$$

$$E_{PC} = -2Z \sum_\mu \int \frac{\rho(\vec{r})}{|\vec{r}-\vec{R}_\mu|} \, d^3r + \int \frac{\rho(\vec{r})\rho(\vec{r}')}{|\vec{r}-\vec{r}'|} \, d^3r \, d^3r' + \sum_{\mu\nu,\mu\neq\nu} \frac{Z_\mu Z_\nu}{|\vec{R}_\mu-\vec{R}_\nu|} \qquad \text{C.1.3}$$

V is the crystal volume.

The remaining terms in equation C.1.1 are as defined in Chapter 2. Using equations 1 and 2 and the definitions of U and D in Chapter 2 one readily obtains:

$$T = \sum_n E_n(\vec{k}) + 2U - \Sigma \int \rho \, V_{xc} \, d^3r \qquad \text{C.1.4}$$

The above expression of E_{PC} yields:

$$E_{PC} = D - U \qquad \text{C.1.5}$$

The last term in equation C.1.1 (sign included) in simply Δ_{xc}. We therefore have:

$$3PV = 2 \sum_n E_n(\vec{k}) + 3U + D - 2X + \Delta_{xc}, \qquad \text{C.1.6}$$

with

$$x = \int \rho \, V_{xc} \, d^3r \qquad \text{C.1.7}$$

This expression can be precisely evaluated by the new version of BNDPKG as shown in program Density provided in appendix A.3. As stated above, this new method does not use a Muffin-Tin[85] or other approximations in obtaining the pressure P.

VITA

Diola Bagayoko, a son of Djigui Bagayoko and Nagnouma Keita, was born on December 12, 1948 in Bamako, Mali. He attended the secondary school of N'Tomikorobougou from 1962 to 1966 and the Prosper Kamara High School from 1966 to 1969, where he majored in mathematics, physics, and chemistry. He majored from 1969 to 1973, in physics and chemistry at the Ecole Normale Superieure de Bamako. Bagayoko earned a national reputation as a good student by systematically holding the 1^{st} rank in his classes from primary school to college.

After two years of teaching physics and chemistry at Askia Mohamed and Sikasso High Schools he enrolled at the American Language Institut at Georgetown University to acquire english proficiency in October of 1975. He earned a Master's degree in physics from Lehigh University in 1978 and joined the group of professor Callaway at Louisiana State University the same year.

A few of the awards and honors Diola Bagayoko accepted include but are not limited to: the Malien Government fellowship from 1966 to 1973, a French government fellowship (Bourse FAC) from 1970 to 1971, Operation Cross-road Africa Award to visit the United States of America in the summer of 1972, a University of Grenoble (France) grant for practical training in the summer of 1973, African graduate fellowship (AFGRAD) offered by the African American Institute, Brandeis and Lehigh Universities from 1975 to 1980, a Physics department teaching assistantship at Louisiana State University from 1978 to 1981 followed by a research assistantship from 1982 to present.

Diola Bagayoko has been holding membership and leadership positions in various student and professional organizations. These include, at the professional level, the American Physical Society (APS), the International Association for the advancement of appropriate technology for developing countries, and, at the social level, the Organization of Lycee Proper Students (President 1968-1969), the Organization of EN Sup Students (public relations officer 1970-1971), the African Student Organization of Louisiana State University (vice-president 1979-1980, president 1981-1982, and 1983 to present), the International Student Association at L.S.U. (vice-president 1980-1981, president 1981-1982).

Bagayoko has been participating in several international physics conferences. Few of those at which he presented a publication are: the APS Annual meeting in New York City (1980), APS meeting in New Orleans, Louisiana in November 1981, the APS annual meeting in Dallas, Texas in March 1982, the Sanibel International symposium in Palm Coast, Florida, in March 1983. Bagayoko delivered invited talks at social conferences on such subjects as world hunger and voluntarism.

He coauthored and/or authored numerous publications in a number of journals (i.e., physics letters, Physical Review and the International Journal of quantum chemistry) on the electronic, magnetic, bulk, optical and other properties of metals as well as computational procedures. Detailed references are available in his Ph.D. dissertation.

Married and father of one, Diola Bagayoko is currently a Ph.D. candidate in physics at Louisiana State University. His present research interests include the electronic energy band theory of metals and related topics, Laser physics, and the search of solution to relativistic quantum mechanical equations.

EXAMINATION AND THESIS REPORT

Candidate: DIOLA BAGAYOKO

Major Field: Physics

Title of Thesis: Electronic Structure of Iron

Approved:

Major Professor and Chairman

Dean of the Graduate School

EXAMINING COMMITTEE:

Date of Examination:

July 15, 1983